Immune-modulatory effects of non-thermal plasma

I n a u g u r a l d i s s e r t a t i o n

zur

Erlangung des akademischen Grades eines

Doktors der Naturwissenschaften

(Dr. rer. nat.)

der

Mathematisch-Naturwissenschaftlichen Fakultät

der

Ernst-Moritz-Arndt-Universität Greifswald

vorgelegt von

Lena Christina Bundscherer

geboren am 29.10.1983

in Erlangen

Greifswald, Dezember 2013

Dekan: Prof. Dr. Klaus Fesser

1. Gutachter: Prof. Dr. Ulrike Lindequist

2. Gutachter: Prof. Dr. Eun Ha Choi

Tag der Promotion: 10.04.2014

Table of Contents

Table of Contents

List of Figures

List of Tables

Abbreviations

7AAD	7-aminoactinomycin D
ACTB	Actin beta
ALL	Acute lymphoblastic leukemia
AML	Acute monocytic leukemia
ANOVA	Analysis of variances
AP	Activator protein
APC	Allophycocyanin
AVBB	Annexin V binding buffer
Ca^{2+}	Calcium cation (2+)
$CaCl_2$	Calcium chloride
CD	Cluster of differentiation
cDNA	Complementary deoxyribonucleic acid
CO	Carbon monoxide
CO_2	Carbon dioxide
$CO_3^{\cdot-}$	Carbonate radical anion
conc.	Concentrated
Cy	Cyanine
DNA	Deoxyribonucleic acid
DNase	Deoxyribonuclease
dNTP	Deoxyribonucleotide triphosphate
dT	Desoxythymidine
DTT	Dithiothreitol
ECM	Extracellular matrix
EDTA	Ethylenediaminetetraacetic acid
ELISA	Enzyme-linked immunosorbent assay
ERK	Extracellular signal-regulated kinase
Eto	Etoposide
FcR	Fc receptor

Abbreviations

FCS	Fetal calf serum
Fe^{2+}	Iron (2+)
FITC	Fluorescein isothiocyanat
FOS	FBJ murine osteosarcoma viral oncogene homolog
FSC	Forward scatter
GM-CSF	Granulocyte macrophage colony-stimulating factor
GO	Gene ontology
GSH	Reduced glutathione
GS$^{\bullet}$	Glutathione-thiyl radical
GSR	Glutathione reductase
GSSG	Oxidized glutathione
HaCaT	Human adult low calcium temperature keratinocytes
HEPES	4-(2-hydroxyethyl)-1-piperazineethanesulfonic acid
HMOX	Heme oxygenase
HNO_2	Nitrous acid
$HO_2^{\bullet}$	Hydroperoxyl radical
H_2O_2	Hydrogen peroxide
HRP	Horseradish peroxidase
HSP	Heat shock protein
IFN	Interferon
IgG	Immunglobulin G
IL	Interleukin
IPA	Ingenuity System Pathway Analysis
JNK	C-Jun N-terminal kinase
JUN	Jun proto-oncogene
kDa	Kilodalton
kVpp	Kilovolts peak to peak
LPS	Lipopolysaccharide
MAPK	Mitogen-activated protein kinase
MAPKAPK2	MAPK-activated protein kinase-2

MEK	MAPK/ ERK kinase
Mg^{2+}	Magnesium (2+)
MHC	Major histocompatibility complex
MHz	Megahertz
MKK	Mitogen-activated protein kinase kinase
mRNA	Messenger ribonucleic acid
n.a.	Not analyzed
NaCl	Sodium chloride
NaOH	Sodium hydroxide
n.c.	Not changed
n.d.	Not detectable
$NO^\bullet$	Nitric oxide
NO^+	Nitrosyl cation
NO^-	Nitrosyl anion
$NO_2^\bullet$	Nitrogen dioxide radical
NRF	Nuclear respiratory factor
$O_2^{\bullet-}$	Superoxide anion
$^1O_2$	Singlet oxygen
O_3	Ozone
$OH^\bullet$	Hydroxyl radical
$ONOO^-$	Peroxynitrite
PAGE	Poly-acrylamide gel electrophoresis
Panther	Protein analysis through evolutionary relationships
PBMC	Peripheral blood mononuclear cell
PBS	Phosphate buffered saline
PCR	Polymerase chain reaction
PE	Phycoerythrin
pH	Negative 10-base logarithm of the positive hydrogen ion concentration
PHA	Phytohemagglutinin
PMSF	Phenylmethanesulfonyl fluoride

Abbreviations

PVDF	Polyvinylidene fluoride
qPCR	Quantitative polymerase chain reaction
Redox	Oxidation-reduction
RIPA	Radioimmunoprecipitation assay
RLP	Ribosomal protein L
RMA	Robust Multichip Average
RNA	Ribonucleic acid
RNase	Ribonuclease
RNS	Reactive nitrogen species
RONS	Reactive oxygen and nitrogen species
ROS	Reactive oxygen species
ROONO	Alkyl peroxynitrites
RPMI	Roswell Park Memorial Institute
RT	Room temperature
SDS	Sodium dodecyl sulfate
sLm	Standard liters per minute
SP	Scaffold protein
SSC	Side scatter
TBS	Tris-buffered saline
TBS-T	TBS-Tween
TCR	T cell receptor
TFRC	Transferrin receptor protein
TGF	Transforming growth factor
TLR	Toll-like receptor
TMB	3,3',5,5'-Tetramethylbenzidine
TNF	Tumor necrosis factor
Tregs	Regulatory T cells
UV	Ultraviolet
VEGF	Vascular endothelial growth factor

X

1 Introduction

1.1 The immune system

The immune system of vertebrates protects the body from infectious agents by various effector cells and molecules. It is classically grouped into the innate and the adaptive immune system. The innate immunity is an unspecific host defense against pathogens immediately after infection. It consists of natural barriers e.g. skin or mucous membranes but also of phagocytic cells moving through the body searching for harmful agents [1, 2]. On the contrary, the adaptive immunity is defined as a specific immune response to pathogens, such as antibody production. Furthermore, it includes the development of an immunological memory [2, 3].

The effector cells of the immune system are also called leukocytes or white blood cells. All leukocytes descend from one hematopoietic stem cell (Figure 1.1).
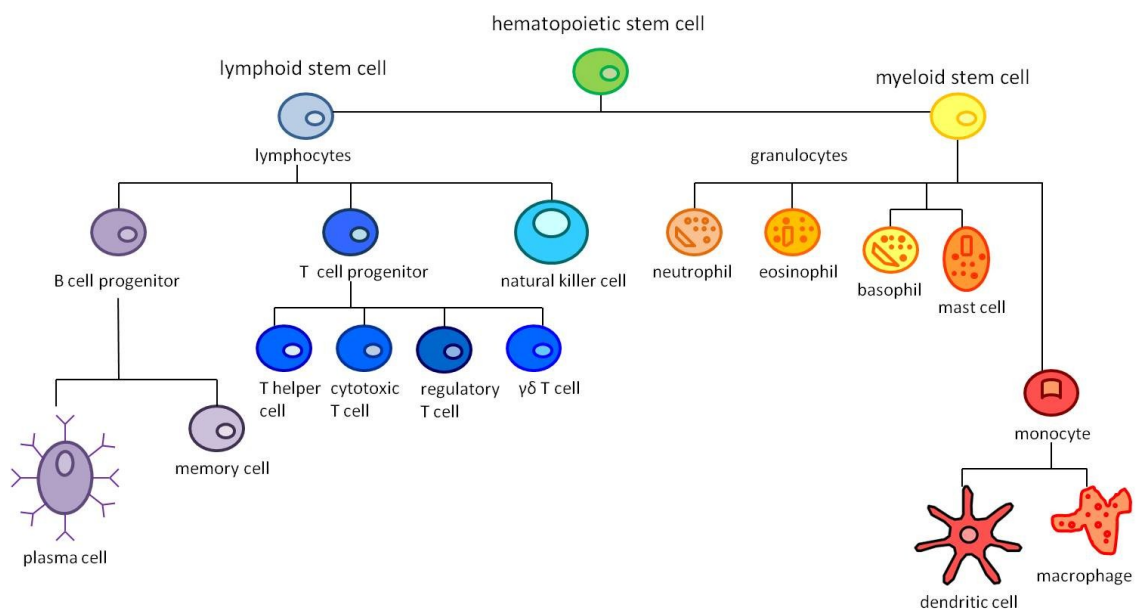
Figure 1.1: Scheme of the immune system.
All leukocytes have their origin in a hematopoietic stem cell (green) that can progress in a lymphoid stem cell (light blue) or a myeloid stem cell (yellow). Lymphoid stem cells are the progenitors of lymphocytes including B cells (plasma and memory B cells, purple), T cells (T helper, cytotoxic, regulatory or γδ T cells; dark blue) and natural killer cells (turquoise). Myeloid stem cells can differentiate into granulocytes (neutrophil, eosinophil, basophil or mast cell; orange) or monocytes, the precursor of dendritic cells and macrophages (all red). Image adapted from [4].

Introduction

This pluripotent hematopoietic stem cell can either develop in lymphoid or myeloid direction. Lymphoid stem cells develop into B-, T- and natural killer cells. In contrast, myeloid stem cells give rise to either granulocytes or monocytes that are able to further differentiate into dendritic cells and macrophages [2, 5, 6].

1.1.1 T cells

T cells derive from lymphoid stem cells and are leukocytes of the adaptive immune system. Naïve T cells are mature T lymphocytes that have not encountered foreign substances (antigens) yet and circulate through the blood or lymphatic vessels searching for foreign substances. Therefore, they express T cell receptors (TCRs) on their surface, which interact with high affinity to molecules of the major histocompatibility complex (MHC) expressed ubiquitously on vertebrate cells. Next to TCRs, the majority of T lymphocytes express one of the CD (cluster of differentiation) cell surface proteins, either CD4 or CD8 that are also of importance for the interaction with target cells [7, 8].

One distinguishes at least four groups of T cells by their CD or TCR, namely T helper cells, cytotoxic T cells, regulatory T cells and γδ T cells. CD4$^+$ T helper cells are activated through dendritic cells that are specialized in capturing, processing and presenting antigens to naïve T cells. Here, the TCR as well as the CD4 molecule of the T helper cell interact with MHC class II (MHC II) molecule of the dendritic cell surface. Activated T helper cells then proliferate and migrate to the site of antigen presence. There, they produce various cytokines amongst others interleukin-4 (IL-4), IL-5 or interferon γ (IFNγ). These cytokines are toxic for target cells or stimulate other T cell effector functions and B cells to produce antigen-specific antibodies or activate inflammatory mechanisms. Another main T cell population are cytotoxic T cells that are CD8$^+$ and known to lyse infected or malignant autologous cells bearing a pathogenic antigen on MHC I molecules. MHC I molecules are expressed ubiquitously on the cell surface of vertebrates and present proteins produced inside the cell.

Regulatory T cells (Tregs) are mainly CD4$^+$ effector T cells, which are responsible for the maintenance of self-tolerance and regulation of immunity to various nonself-antigens [7, 9, 10]. All T cells mentioned above express αβTCRs, which have a very diverse antigen repertoire. In contrast, the small population of γδ T cells expresses γδTCR, which is less heterogenic. These T cells are known to be involved in skin inflammation [7, 11]. Commercially available are many cell lines for different T cell types. One widely used CD4$^+$ T helper cell line is the Jurkat cell line that was derived from peripheral blood cells of a 14 year old ALL (acute lymphoblastic leukemia) patient [12].

1.1.2 Monocytes

Monocytes originate from myeloid stem cells and are effector cells of the innate immune system. They are short living leukocytes, circulating through the blood from 1 to 3 days. Monocytes belong to peripheral blood mononuclear cells (PBMC) and next to neutrophils and macrophages to the mononuclear phagocytic system [13-15]. Phagocytes are able to engulf cell debris and pathogens that invaded the body. Thus, they have pattern-recognition receptors including the Toll-like receptors (TLRs). These TLRs recognize bacterial products and other pathogen-related molecules. In association with regulatory surface proteins pathogen recognition and receptor-mediated endocytosis can be enhanced. One such regulator for TLR4 is CD14, which is required for endocytosis of lipopolysaccharides (LPS) – components of gram negative bacteria. This leads to activation of TLR signaling pathways and subsequently production of inflammatory cytokines e.g. IL-6 [16-18].

Monocytes are not only important for the innate but also for the adaptive immunity, since they are able to invade tissue to differentiate into macrophages and dendritic cells [18, 19]. Monocytes as well as macrophages are known to produce reactive nitrogen species (RNS) like nitric oxide radical (NO$^•$) and reactive oxygen species (ROS) including hydrogen peroxide (H$_2$O$_2$) to destroy phagocytized bacteria. Hence, they are also major players in the wound healing process due to their local action [20-23]. There are also different monocyte cell

lines commonly used as monocyte models. One example is the cell line THP-1 that is derived from the peripheral blood of a 1 year old boy with AML (acute monocytic leukemia) [24].

1.2 Wound healing

Wound healing requires the interplay of various cell types, growth factors, cytokines and extracellular matrix (ECM) components [25]. Here, not only skin but also immune cells are involved [26].

1.2.1 The acute wound healing procedure

The process of acute wound healing consists of different but overlapping phases – hemostasis, inflammation, proliferation and remodeling [27, 28]. Immediately after the skin and blood vessels are damaged, hemostasis is initiated, which lasts up to 30 min. Throughout this phase, blood vessels constrict and clot formation takes place to stop the bleeding. Platelets that are embedded in cross-linked fibrin fibers form the clot to temporarily protect the wound. Platelets of this clot also provide pro-inflammatory cytokines and growth factors to attract phagocytic immune cells [29]. Here, IL-8, VEGF (vascular endothelial growth factor) and TGFβ (transforming growth factor β) belong to the main chemoattractants [30]. During inflammation phase that occurs up to 3 days (Figure 1.2), first neutrophils and subsequently monocytes are recruited from the circulating blood to the wound bed via diapedesis [23, 31]. Neutrophils are able to secrete pro-inflammatory cytokines including IL-6 or tumor necrosis factor α (TNFα) [30]. Next to bacterial products like LPS, these mediators induce the differentiation from monocytes to M1 macrophages. M1 macrophages display antimicrobial activities e.g. secretion of the inflammatory mediators NO$^•$ and IL-6 [23]. Furthermore, neutrophils as well as M1 macrophages are able to engulf and remove foreign particles, microbes and cell debris via phagocytosis [15]. Subsequently, the proliferation- or granulation phase is initiated that lasts up to 2 weeks [31]. During this stage, the vascular network is restored, which is called angiogenesis. Furthermore, skin cells like

keratinocytes and fibroblasts migrate and proliferate at the wound edge to form granulation tissue [30]. Moreover, M1 macrophages convert to M2 macrophages, which are crucial for tissue regeneration, since they contribute to the resolution of inflammation and are known to be involved in angiogenesis [23, 32]. Additionally, re-epithelialization is initiated, in which the wound is closed. Cytokines released during re-epithelialization attract keratinocytes and fibroblasts, which contribute to wound closure. During the remodeling phase that can last up to several weeks, granulation of the tissue is stopped and a scar is formed. This is stimulated by various cytokines released by T helper cells including IL-2, TNFα, IL-4 and IL-10 [27, 31, 33].
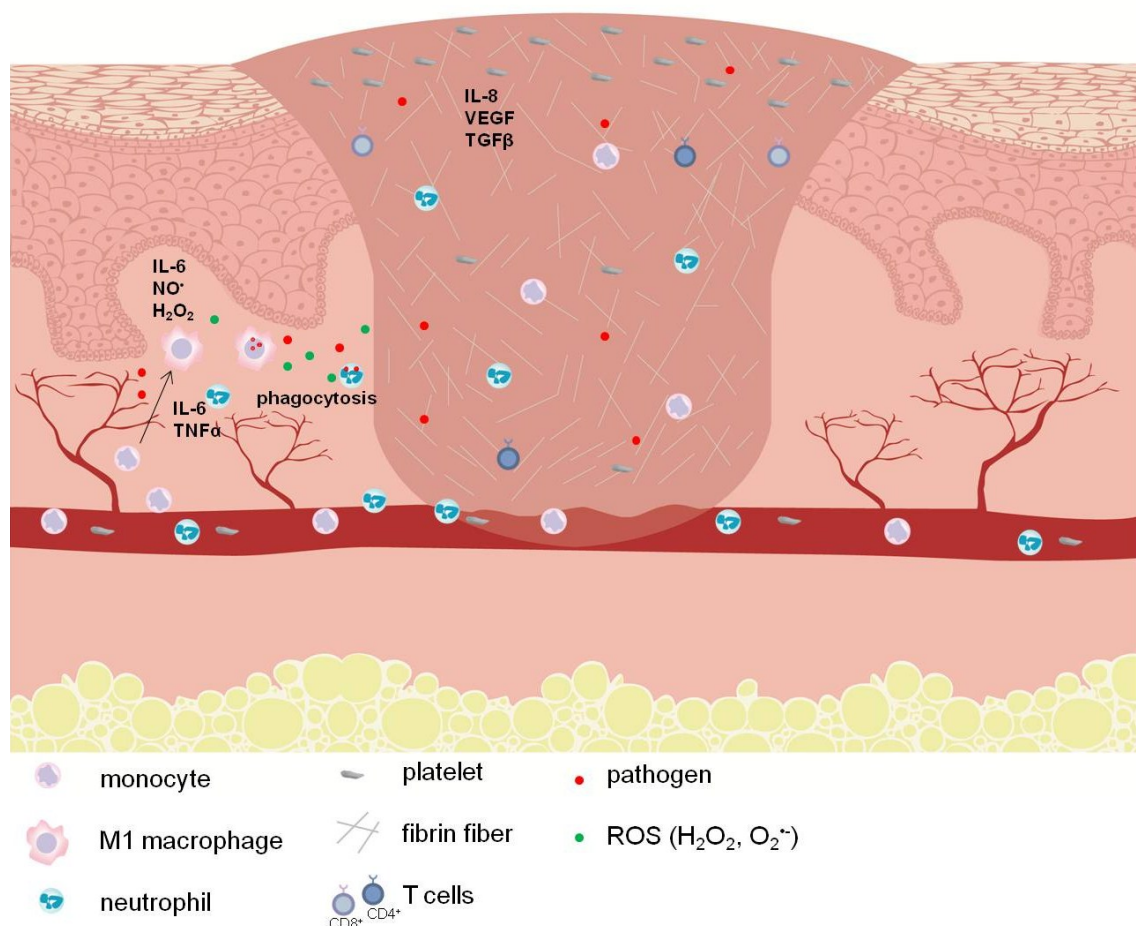
Figure 1.2: The inflammatory phase of wound healing.
During inflammation phase, neutrophils as well as monocytes invade the wound bed due to chemoattractants released by platelets (e.g. IL-8, VEGF or TGFß). Monocytes differentiate to M1 macrophages in response to immune-modulatory molecules including LPS or IL-6 and TNFα, secreted from neutrophils. Subsequently, M1 macrophages and neutrophils phagocytize infiltrating pathogens and cell debris and produce pro-inflammatory cytokines (IL-6 and TNFα) and anti-microbial molecules (NO$^{\bullet}$, H_2O_2). Image courtesy of INP Greifswald.

Introduction

1.2.2 Chronic wounds

While a normal wound is usually healed within 4 weeks, chronic wounds remain open. Chronic wounds exhibit a disturbed wound healing process and remain in a persistent state of inflammation. Because wound healing is a complex process, defects in the different stages are not uncommon, whereas inflammation and proliferation phase are mostly affected [27, 31].

Figure 1.3 displays a chronic wound including its involved cells and molecules. One main characteristic of chronic wounds is the enormous infiltration of neutrophils and M1 macrophages. They are the major sources for pro-inflammatory cytokines and growth factors. Amongst others, enhanced levels of TNFα, IL-1β, IL-6 and TGFβ have been found in chronic wound fluids. Next to cells of the wound edge (keratinocytes, fibroblasts and endothelial cells), these leukocytes are additionally responsible for the generation or up-regulated activity of proteases. For instance, metalloproteinases have been found in chronic wound fluids but are absent in acute wound fluids [27, 31]. Enhanced catalytic activity results in the degradation of growth factors and structural proteins necessary for the repair. Moreover, a pro-oxidant microenvironment has been found to be associated with chronic wounds. This can be explained with the release of ROS e.g. $O_2^{\bullet-}$, H_2O_2 into the wound fluid due to leukocytes, mainly neutrophils. Next to the direct tissue damage, ROS is known to provoke the activation of signaling pathways leading to production of pro-inflammatory cytokines and proteases [27]. However, the RNS $NO^{\bullet}$ was found to be reduced in chronic wound environments [34]. In contrast to $CD8^+$ T cells, $CD4^+$ T cells have been shown to be decreased in chronic wounds in comparison with healing wounds [35]. Next to venous insufficiency a main characteristic of chronic wounds is the presence of bacteria that grow in matrix enclosed biofilms [36-38]. Bacterial components may additionally contribute to impaired wound repair or attenuation of inflammatory response due to interference with the cell-matrix interactions or by promoting the inflammatory response [27].

6
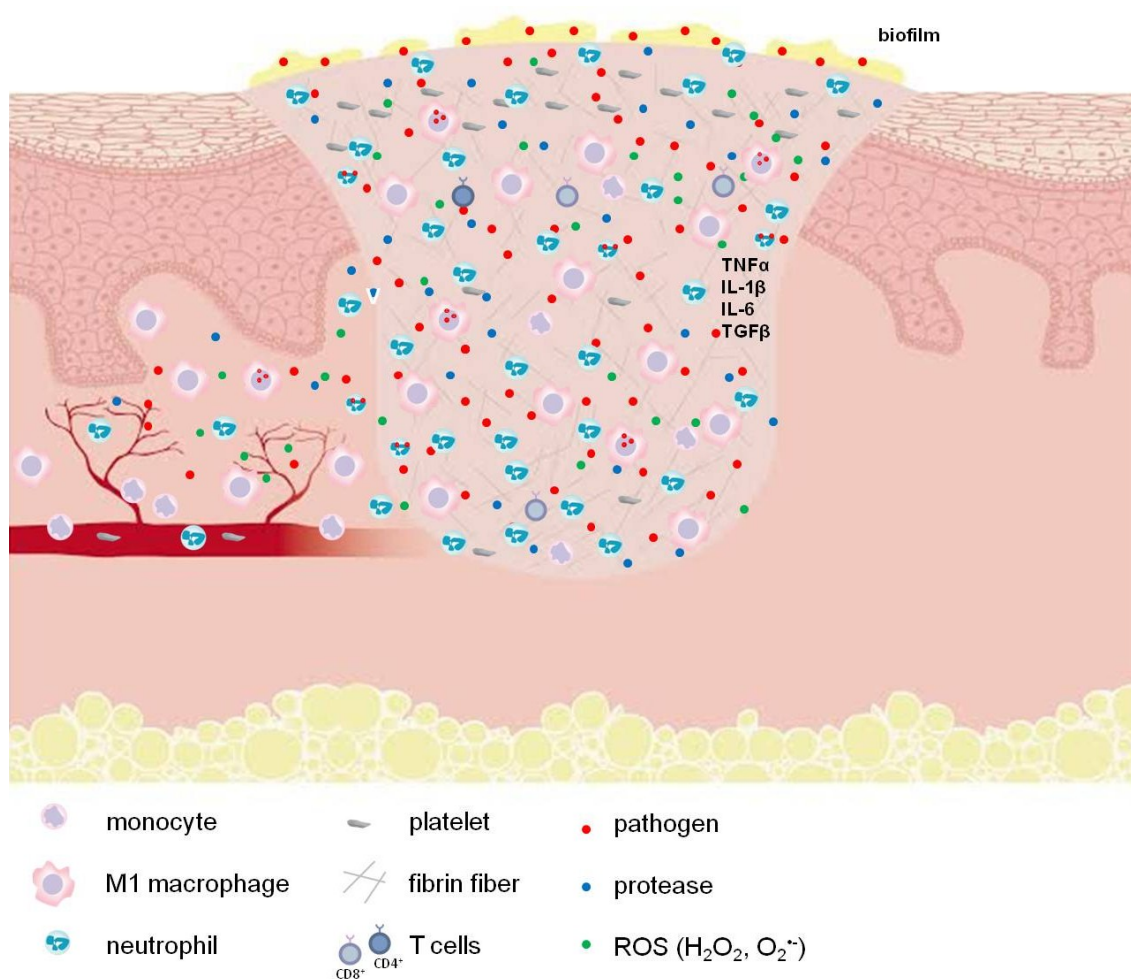
Figure 1.3: Scheme of a chronic wound.
Chronic wounds are usually characterized by an enormous amount of bacteria that are also responsible for biofilm generation at external part of the wound. There is an immense infiltration of neutrophils and M1 macrophages, which produce a huge amount of pro-inflammatory cytokines like TNFα, IL-1β, IL-6 and TGFß. They are also producing proteases and ROS (H_2O_2 and $O_2^{\bullet-}$) that are responsible for a pro-oxidant milieu. Additionally, the CD4$^+$/ CD8$^+$ ratio of T cells is lower as in healing wounds. Some chronic wounds reveal disturbed blood supply. Image courtesy of INP Greifswald.

Dependent on the kind of chronic wound there are also intrinsic factors that contribute to impaired wound healing [31]. For instance hyperglycemia provokes permanent irritation of the vascular wall in diabetic patients [39]. Another example is an increased hydrostatic pressure that is associated with venous diseases [27].

However, the etiology of chronic wounds is poorly understood. That is the reason why healing mechanisms of chronic wounds are subject of current investigations [40, 41].

Introduction

Chronic, non-healing wounds are a huge factor with financial respect to the healthcare sector, since about 1 – 2 % of the population of industrial countries is affected. However, healing of chronic wounds is still enormously challenging for clinicians since effective therapies are urgently needed. Thus, promising treatment strategies are sought for [42, 43].

1.3 Cell signaling

Cell signaling is defined as the stimulation or inhibition process of cells in response to signaling mediators, which are mainly extracellular signaling molecules e.g. cytokines, growth factors or chemicals. A receptor protein at the cell surface is activated by binding of a signal molecule. Subsequently, a chain of reactions transmits the signal inside the cell by induction of one or more intracellular signaling pathways. A signaling pathway usually consists of several intracellular signaling proteins that process the signal inside the cell and distribute it to the appropriate target. These targets are mainly effector proteins, which are then altered through the signaling pathway and can be amongst others metabolic enzymes, gene transcription factors or cytoskeleton proteins [44, 45].

1.3.1 Canonical MAPK signaling

One example of signaling pathways are the mitogen-activated protein kinases (MAPKs), which are serine/ threonine kinases ubiquitously expressed in eukaryotes. All MAPKs are induced by a distinct kinase cascade, in which upstream kinases activate the MAPKs through dual phosphorylation of threonine and tyrosine residues within a conserved tripeptide motif [46]. They play essential roles in cell fate decisions, whether a cell is going to die or will survive [47]. There are three canonical MAPK signal transduction pathways (Figure 1.4).
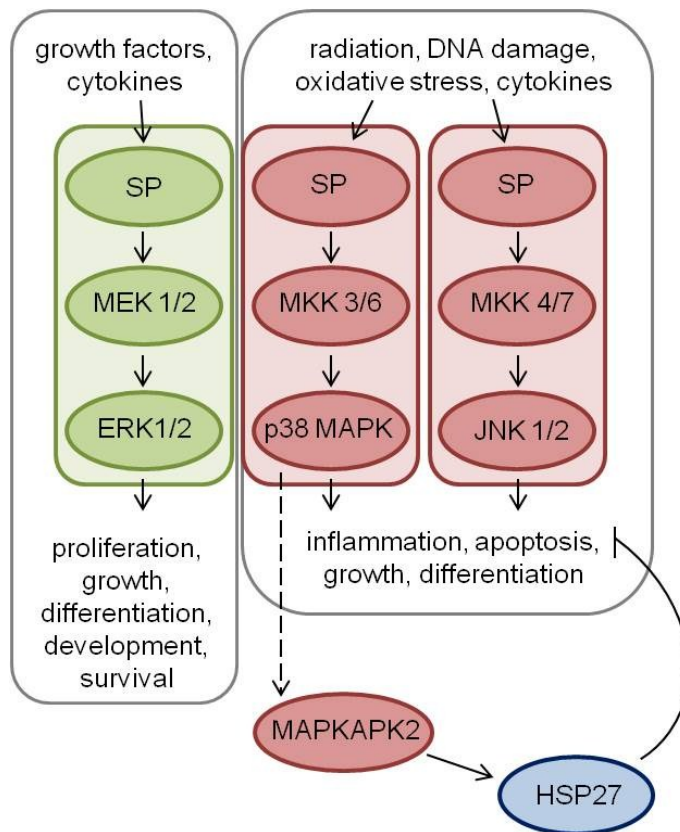
Figure 1.4: Schematic illustration of the canonical MAPK signaling pathways.
Scaffold proteins (SP) are various kinases that are upstream of the MAP kinases, which are activated through extracellular signaling molecules. On the one hand, the MEK-ERK signaling pathway is induced by growth factors and cytokines and leads to proliferation, growth, differentiation, development or survival. On the other hand radiation, DNA damage, oxidative stress or cytokines are inducers of p38 MAPK or JNK 1/2 via MKKs (mitogen-activated protein kinase kinases) that also belong to the SPs. Activated p38 MAPK can result in activation of MAPKAPK2 and subsequently in induction of the apoptosis inhibitor HSP27. Image adapted from [48].

The kinase ERK 1/2 (extracellular signal-regulated kinase 1/2) and its upstream regulator MEK 1/2 (MAPK/ ERK kinase 1/2) are mainly induced by growth factors or cytokines. This MEK-ERK pathway is involved in cell growth, differentiation, proliferation as well as development. It additionally functions as survival-promoting factor in response to cell stress and death [49-51]. In contrast, JNK 1/2 (c-Jun N-terminal kinase 1/2) and p38 MAPK are usually activated by stress signals like radiation, DNA damage, oxidative stress and cytokines. Induction of these pathways mainly leads to initiation of inflammation and later on to apoptosis, the programmed cell death. However, they are also able to activate growth and differentiation [46, 52, 53]. Heat shock protein 27 (HSP27), a chaperone protein, is known to refold denatured proteins and to stabilize the actin cytoskeleton in order to inhibit death receptor mediated apoptosis [50, 54-56]. HSP27 can be activated by the MAPK-activated protein

kinase-2 (MAPKAPK2), which itself can become induced by p38 MAPK signaling [50, 57, 58].

1.3.2 MAPK signaling involved in wound healing

Various studies evidence the involvement of the MAPK cascades in wound regeneration [59, 60]. In monocytes, all three canonical MAPK pathways are activated through the bacterial endotoxin LPS [61-63]. Furthermore, MAPKs are of importance during initiation of inflammation, amongst others in the regulation of different inflammatory cytokines. The JNK pathway has been reported to be essential for the IL-8 and IL-6 gene expression. Additionally, ERK 1/2 is known to weakly activate the gene transcription of IL-8. An active p38 MAPK pathway was shown to stabilize the mRNAs (messenger ribonucleic acids) of both IL-8 and IL-6. Furthermore, impaired expression of p38 MAPK and ERK 1/2 was associated with down-regulation of IL-6 secretion [48, 64-66]. IL-8 is an important mediator for wound healing since it is one major chemoattractant for neutrophils. Next to IL-8, IL-6 is essential for wound repair, e.g. stimulation of skin cell proliferation or regulation of immune responses [30, 48, 67]. The better the understanding of wound healing processes, the better is the change to contribute. One promising tool to enable wound regeneration processes is non-thermal plasma.

1.4 Physical plasma

Next to solid, liquid and gaseous state, physical plasma is referred to as the fourth state of matter (Figure 1.5). In the solid phase (first state of matter), the atoms are arranged in a fixed crystalline lattice. When sufficient energy is applied to a solid, the lattice structure is broken apart and a liquid (second state of matter) is formed. In this phase, intermolecular bonds between free moving atoms and molecules are formed. If enough energy is transferred to a liquid, atoms vaporize and the gaseous phase (third state of matter) is reached, where atoms are independently moving. Plasma is generated by the input of sufficient energy (beams, thermal or electric field energy) to the gas that atoms collide

with each other and knock their electrons off. It is defined as an ionized gas with quasineutral characteristics [68, 69]. Plasma has a complex composition. It consists of ions, electrons, exited and neutral atoms, free radicals (ROS and RNS), ultraviolet (UV), thermal and infra-red radiation, electric fields and molecules [70, 71].

| solid | liquid | gas | plasma |
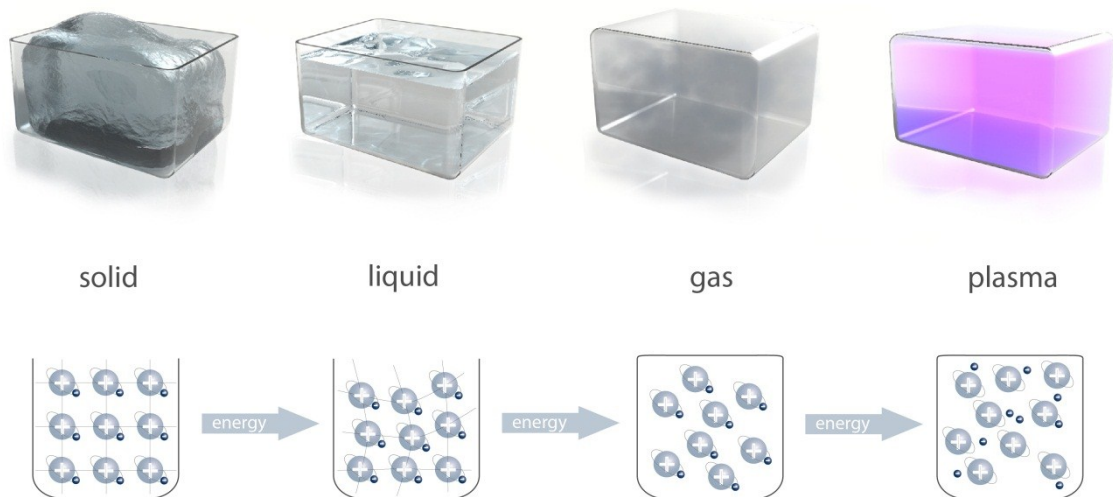
Figure 1.5: Generation of physical plasma.
Plasma consists of ionized gas and is known to be the fourth state of matter. It can be generated by energy transfer from the solid matter, over the liquid and the gaseous phase. Image courtesy of INP Greifswald.

1.4.1 Thermal plasma

Although it is not obvious at first side, we are surrounded by plasma. Remarkably, about 99 % of the visible universe consists of plasma matter, for instance the sun, polar lights or lightening. These natural plasmas exhibit temperatures up to 10^7 Kelvin (K) and are called thermal plasmas. Moreover, they consist of almost completely ionized particles and are in or nearby the thermal equilibrium. Next to natural plasmas, plasmas can be artificially generated, which can be found in fluorescent lamps or plasma displays [68, 72]. Recently many new plasma sources were emerged to make plasma applicable to living tissue. Therefore, it needed to exhibit lower temperatures and work at atmospheric pressure. Hence, non-thermal atmospheric pressure plasma was created [73].

Introduction

1.4.2 Non-thermal plasma

In contrast to thermal plasma, non-thermal plasma is characterized by a low degree of ionization (around 1 %). Its reaction mixture is far from thermal equilibrium. Hot free electrons ($T_e \geq 10^4$ K) are responsible for the initiation of chemical conversions. However, they are surrounded by gas with relative low temperatures ($T_g \leq 10^3$ K) [74]. Thus, lower energy levels are transferred to the ions, molecules and atoms of the plasma leading to a relative low total plasma temperature of a few hundred K [75]. An essential advantage for the industrial utilization of non-thermal plasmas is the minimization of the thermal stress of treated interfaces, which allows using heat-sensitive materials [74].

Non-thermal plasma reactors are often operated under low pressure conditions. However, this requires the installation of an expensive vacuum technique and limits the introduction of plasma processes in technical lines. Therefore, during the last decades, non-thermal plasma sources have been developed that work under atmospheric pressure [74]. There are different kinds of non-thermal atmospheric pressure plasma sources, namely barrier discharges (BDs), plasma jets, and corona discharges. In this study, the atmospheric pressure plasma jet kinpen 09 (neoplas GmbH), displayed in Figure 1.6, has been used. The kinpen 09 contains a centered pin-type electrode, located in a ceramic capillary, and a grounded ring electrode. The plasma that is generated from the top of the centered electrode expands to the surrounding air outside the nozzle as an effluent. It can be utilized with a variety of gases including nitrogen, oxygen, argon or admixtures [73]. In this study the inert gas argon was used as carrier gas. So far, different active components have been identified to be produced by the reaction of the effluent with the surrounding air for this setup. Amongst others ozone (O_3) and nitric oxide radical ($NO^\bullet$) were found in the plasma effluent of the kinpen 09, which belong to the reactive oxygen species and nitrogen species (RONS) of biological importance [76-78]. This device is of great usage to generate and transport RONS specifically and timely defined to the desired place. With special focus at wound healing, plasma jets like the

12

kinpen 09 hold the capacity to penetrate into bodily parts with complex geometries and cavities [73].
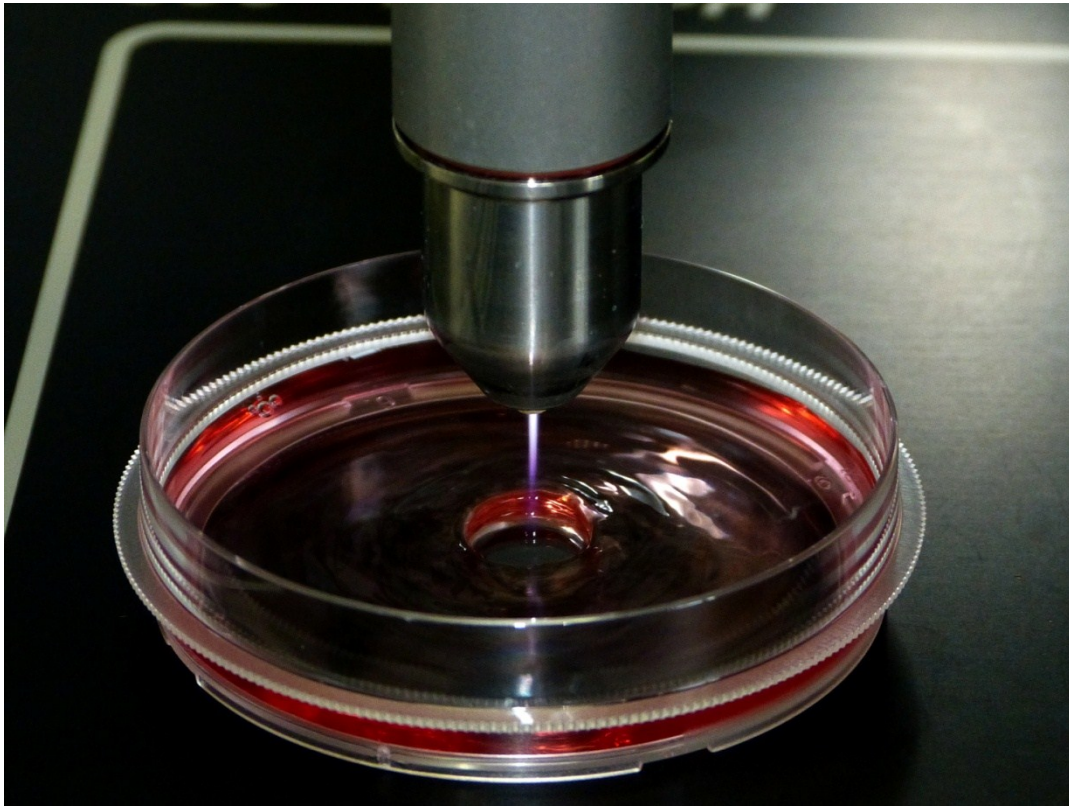
Figure 1.6: Photograph of the kinpen 09 treating cell culture medium in a Petri dish.
Non-thermal plasma treatment of cell culture medium in a 60 mm Petri dish with the jet kinpen 09. Image courtesy of Dr. Kristian Wende.

1.5 Plasma medicine

Non-thermal atmospheric pressure plasma has drawn more and more attention worldwide in the biomedical sector over the last two decades. Next to temperatures below those inducing thermal cell damage it is characterized by its unique composition including free radicals, excited and neutral species, ions, electrons, electric fields, ultraviolet, thermal and infra-red radiation [70, 71]. Especially RONS are of importance in oxidation-reduction (redox) biology. Some of the main important RONS for biochemical processes are summarized in Table 1.1. In addition to the involvement of these molecules in diseases (e.g. type 2 diabetes or cancer) they are essential anti-microbial key players in immune reactions, mainly synthesized by phagocytes like neutrophils,

monocytes and macrophages. Especially, hydrogen peroxide (H_2O_2) and nitric oxide radical ($NO^\bullet$) produced during respiratory burst of phagocytes are important effector molecules, which play key roles in the inflammation phase of wound healing [78-80].

Table 1.1: Biological essential RONS.

Reactive oxygen species		Reactive nitrogen species	
Radical	**Non-radical**	**Radical**	**Non-radical**
Superoxide anion $O_2^{\bullet-}$	Ozone O_3	Nitric oxide radical $NO^\bullet$	Nitrous acid HNO_2
Hydroxyl radical $OH^\bullet$	Singlet oxygen $^1O_2$	Nitrogen dioxide radical $NO_2^\bullet$	Nitrosyl cation NO^+
Hydroperoxyl radical $HO_2^\bullet$	Hydrogen peroxide H_2O_2		Nitrosyl anion NO^-
Carbonate radical anion $CO_3^{\bullet-}$			Alkyl peroxynitrites $ROONO$
			Peroxynitrite $ONOO^-$

List adapted from [78, 81].

Thus, it is not surprising that RONS are already used for wound treatment. H_2O_2 is commonly utilized to disinfect wounds due to its broad anti-microbial activities [50, 82]. Application of $NO^\bullet$ through semi-permeable membranes has been recently discovered to promote wound healing through vasodilatory and anti-microbial effects [83]. Not only RONS but also other plasma components are utilized for dermatological application. Amongst others, UV radiation is used in phototherapy to treat skin diseases by inducing ongoing cellular regeneration. Plasma has the benefit that it combines all these active principles [50, 84]. In future, variation of plasma components might lead to tailored plasma adapted to specific skin diseases [85].

So far, several studies have evidenced that non-thermal plasma exhibits anti-bacterial effects [86, 87]. Consequently, there are various applications in medicine, e.g. decontamination of heat sensitive endoscopes or ablation of dental biofilms [48, 88, 89]. Additionally, it was proven that non-thermal plasma application is able to sterilize human tissue [90]. First trials even revealed that its application on chronic wounds is able to reduce the bacterial load significantly [91].

Besides, non-thermal plasma is able to inhibit cell growth of eukaryotic cells, which can be beneficial for cancer treatment [92]. However, it also has potentially stimulating impacts on mammalian cells [93-95]. Additionally, first studies showed that gene transcription and secretion of wound-healing related cytokines were induced by plasma-treated skin cells. In particular, Barton *et al.* discovered the plasma-induced gene expression and secretion of IL-6, GM-CSF (granulocyte macrophage colony-stimulating factor) and VEGF-A in keratinocytes, while Arndt *et al.* enlightened the increased gene transcription of IL-6, IL-8 and TGFβ in fibroblasts [96, 97]. Some studies already evidenced positive effects of non-thermal plasma on human blood coagulation and wound repair [50, 90, 98, 99]. Thus, non-thermal plasma treatment seems to be a promising tool regarding chronic wound care management, whereas effective therapies are urgently needed. However, future plasma applications require thorough examination of plasma-cell interactions ensuring safety and reliability of devices in advance of its clinical use [100].

So far, the impact of plasma on wound healing properties has been studied mainly for skin cells. Although immune cells provide a considerable contribution in wound healing and removal of pathogens, they have been widely neglected in plasma research until now [23, 50, 101]. First studies investigated leukocyte survival after non-thermal plasma treatment. Bekeschus *et al.* revealed decreased viability and proliferation capacity of human peripheral blood mononuclear cells, while Haertel *et al.* showed distinct sensitivities of different rat lymphocyte subpopulations towards plasma treatment. Moreover, Shi *et al.* demonstrated that plasma induced apoptosis in human peripheral blood lymphocytes [50, 102-104].

1.6 Aim of the study

Very little is known about the immune-modulatory effects of non-thermal atmospheric pressure plasma. Therefore, the aim of this thesis was the investigation of non-thermal plasma-treated (kinpen 09) *in vitro* cultured immune cells, in particular CD4$^+$ T helper cells and monocytes. Next to the human cell lines Jurkat (CD4$^+$ T cells) and THP-1 (monocytes), human primary peripheral blood cells were isolated, plasma treated and examined. In order to get deeper insights in the underlying mechanisms of plasma-cell interactions, investigations followed gene expression, protein activation and protein secretion. Those studies should help to identify key molecules regulated by non-thermal plasma, in order to modify cellular reactions by plasma.

To distinguish different plasma sensitivities of the examined cell types, first cell survival studies (growth curves) as well as flow cytometric apoptosis assays were performed. Subsequently, plasma-modulated gene activities were identified by unbiased genome-wide gene expression analysis using DNA microarrays. Specific non-thermal plasma induced target genes were further validated using quantitative PCR. In addition, plasma-modulated activation of MAPK signaling, which was shown to be related to the examined target genes, was studied by western blot analysis. Finally, this research aimed to study the inflammatory cytokine production in response to non-thermal plasma treatment either by ELISA or intracellular flow cytometry.

2   Material and Methods

If not indicated differently, all cell culture ingredients were purchased from Lonza, cell isolation components from Miltenyi Biotec, while chemicals were obtained from Sigma-Aldrich.

2.1   Cell culture

Next to the monocyte cell line THP-1 and the CD4$^+$ T helper cell line Jurkat, the according primary cells that were isolated from human buffy coat were used for this study as described in the following part.

2.1.1   Culture of the cell lines THP-1 and Jurkat[x]

For this study, the CD4$^+$ T helper cell line Jurkat and the monocyte cell line THP-1 were used as models for CD4$^+$ T helper cells and monocytes, respectively. The Jurkat cell line was retrieved from DSMZ (German Collection of Microorganisms and Cell Cultures), while the monocyte cell line THP-1 was obtained from CLS (Cell Lines Service GmbH).

Both cell lines were cultured in RPMI (Roswell Park Memorial Institute) 1640 medium supplemented with 8 % (Jurkat) or 10 % (THP-1) fetal calf serum (FCS), 2 mM L-glutamine, 0.1 mg/mL streptomycin and 100 U/mL penicillin at 37°C, 95 % relative humidity and 5 % CO_2. Every second or third day, both cell lines were passaged, whereas they were seeded with an initial density of 0.5×10^6 (Jurkat cells) or 0.2×10^6 cells/mL (THP-1 cells). Cell counting was performed by trypan blue (0.2 %; Roche) staining using a Cedex XS Cell counting System (Roche).

---

[x] this section is partly adapted from Bundscherer *et al.* [50]

Material and Methods

2.1.2 Isolation and cultivation of human primary monocytes[x]

Human buffy coats, derived from healthy blood donors, were kindly provided by the Institute of Transfusion Medicine from the University of Greifswald. After dilution with three volumes of 1 × PBS (phosphate buffered saline), 35 mL of this buffy coat sample was subjected to density gradient centrifugation (400 × g, 30 min, 4°C) on 15 mL Lymphocyte Separation Medium 1077 (density 1.077 g/ml, PAA Laboratories GmbH). Subsequently, peripheral blood mononuclear cells (PBMCs) were retrieved from the interphase and washed three times with 1 × PBS (300 × g, 10 min, 4°C). Remaining erythrocytes were lysed with 1 × Red Blood Cell Lysis Buffer (Biolegend) for 5 min, which was followed by one washing step (300 × g, 10 min, 4°C). Cell counting was performed with trypan blue staining in a Neubauer chamber (Carl Roth). Subsequently, untouched monocytes were isolated with the Pan Monocyte Isolation Kit ($CD14^{++}/CD16^{-}$, $CD14^{+}/CD16^{++}$ and $CD14^{++}$, $CD16^{+}$ monocytes; for the annexin V/ 7AAD assay) or Monocyte Isolation Kit II ($CD14^{+}$ monocytes; for the MAPK and cytokine analysis) by negative selection according to the manufacturer´s instructions (Miltenyi Biotec) as described below for up to 10^7 cells. The cell pellet was resuspended in 30 µL buffer (autoMACS Running Buffer) and mixed with 10 µL FcR Blocking Reagent and 10 µL Biotin-Antibody Cocktail. After an incubation time of 10 min at 4°C, 30 µL of buffer and 20 µL Anti-Biotin MicroBeads were admixed, followed by an incubation step at 4°C for 15 min. Subsequently, cells were washed with 1 mL added buffer at 300 × g for 10 min. After removing the supernatant, up to 10^8 cells were resuspended in 500 µL buffer. The cells were then filtered through Pre-Separation Filters (30 µm) and applied to the pre-equilibrated magnetic column. The cell suspension passing through was collected. Then, the column was washed three times with 3 mL buffer. The entire effluent, which passed through the column, consisted of the enriched untouched monocytes. Retained cells, which were composed of magnetically labeled non-monocytes, were eluted in 5 mL buffer outside the magnetic field. The monocyte purity was analyzed by flow cytometry

---

[x] this section is partly adapted from Bundscherer *et al.* [100]

18

(part 2.4.2), whereas the assessed monocyte purity was greater than 80 % for all experiments.

In cooperation, Sander Bekeschus isolated primary $CD4^+$ T helper cells by positive selection according to the manufacturer´s instructions (Stem Cell Technology) for investigation of plasma-mediated apoptosis (annexin V/ 7AAD assay). The T helper cell purity was greater than 85 % (data not shown) as evaluated by staining with specific fluorochrome-conjugated CD4 antibodies and flow cytometry measurements (part 2.4.2).

Both, primary $CD14^+$ monocytes as well as primary $CD4^+$ T lymphocytes were cultivated in cell culture medium as described in part 2.1.1 (supplemented with 10 % FCS).

2.2 Plasma treatment[x]

18 h before plasma treatment, cell culture medium was pre-incubated at a CO_2-incubator to ensure a stable pH value and an optimal temperature of the medium during plasma exposure. Non-thermal plasma treatment was performed with the atmospheric pressure jet kinpen 09 (neoplas GmbH), based on the setup of Weltmann *et al.* in 2009 [105]. Noteworthy, the quartz capillary was replaced by a ceramic one. Plasma was generated under atmospheric pressure, while a voltage of 2 – 6 kV_{pp} and a frequency of around 1 MHz were applied. The kinpen 09 was operated with argon (purity of 99.999 %). The gas flow rate was 3 sLm (standard liters per minute) as controlled by a mass flow controller (MKS Instruments). To reduce the strong effect of feed gas humidity on the cells [106], stainless steel tubing was used in the setup. The kinpen 09 was fixed at a computer controlled xyz table that was conducting meander-shaped movements (Figure 2.1) over the liquid surface of a cell culture medium

---

[x] this section is partly adapted from Bundscherer *et al.* [48]

filled 60 mm dish to ensure equal distribution of the plasma-generated species in the liquid.

Figure 2.1: Moving track of the kinpen 09.
5 mL cell culture medium in a 60 mm dish was plasma-treated with the jet along the meander-shaped track by a computer controlled xyz table. Image courtesy of ZIK *plasmatis*, INP Greifswald.

Plasma treatment of the investigated cells was performed indirectly, meaning 5 mL of culture medium was plasma treated in a 60 mm dish for a distinct time and then added to 1×10^6 cells. Immediately after treatment, appropriate volumes of sterile distilled cell culture water were added to the culture medium to compensate molarity changes caused by evaporation during plasma exposure. Besides the plasma treatment, cells were incubated in medium, which was left untreated (0 s). Simultaneously, different positive controls were conducted dependent on the experiment and cell type. To induce proliferation, monocytes (THP-1 cells and primary cells) were incubated with medium containing 1 µg/mL LPS, while CD4$^+$ Jurkat T helper cells were cultivated with medium including 1 µg/mL phytohemagglutinin (PHA, Biochrom). In contrast, apoptosis was activated by treatment with medium including 100 µM H_2O_2 or 10 µM etoposide (Eto, Axxora). Subsequently, cells were incubated at 37°C, 95 % relative humidity and 5 % CO_2 for indicated time periods.

2.3 Gene expression analysis

To examine the plasma-modulated gene transcription in the immune cells, genome-wide gene expression analyses were performed by DNA microarray. Only the cell lines Jurkat and THP-1 were used for these studies. The primary cells were also tried but they contained not enough RNA for this isolation

method. Subsequently, distinct target genes were validated by quantitative PCR. The following sections describe these methods.

2.3.1 RNA isolation

RNA isolation was done with RNA micro Kit from Bio & Sell. All steps were performed at room temperature (RT) according to the manufacturer´s instruction. Briefly, 400 µL lysis buffer SM was added to each cell pellet from up to 4×10^6 cells. After an incubation time of 2 min, cells were completely resuspended in lysis buffer SM by roughly pipetting. This was followed by a further incubation step of 3 min. The lysed sample was transferred onto a centrifugation column D, which was placed in a 2.0 mL collection tube. Then, it was centrifuged at 10,000 × g for 2 min and 400 µL 70 % ethanol (Carl Roth) were admixed to the filtrate. Subsequently, a centrifugation column R was placed in a new 2.0 mL collection tube, on which the sample solution was pipetted. After another centrifugation step at 10,000 × g for 2 min, the centrifugation column R was transferred to a new 2.0 mL collection tube. DNase (deoxyribonuclease) digestion was performed with 40 µL RNase (ribonuclease) free DNase (Qiagen) for 15 min. This was followed by two washing steps of the column. First, 500 µL wash buffer JT was added to the column, which then was subjected to 10,000 × g for 1 min. Centrifugation column R was then placed onto a new 2.0 mL collection tube. Second, 700 µL wash buffer MT was pipetted on the column and then spun down at 10,000 × g for 1 min. Centrifugation column R was placed onto a new 2.0 mL collection tube, which then was dried at 10,000 × g for 3 min. Subsequently, centrifugation column R was transferred to a 1.5 mL elution tube and 30 µL RNase free water was applied to the column. Elution of the RNA took place at 6,000 × g for 1 min. RNA was frozen at -80°C until further use.

2.3.2 cDNA transcription

After thawing the RNA samples their concentration was determined by a NanoDrop 2000c Spectrophotometer (Thermo Scientific). Then, mRNA

(messenger ribonucleic acid) was transcribed into first strand cDNA (complementary DNA) by Transcriptor First Strand cDNA Synthesis Kit from Roche. To do so, 1 µg total RNA was mixed with 2.5 µM (1 µL) Anchored-oligo(dT)$_{18}$ Primer and PCR-grade water up to a volume of 13 µL in a nuclease-free PCR tube. Denaturation of the template-primer mixture took place at 65°C for 10 min in a thermocycler (T Professional Thermocycler, Biometra). Immediately after the denaturation step, samples were cooled on ice. Then, 7 µL transcription master mix (Table 2.1) were admixed to a final sample volume of 20 µL. Samples were incubated in a thermocycler for 45 min at 55°C. Subsequently, Transcriptor Reverse Transcriptase was inactivated at 85°C for 5 min. Then, samples were frozen at -20°C until further examination.

Table 2.1: Composition of transcription master mix per sample.

Volume [µL]	Reagent	Concentration/ Molarity
4.0	Transcriptor Reverse Transcriptase Reaction Buffer	5 × conc.
0.5	Protector RNase Inhibitor	40 U/µL
2.0	Deoxynucleotide Mix	10 mM
0.5	Transcriptor Reverse Transcriptase	20 U/µL
7.0	**Total**	

2.3.3 DNA microarray

For DNA microarray analysis, RNA samples of four independent experiments were pooled for each condition before transcription into first strand cDNA (part 2.3.1 and 2.3.2). DNA microarray analysis was performed with NimbleGen 4-plex arrays (4×72K), with 24,000 different human gene-specific probes per slide, from Roche NimbleGen with the provided substances.

Second Strand cDNA Synthesis

After thawing, first strand cDNA of two independent experiments were pooled to a final volume of 40 µL (in total n = 8). Then 38.4 µL cDNA was admixed to 11.6 µL second strand cDNA master mix on ice (Table 2.2).

Table 2.2: Second strand master mix.

Volume [µL]	Reagent	Concentration/ Molarity
9.0	Second Strand Buffer	5 × conc.
0.9	dNTPs	10 mM
0.3	DNA Ligase	10 U/µL
1.1	DNA Polymerase	10 U/µL
0.3	RNase H	2 U/µL
11.6	**Total**	

This reaction mix was incubated at 16°C for 2 h in a thermocycler. Subsequently, 0.7 µL T4 DNA polymerase (5 U/µL) was added to each reaction and incubated for additional 5 min at 16°C. The reaction was stopped by placing the tubes on ice and admixture of 3.3 µL EDTA (0.5 M).

cDNA precipitation

After addition of 5.4 µL ammonium acetate (7.5 M) to each sample, it was mixed by repeated inversion. First, 2.3 µL glycogen (5 mg/mL) and subsequently 120 µL of ice-cold absolute ethanol were admixed by repeated inversion. Samples were centrifuged at 12,000 × g for 20 min at 4°C. Then, supernatant was aspirated and the pellet was resuspended in 200 µL ice-cold 80 % ethanol by repeated inversion. This was followed by a centrifugation step at 12,000 × g for 5 min at 4°C. After removing the supernatant, the pellet was again resuspended in 200 µL ice-cold 80 % ethanol and spun down at 12,000 × g for 5 min at 4°C. The supernatant was aspirated and the pellet dried in a vacuum centrifuge. The pellet was rehydrated in 20 µL nuclease-free water. Quantification of cDNA took place with a NanoDrop 2000c Spectrophotometer.

Sample labeling

First, Random Primer Buffer was established by admixing of 1,100 µL Random Primer Buffer to 2 µL β-mercaptoethanol. The Cy3 (Cyanine 3) Random Nonamers were diluted in 1,050 µL Random Primer Buffer. A 40 µL aliquot of this mixture was then added to 1 µg precipitated cDNA, which was filled up to 80 µL with nuclease-free water. Heat denaturation took place at 98°C for 10 min

followed by a quick-chill in an ice-water bath for 2 min. Afterwards, 20 µL deoxyribonucleotide triphosphate (dNTP)/ Klenow master mix was assembled on ice (Table 2.3.), added to each sample (final volume 100 µL) and mixed by pipetting up and down.

Table 2.3: dNTP/ Klenow master mix composition.

Volume [µL]	Reagent	Concentration/ Molarity
10.0	dNTP Mix	10 mM
8.0	Nuclease-free water	
2.0	Klenow Fragment (3´ → 5´ exo)	500 U/µL
20.0	**Total**	

Subsequently, samples were incubated at 37°C for 2 h in a thermocycler. The reaction was stopped by addition of 21.5 µL Stop Solution. After vortexing, the entire content was admixed to 110 µL isopropanol in a 1.5 mL tube and incubated for 10 min in the dark at RT. Samples were centrifuged at 12,000 × g for 10 min and the supernatant was removed. Then, sample pellets were rinsed with 500 µL 80 % ice-cold ethanol each and centrifuged for 12,000 × g for 2 min. After aspirating the supernatant, Cy3-labeled cDNA samples were dried in a vacuum centrifuge and rehydrated in 25 µL nuclease-free water. Samples were vortexed for 30 s. This step was repeated until the pellet was completely rehydrated. Concentration of cDNA was quantified using a NanoDrop 2000c Spectrophotometer. The appropriate volume of 4 µg Cy3-labeled cDNA was aliquoted in 1.5 mL tubes for each sample. Subsequently, samples were dried in a vacuum centrifuge.

Hybridization

3 h before hybridization, the hybridization system was set at 42°C. Each dried cDNA sample was resuspended in 3.3 µL Sample Tracking Control, whereas each sample to be hybridized to a 4×72K array was rehydrated in a unique Sample Tracking Control. This was followed by a vortexing step. Then, the hybridization solution master mix was prepared as depicted in Table 2.4, which was sufficient for all four arrays of one slide.

Table 2.4: Hybridization solution master mix composition.

Volume [µL]	Reagent	Concentration/ Molarity
29.5	Hybridization Buffer	2 × conc.
11.8	Hybridization Component A	
1.2	Alignment Oligo	
42.5	**Total**	

Each sample was admixed to 8.7 µL hybridization solution master mix to a final volume of 12 µL. After vortexing, samples were incubated at 95°C for 5 min. Samples were placed at 42°C (hybridization system) for 5 min and vortexed. Mixers were prepared as described in the manufacturer´s instructions (NimbleGen Roche). Then, 8 µL of one sample was applied into the filling port of each array. All fill and vent ports were covered with one mixer multi-port seal and the slides were placed into the Hybridization System. Subsequently, the Mixing Panel of the Hybridization System was turned on and the mixing procedure was started. Sample hybridization took place at 42°C for 20 h.

Washing

This was followed by three washing steps. Therefore, 27 mL of Wash I, II and III (all 10 × conc.) was admixed to 27 mL DTT solution and 216 mL nuclease-free water. Wash I was pre-heated to 42°C, while Wash II and III were used at RT. After applying the mixer-slide assembly to Wash I solution, the mixer was removed with a mixer-slide disassembly tool. The slide was agitated gently for 2 min in Wash I and then transferred to Wash II. Here, it was washed for 1 min with vigorous, constant agitation. After that it was placed inside Wash III for 15 s and washed as described before. Then, slides were removed from Wash II and spin-dried for 2 min.

Array Scanning and Analysis

After washing, microarray slides were scanned using a MS 200 Microarray Scanner and the appropriate MS 200 Data Collection Software according to the manufacturer´s instructions. Image generation and quality analysis were done with NimbleScan Software v2.6 with a resolution of 2 µm. Here, sample tracking

analysis and generation of metrics reports were performed of background-corrected signal intensities. Furthermore, Robust Multichip Average (RMA) analyses were done with quantile normalization [107, 108]. Subsequently, data were further processed using Patek Genomics Suite, in which gene lists were generated with at least two-fold regulated (p ≤ 0.05) genes in plasma-treated samples compared with untreated control. These genes were clustered in a heatmap format according to their fold change values. Ingenuity System Pathway Analysis (IPA) software provided the pathways involved in plasma-mediated regulation. Next to IPA, gene ontology (GO) analysis was done with Panther (Protein analysis through evolutionary relationships) classification system.

2.3.4 Quantitative polymerase chain reaction

Quantification of gene expression was performed by quantitative polymerase chain reaction (qPCR) with the RealTime ready Catalog Assay kit (Roche). All steps of preparation took place on ice. Thawed cDNA samples were diluted 1:20 with nuclease-free water to a concentration of 2.5 ng/µL. Then, qPCR mix was prepared as summarized in Table 2.5. Used primers are displayed in Table 2.6. 15 µL qPCR mix were admixed to 5 µL cDNA sample to a final volume of 20 µL in each well of a LightCycler 480 Multiwell Plate (Roche). Subsequently, the Multiwell Plate was sealed with a LightCycler Sealing Foil and centrifuged for 2 min at 15,000 × g at 4°C. Immediately, the plate was transferred into a LightCycler 480 II Instrument (Roche) and the qPCR program (Table 2.7) was started.

Table 2.5: Composition of qPCR mix per sample.

Volume [µL]	Reagent	Concentration/ Molarity
4.0	Nuclease-free water	-
10.0	LightCycler 480 Probes Master	2 × conc.
1.0	Real time ready Assay Primers	160 pmol each; 20 × conc.
15.0	**Total**	

Table 2.6: Real Time Ready Single Assay primers.

Gene	Organism	Manufacturer	Assay ID	Catalogue number
FOS	*H. sapiens*	Roche	100917	05532957001
JUN	*H. sapiens*	Roche	111353	05532957001
JUND	*H. sapiens*	Roche	111353	05532957001
IL-8	*H. sapiens*	Roche	103136	05532957001
HMOX1	*H. sapiens*	Roche	110977	05532957001
RLP13A	*H. sapiens*	Roche	102119	05532957001
TFRC	*H. sapiens*	Roche	102422	05532957001
ACTB	*H. sapiens*	Roche	143636	05532957001

Table 2.7: Light Cycler program for real time ready qPCRs.

Program	Cycles		Analysis Mode
Pre-Incubation	1.0		None
Amplification	45.0		Quantification
Cooling	1.0		None
Temperatur [°C]	**Acquisition Mode**	**Hold [hh:mm:ss]**	**Ramp Rate [°C/s]**
Pre-Incubation			
95	None	00:10:00	4.4
Amplification			
95	None	00:00:10	4.4
60	None	00:00:30	2.2
72	Single	00:00:01	4.4
Cooling			
40	None	00:00:30	2.2

2.4 Protein analysis

Besides genomic alterations, plasma-mediated changes of the cellular protein activation or production level were under investigation in this study. Hence, western blot analyses, flow cytometry measurements and ELISA assays were performed with plasma-treated cells as described in the following parts.

2.4.1 Western blot[x]

MAPK signaling was analyzed by western blot with the cell lines Jurkat and THP-1 as well as primary monocytes. Due to technical reasons primary CD4^{+} T helper cells were not included. To examine the proliferative MEK-ERK

---

[x] this section is partly adapted from Bundscherer *et al.* [48, 50]

signaling pathway, cells were lysed 15 min after plasma treatment, while the apoptotic cascades p38 MAPK and JNK 1/2 were studied 3 h after plasma exposure.

Sample preparation

Suspension cells were collected in falcon tubes while adherent cells (primary monocytes) were washed once with 1 × PBS and then trypsinized for 5 min. Then, suspension and adherent cells were recombined and rinsed once with 1 × PBS at 230 × g for 5 min. Subsequently, cell lysis took place in 150 µL ice-cold RIPA (radioimmunoprecipitation assay) buffer (Table 2.8) containing one tablet of protease as well as phosphatase inhibitors (cOmplete Mini and phosSTOP, Roche) per 10 mL and freshly added 2 mM phenylmethanesulfonyl fluoride (PMSF, Carl Roth). To ensure complete cell lysis, cells were kept on ice for 30 min, while vortexing every 10 min, which was followed by a sonication step (Labsonic M, Satorius AG). Samples were then centrifuged at 10,000 × g for 5 min at 4°C. Supernatants containing the cellular proteins were collected and the protein concentration was determined with the DC^{TM} Protein Assay (Bio-Rad Laboratories GmbH).

Table 2.8: Composition of RIPA buffer.

Reagent	Concentration/ Molarity
PBS (without Ca^{2+}/ Mg^{2+})	1 × conc.
Igepal CA-630 substance	1 %
sodium deoxycholate	0.5 %
SDS (Carl Roth)	0.1 %
EDTA	20 mM

SDS PAGE

Protein concentration of all samples was adjusted and proteins were subsequently denatured in 1 × sample buffer (Table 2.9) at 95°C for 5 min. Then, samples and a protein size-marker (PageRuler^{TM} Prestained Protein Ladder, Fermentas) were subjected to SDS-PAGE (sodium dodecyl sulfate

poly-acrylamide gel electrophoresis) on precast 10 % PAGE gels (Anamed Gelelektrophorese GmbH), while a constant voltage of 125 V was applied.

Table 2.9: Composition of 1 × sample buffer.

Reagent	Concentration/ Molarity
tris (Carl Roth)	0.25 M, pH 6.8
SDS	2 %
glycerol (Carl Roth)	10 %
β-mercaptoethanol	2 %
bromophenol blue	0.004 %

Western blotting and detection

The blotting step onto Roti-PVDF membranes (Carl Roth) took place with a Trans-Blot Turbo^{TM} (Bio-Rad Laboratories GmbH) according to the manufacturer´s instructions (30 min at 25 V, up to 1.0 A). Subsequently, unspecific binding was blocked with 5 % nonfat milk powder (Premier Foods Marvel) in tris-buffered saline Tween 20 (TBS-T, Table 2.10) for 30 min. After this, the membrane was incubated with the corresponding primary phospho-specific antibody 1:1,000 (Table 2.11; all from Cell Signaling) in TBS-T at 4°C over night. Incubation was followed by three washing steps with TBS-T and incubation with horseradish peroxidase-coupled secondary antibodies 1:10,000 (Table 2.12; all from Jackson ImmunoResearch) for 1 h at room temperature. After three washing steps in TBS-T, membranes were incubated with the chemiluminescence detection reagent Serva Light Polaris (Serva Electrophoresis GmbH) and imaged using the ImageQuantLAS4000 (GE Healthcare). Subsequently, the membrane-bound antibodies were stripped off the membranes. Therefore, the membranes were incubated in stripping buffer (Table 2.13) for 25 min at 70°C. Then, they were reprobed with antibodies directed against the corresponding total protein. This stripping procedure was repeated and membranes were incubated with β-Actin antibodies that served as a loading control (Table 2.11). Band intensities were quantified using ImageQuantTL Software (GE Healthcare) and normalized by dividing band intensities of phospho-proteins by those of the total protein using Excel.

Material and Methods

Table 2.10: Composition of TBS-T (pH 7.6).

Reagent	Concentration/ Molarity
Tris	20 mM
NaCl (Carl Roth)	13.7 mM
Tween (Carl Roth)	0.1 %

Table 2.11: Primary antibodies for western blotting.

Target	Molecular mass of target [kDa]	Phosphorylation site	Host organism	Product number
β-Actin	45	-	Rabbit	4970
ERK 1/2	42/ 44	-	Rabbit	9102
HSP27	27	-	Mouse	2402
JNK 1/2	46/ 55	-	Rabbit	9258
MEK 1/2	45	-	Rabbit	9126
p38 MAPK	43	-	Rabbit	9212
Phospho-ERK 1/2	42/ 44	T202/ Y204	Rabbit	4370
Phospho-HSP27	27	S78	Rabbit	2405
Phospho-JNK 1/2	46/ 54	T183/ Y185	Rabbit	4668
Phospho-MEK 1/2	45	S217/ S221	Rabbit	9154
Phospho-p38 MAPK	43	T180/ Y182	Mouse	9216

Table 2.12: Secondary antibodies for western blotting.

Target	Host organism	Product number
Mouse IgG	Goat	115-035-174
Rabbit IgG	Mouse	211-032-171

Table 2.13: Composition of stripping buffer (pH 6.7).

Reagent	Concentration/ Molarity
tris	62.5 mM
SDS	1 %
β-mercaptoethanol	111 mM

2.4.2 Flow cytometry

Flow cytometry analysis was performed using a Gallios^{TM} flow cytometer and data were analyzed by Kaluza 1.2 and FlowJo 7.6.5 software.

Determination of primary cell purity

Immediately after isolation of primary monocytes or CD4$^+$ T helper cells as described in part 2.1.2, the purity of these cells was examined by flow cytometry (in cooperation with S. Bekeschus). First, 1×10^6 cells were resuspended in

70 µL buffer (autoMACS Running Buffer) and treated with 10 µL FcR blocking reagent. After an incubation step of 10 min at 4°C, the specific antibodies were added. Monocytes were admixed to 10 µL FITC (fluorescein isothiocyanat)-conjugated CD14 and 10 µL APC (allophycocyanin)-labeled biotin antibodies, while CD4$^+$ T helper cells were stained with 10 µL APC-conjugated CD4 antibodies. Simultaneously, staining with the according isotype antibodies were used as controls for unspecific binding (Table 2.14). Staining took place for 10 min at 4°C in the dark. Subsequently, two washing steps were performed with 1 mL buffer at 300 × g for 10 min at 4°C. Each pellet was resuspended in 300 µL buffer and measured by flow cytometry.

Table 2.14: Flow cytometric antibodies used for purity determination.

Marker	Fluorochrome	Antibody class	Manufacturer	Catalogue number
CD14	FITC	IgG2a	Miltenyi Biotec	130-080-701
Biotin	APC	IgG1	Miltenyi Biotec	130-090865
CD4	APC	IgG2a	Miltenyi Biotec	130-092-374
Isotype	FITC	IgG2a	Miltenyi Biotec	130-098-877
Isotype	APC	IgG1	Miltenyi Biotec	130-092-214
Isotype	APC	IgG2a	Miltenyi Biotec	130-091-836

Annexin V/ 7AAD staining[x]

The annexin V/ 7AAD apoptosis assay was performed with the cell lines Jurkat and THP-1 as well as primary CD4$^+$ T helper cells and monocytes. For the determination of early and late apoptosis, cells were harvested 12 h after plasma or H$_2$O$_2$ treatment, and 0.5 × 10^6 cells were stained with 1 µL of the apoptosis marker annexin V (1 µg/µL, FITC-conjugated, Enzo Life Sciences) in 300 µL annexin V binding buffer (AVBB; Table 2.15) for 10 min in the dark at RT. Cells were washed once with 0.5 mL AVBB at 1,000 × g for 5 min and resuspended in 300 µL of AVBB. Late apoptotic or necrotic cells were stained with 1 µL 7-aminoactinomycin (7AAD; eBioscience) for 5 min at RT.

---

[x] this section is partly adapted from Bundscherer *et al.* [100]

Material and Methods

Subsequently, the percentage of early (annexin V positive/ 7AAD negative) and late (annexin V and 7AAD double positive) apoptotic cells was measured by flow cytometry.

Table 2.15: Composition of annexin V binding buffer.

Reagent	Molarity
HEPES/ NaOH	10 mM, pH 7.4
NaCl	140 mM
CaCl$_2$	2.5 mM

Caspase 3 staining[x]

After an incubation time of 18 h after plasma treatment at 37°C, Jurkat, THP-1 cells and primary monocytes were analyzed by flow cytometry in respect to their caspase 3 activation level to determine the amount of cells undergoing late apoptosis. After cell harvesting, the absolute cell number of THP-1 and Jurkat cells was determined. Subsequently, activated caspase 3 cells were stained with Green Caspase-3 Staining Kit (PromoCell) according to the manufacturer´s instructions. First, 0.3×10^6 cells were resuspended in 300 µL cell culture medium and admixed to 1 µL FITC-DEVD-FMK, a dye detecting activated caspase 3. Staining of the cells took place for 30 min in the dark at 37°C incubator with 5 % CO$_2$. Cells were washed twice with 0.5 mL Wash Buffer at 1,000 × g. Each pellet was resuspended in 300 µL Wash Buffer and caspase 3 activation was measured by flow cytometry.

Intracellular cytokine staining[xx]

Immediately after plasma treatment 4 µL BD GolgiStop™ (BD Biosciences) was added to each primary monocyte sample to inhibit cytokine release into the cell culture medium and to accumulate them inside the cells. Intracellular detection

---

[x] this section is partly adapted from Bundscherer *et al.* [50]

[xx] this section is partly adapted from Bundscherer *et al.* [48]

of IL-8 and IL-6 production was determined 6 h after plasma treatment. Therefore, monocytes were harvested as described in part 2.4.1. Then, cells were permeabilized with the BD Cytofix/Cytoperm™ Kit (BD Biosciences). First, each cell pellet was resuspended in 100 µL 1 × BD Perm/Wash™ buffer, admixed to 250 µL of the Fixation/Permeabilization solution and incubated for 20 min at 4°C. This was followed by two washing steps with 1 mL 1 × BD Perm/Wash™ buffer at 1,000 × g for 5 min at 4°C. Then, permeabilized cells were resuspended in 50 µL 1 × BD Perm/Wash™ buffer and 10 µL of each fluorochrome-conjugated cytokine antibodies or the according isotype antibodies (Table 2.16) were added. After an incubation step for 30 min at 4°C in the dark, cells were washed twice (1,000 × g, 5 min, 4°C) with 1 mL 1 × BD Perm/Wash™ buffer. Cell pellets were resuspended in 300 µL buffer and analyzed by flow cytometry regarding their intracellular cytokine expression levels.

Table 2.16: Flow cytometric antibodies used for intracellular cytokine staining.

Marker	Fluorochrome	Antibody class	Manufacturer	Catalogue number
IL-8	APC	IgG1	Biolegend	511410
IL-6	PE (phycoerythrin)	IgG1	Biologend	501106
Isotype	APC	IgG1	Miltenyi Biotec	130-093-189
Isotype	PE	IgG1	BD Pharmingen	550617

2.4.3 Enzyme-linked immunosorbent assay (ELISA)

Next to intracellular cytokine staining, cytokine concentrations of the cell supernatants were determined by enzyme-linked immunosorbent assay (ELISA) after different incubation times after plasma exposure with Jurkat, THP-1, primary monocytes and co-cultured THP-1 and HaCaT cells. Therefore, cells were harvested and spun down at 230 × g for 5 min. Supernatants were collected and frozen at -80°C until further investigation.

After thawing the cell supernatants, ELISA was performed with different ELISA kits, listed in Table 2.17. Human Inflammatory Cytokines Multi-Analyte

Material and Methods

ELISArray Kit (Qiagen) is able to detect following cytokines in one assay: IL-1α, IL-1β, IL-2, IL-4, IL-6, IL-8, IL-10, IL-12, IL-17A, IFNγ, TNFα and GM-CSF.

Table 2.17: ELISA kits used for cytokine detection.

ELISA kit	Manufacturer	Catalogue number
Human Inflammatory Cytokines Multi-Analyte ELISArray Kit	Qiagen	MEH-004A
IL-22 ELISA Ready-SET-Go! (human)	eBioscience	88-7522-88
TGF β ELISA Ready-SET-Go! (human)	eBioscience	88-8350-88
Human IL-6 ELISA MAX™ Deluxe	Biolegend	430504
Human IL-8 ELISA MAX™ Deluxe	Biolegend	431504
LEGEND MAX™ Human IL-8	Biolegend	431507
LEGEND MAX™ Human GM-CSF	Biolegend	432007
LEGEND MAX™ Human TNFα	Biolegend	430207

All kits used in this study were performed according to the manufacturer´s instructions and are sandwich ELISAs. In the following the Max^{TM} Deluxe ELISA set of Biolegend is described in detail.

Each well of a 96-well plate was coated with 100 µL Capture Antibody solution and incubated over night at 4°C. The next day the plate was washed four times with 300 µL Wash Buffer per well. Afterwards, non-specific binding was blocked with 200 µL 1 × Assay Diluent A per well and incubated for 1 h at RT, while shaking. In the meantime, two independent standard dilutions were assembled: 1,000 µL of the top standard (e.g. 1,000 pg/mL for IL-8) was prepared from the stock solution and followed by six-fold serial dilutions with 1 × Assay Diluent A in separate tubes. 1 × Assay Diluent A served as zero standard (0 pg/mL). If necessary, samples were diluted with appropriate volumes of 1 × Assay Diluent A. Incubation of the 96-well plate was followed by four wash steps as described above. Then 100 µL of each standard or sample was applied to each well and incubated for 2 h at RT while shaking. In this step, cytokines in the standard or sample bind to the corresponding Capture Antibody. Next, each well was washed four times with 300 µL Wash Buffer. Subsequently, 100 µL of cytokine-specific biotinylated Detection Antibody solution was pipetted in each well and incubated for 1 h at RT with shaking. After four washing steps (300 µL Wash Buffer/ well), 100 µL of HRP-conjugated Avidin was added to each well. Incubation took place for 30 min at RT while shaking, followed by five washing

steps (300 µL Wash Buffer/ well), whereas Wash buffer was incubated for 1 min to each well. 100 µL TMB (3,3',5,5'-Tetramethylbenzidine) of the Substrate Solution C was added to each well and incubated for 15 min in the dark. Reaction was stopped by applying 100 µL Stop Solution (2 N sulfuric acid, Carl Roth) to each well. Absorbance was determined with a plate reader (Infinite M200 PRO, Tecan) at 450 nm and the reference at 570 nm. The conducted standard curve was used to calculate cytokine concentrations of the samples.

2.5 Statistics[x]

Data obtained were illustrated using Prism 6.0 (GraphPad software). One-way analysis of variances (ANOVA) and Dunnett´s post hoc-test were used to calculate statistical significance of the samples referring to the negative untreated control. Means of three independent experiments were plotted as bar graphs with error bars, which represent standard deviation. For the comparison of cell lines to primary cells (annexin V/ 7AAD staining) Two-way ANOVA and Holm-Sidak´s post hoc-test were used to calculate statistical significance. Here, the mean of three independent experiments per cell line was compared with samples from three individual donors. Bars and error bars represent mean and range of duplicates per donor and triplicates of the cell lines, respectively. Statistical analysis of Patek Genomics Suite was performed with One-way ANOVA. Statistical significance is displayed in the following way: $p < 0.05$ (*), $p < 0.01$ (**), $p < 0.001$ (***).

---

[x] this section is partly adapted from publications of Bundscherer *et al.* [50, 100]

3 Results

3.1 Cell growth of Jurkat and THP-1 cells after plasma treatment

To estimate the impact of plasma treatment on cell proliferation, growth curves were performed with the Jurkat and THP-1 cell lines for a time span of 144 h (6 days) after plasma treatment. Here, every 24 h a cell sample was taken and counted. Since preliminary cell counting experiments revealed different plasma sensitivities of the investigated cells, Jurkat cells were treated from 5 s to 60 s and THP-1 cells were plasma-exposed for 30 s to 360 s.

Jurkat cells

Figure 3.1 displays the received growth behavior of the lymphocyte cell line Jurkat. Cell proliferation decreased in a plasma treatment time dependent manner – the higher the plasma exposure duration the lower the cell survival. Considerable growth retardation could be found for cells treated for 15 s, 30 s and 60 s. Cells of different plasma treatment conditions reached lower maximal cell numbers than the untreated control after an incubation time of 144 h. In contrast, cell growth behavior of 5 s exposed Jurkat cells resembled the untreated control. Incubation with 100 µM H_2O_2 resulted in significantly delayed cell growth with even higher inhibitory effects than the longest plasma exposure (60 s).
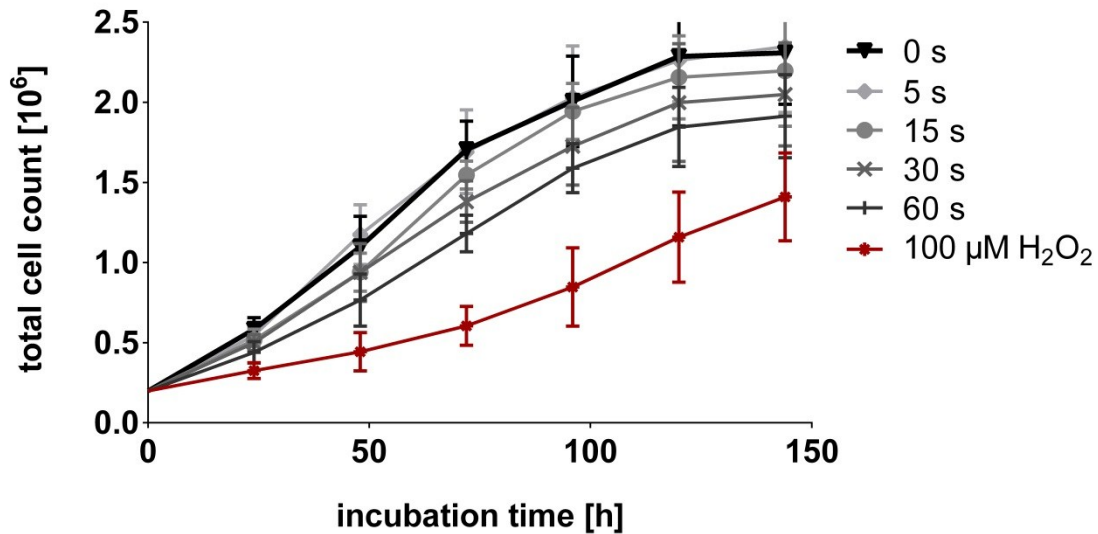
Figure 3.1: Growth curve of plasma-treated Jurkat cells.
After exposure with plasma-treated cell culture medium, total cell count was determined every 24 h until maximum incubation duration of 144 h. Untreated cells (0 s, black) and 100 µM H_2O_2 (red) were used as controls for normal and ROS influenced growth, respectively. Cell numbers and error bars plotted in the diagram are the mean and standard deviation of three independent experiments.

THP-1 cells

Figure 3.2 illustrates the growth curves of THP-1 cells after non-thermal plasma treatment. Due to the better resistance to plasma exposure longer treatment times were chosen for this monocyte cell line than for the Jurkat cell line. However, only the longest plasma exposure of 360 s revealed a delayed proliferation behavior in comparison to the untreated control. Treatment for 30 s and 60 s even seemed to enhance THP-1 cell growth since the corresponding growth curve progressions were increased compared with the control. Proliferation of the 180 s treated sample resembled the curve characteristics of the untreated control. Except the longest plasma treatment time of 360 s, no alteration in the maximum cell number after 142 h of incubation was detected. Incubation with 100 µM H_2O_2 only slightly decreased cell survival. This result is in strong contrast to Jurkat cell growth after plasma and H_2O_2 treatment.
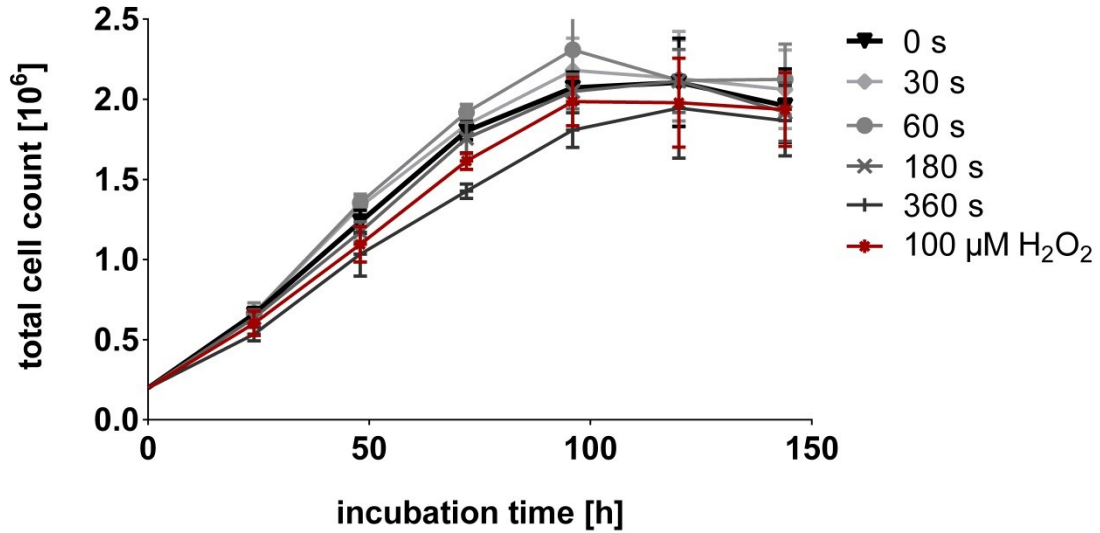
Figure 3.2: Growth curve of plasma-treated THP-1 cells.
After exposure with plasma-treated cell culture medium, total cell count was determined every 24 h until maximum incubation duration of 144 h. Untreated cells (0 s, black) and 100 μM H_2O_2 (red) were used as controls for normal and ROS influenced growth, respectively. Cell numbers and error bars plotted in the diagram are the mean and standard deviation of three independent experiments.

3.2 Apoptosis induction by plasma treatment

Apoptosis is the process of programmed cell death that can be either triggered by intrinsic stimuli due to development and aging or by extrinsic stimuli like toxins. During apoptosis, different morphological changes occur in a cell, like cell shrinkage, membrane blebbing and DNA fragmentation [109]. In early apoptotic stages cells expose phosphatidylserine on their surface to trigger their own engulfment by phagocytes [110]. This can be detected by annexin V, which binds to phosphatidylserine [111]. In contrast, late apoptotic cells that already exhibit a porous cell membrane can be stained with the DNA binding agent 7-aminoactinomycin D (7AAD) [112]. Additionally, late apoptotic cells can be detected via activation of caspase 3, a final member of the caspase cascade during apoptosis [113].

In literature, apoptosis-inducing effects of non-thermal plasma treatment have already been shown for distinct eukaryotic cell types [114, 115]. Therefore, both the early as well as the late apoptotic events were analyzed in this study regarding CD4$^+$ T helper cells and monocytes. Preliminary time course

experiments demonstrated that annexin V/ 7AAD (early/ late apoptotic marker) were maximal detected 12 h after plasma exposure, while caspase 3 (late apoptotic marker) was maximal activated after an incubation time of 18 h, in the investigated cells (data not shown). Thus, an incubation time of 12 h was chosen for the investigation of annexin V/ 7AAD staining and an incubation time of 18 h for the caspase 3 assay, respectively. First, plasma-treated primary CD4$^+$ T helper cells and monocytes were compared with their respective cell lines in an annexin V/ 7AAD assay. Thereafter, Jurkat cells, THP-1 cells and primary cells were analyzed regarding their caspase 3 activation level in response to plasma treatment.

3.2.1 Early and late apoptosis in cell lines compared with primary leucocytes[x]

In Figure 3.3 the gating strategy of the flow cytometric annexin V/ 7AAD apoptosis assay is depicted, which allows recording both early and late apoptotic cells at one time point. After gating all cells in a FSC/ SSC dot plot, they were separated by their annexin V and 7AAD staining properties. Cells that were negative for both annexin V and 7AAD (annexin V$^-$/ 7AAD$^-$) were regarded as living cells. Cells that stained positive for annexin V but negative for 7AAD (annexin V$^+$/ 7AAD$^-$) were undergoing early apoptosis. Moreover, cells positive for both annexin V and 7AAD (annexin V$^+$/ 7AAD$^+$) were already in a late apoptotic stage. In contrast to apoptotic cells, necrotic cells can be stained with 7AAD but not with the marker annexin V (annexin V$^-$/ 7AAD$^+$). Preliminary time course experiments showed that plasma treatment with the kinpen 09 induced only apoptotic processes in all investigated cells, while almost no necrotic cell could be detected (data not shown) as already described by Bekeschus *et al.* for PBMC [104]. Thus, inflammatory reactions due to necrosis could be neglected.

[x] this section is partly adapted from Bundscherer *et al.* [100]
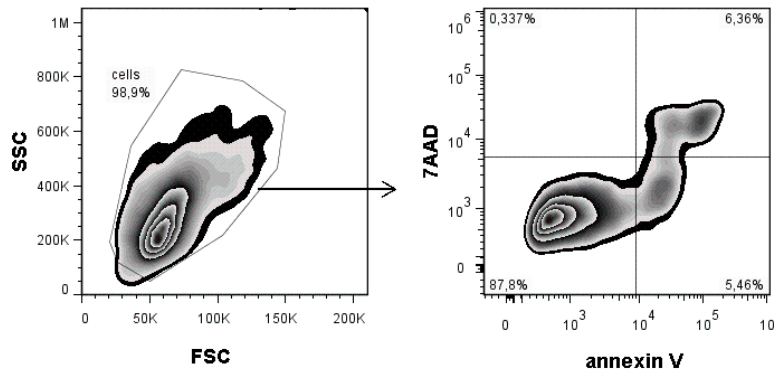
Figure 3.3: Flow cytometric gating strategy for early and late apoptotic cells.
All cells excluding cell debris were first gated in a FSC/ SSC plot and subsequently subgrouped regarding their staining ability of the apoptotic marker annexin V and the late apoptotic/ necrotic dye 7AAD. Percentage of early (annexin V$^+$/ 7AAD$^-$; bottom right quadrant) and late (annexin V$^+$/ 7AAD$^+$; top right quadrant) cells were further analyzed. No necrotic cells could be detected.

CD4$^+$ T helper cells

Figure 3.4 represents the percentages of early (Figure 3.4A) and late (Figure 3.4B) apoptotic blood CD4$^+$ T helper cells compared with the Jurkat cell line after plasma treatment. Percentages of both, early and late apoptotic CD4$^+$ T helper cells and Jurkat cells increased with prolonged plasma treatment time up to 120 s. Due to donor variations, CD4$^+$ T helper cells treated for 180 s behaved differently: While the percentage of early apoptotic cells of donor II further increased, the ones of donor I and III even dropped under the value of the cell sample treated for 120 s. In contrast to the level of late apoptotic cells of donor I and III that further increased, donor II reached a plateau. Apoptotic rates of primary CD4$^+$ T helper cells always exceeded the ones of the Jurkat cell line. Nevertheless, strong differences between the donors of the primary cells were detected. There was no significant increase of cell death after 5 s of plasma treatment for all investigated freshly isolated CD4$^+$ T helper cells compared with Jurkat cells. While early apoptosis after 15 s plasma treatment occurred significantly higher for cells of two blood donors, only one donor revealed a significant increase in late apoptotic CD4$^+$ T helper cells. Plasma treatment for 60 s and longer resulted for nearly all tested samples in a significant difference between primary CD4$^+$ T helper cells of these three donors and the Jurkat cell line (from $p < 0.05$, * to $p < 0.001$, ***). In comparison, H_2O_2 treatment of

primary CD4$^+$ T helper cells led to an increased number of early but not of late apoptotic cells compared with Jurkat cells.

(A)

(B)
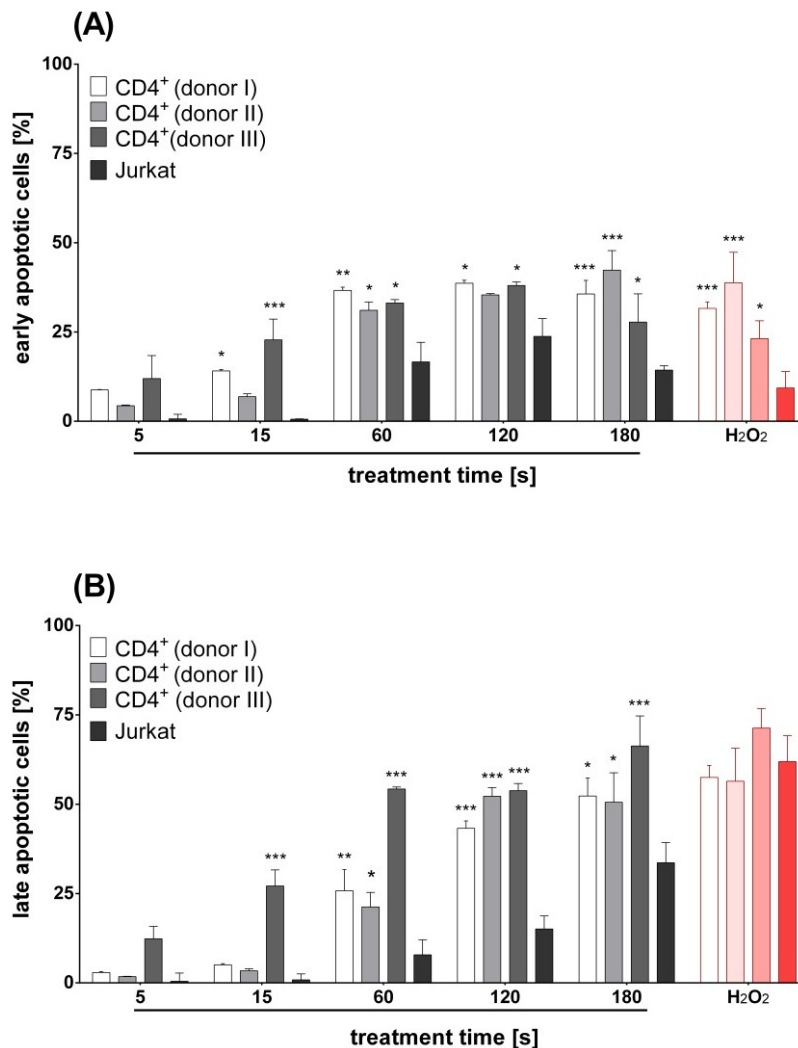
Figure 3.4: Comparison of apoptotic rates of isolated CD4$^+$ T helper cells to Jurkat cell line after plasma treatment.
Percentages of early (A; annexin V$^+$/ 7AAD$^-$) and late (B; annexin V$^+$/ 7AAD$^+$) apoptotic cells are displayed as bar diagrams, with the proportion of apoptotic untreated cells subtracted for each investigated cell types. 100 µM H$_2$O$_2$ (red) was used to trigger apoptosis. Representative data are shown from three independent experiments. Statistical significance of differences between primary CD4$^+$ T cells and Jurkat cells was determined by two-way ANOVA and Holm-Sidak´s post hoc-test and is displayed in the following way: $p < 0.05$ (*), $p < 0.01$ (**), $p < 0.001$ (***).

Monocytes

In Figure 3.5 percentages of early (Figure 3.5A) and late apoptotic (Figure 3.5B) cells of freshly isolated monocytes were compared with the THP-1 cell line.

Results

(A)

(B)
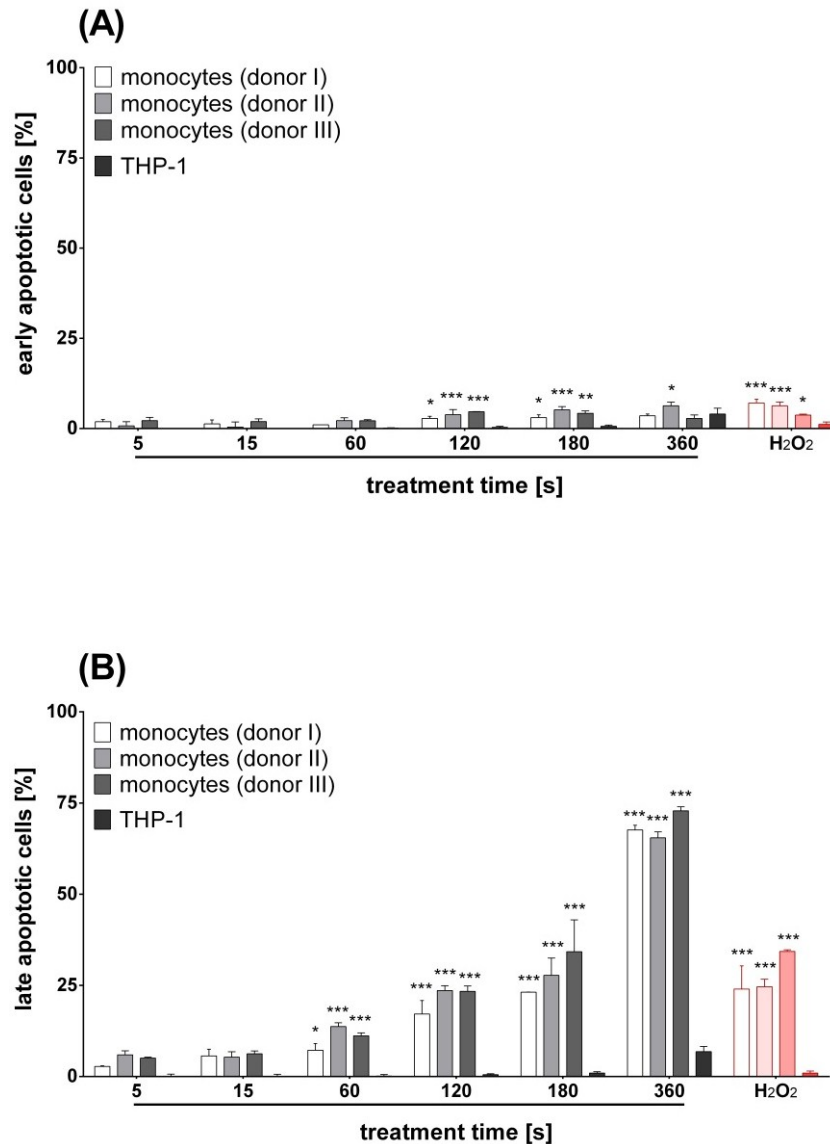
Figure 3.5: Comparison of apoptotic rates of isolated monocytes to THP-1 cell line after plasma treatment.
Percentages of early (A; annexin V$^+$/ 7AAD$^-$) and late (B; annexin V$^+$/ 7AAD$^+$) apoptotic cells are displayed as bar diagrams, with the proportion of apoptotic untreated cells subtracted for each investigated cell types. 100 µM H$_2$O$_2$ (red) was used to trigger apoptosis. Representative data are shown from three independent experiments. Statistical significance of differences between primary monocytes and THP-1 cells was determined by two-way ANOVA and Holm-Sidak´s post hoc-test and is displayed in the following way: $p < 0.05$ (*), $p < 0.01$ (**), $p < 0.001$ (***).

Similar to the T helper cells, the percentage of apoptotic cells increased in a plasma treatment time dependent manner in both investigated cell types. For the THP-1 cell line, only a small increase in early and late apoptosis was detected after 360 s plasma treatment. Furthermore, all examined cells displayed much lower percentages of early apoptotic cells than the corresponding late apoptotic cell numbers, indicating a fast apoptosis process. Primary monocytes showed significantly higher (from $p < 0.05$, * to $p < 0.001$,

***) early and late apoptosis rates compared with THP-1 cells for treatment times exceeding 60 s and 15 s of plasma exposure, respectively. Thus, isolated monocytes were more susceptible to non-thermal plasma treatment than the THP-1 cell line. Additionally, incubation with 100 µM H_2O_2 significantly increased early and late apoptosis in primary monocytes compared with THP-1 cells.

3.2.2 Plasma-induced caspase 3 activation[x]

Activation of the effector caspase 3 occurs as a last step of the apoptotic caspase cascade and is therefore regarded as a late apoptotic signal [116]. 18 h after plasma treatment Jurkat, THP-1 and primary monocyte cell samples were counted and the percentage of late apoptotic cells was determined by staining caspase 3 positive cells and subsequent flow cytometric measurements. Figure 3.6 displays the flow cytometric gating strategy used in this study. First, all cells were gated in a FSC/ SSC dot plot. This ensures that cells, which already underwent apoptosis, were included, while debris and cell aggregates were gated out. Then, cells were plotted in a FL-1 histogram, where caspase 3 positive cells were gated.
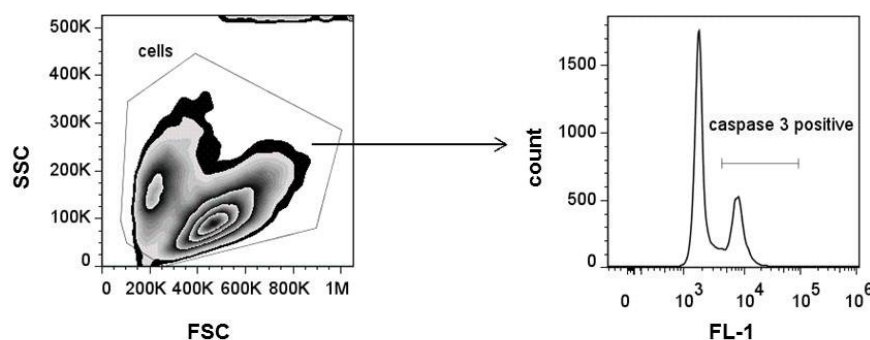
Figure 3.6: Flow cytometric gating strategy for caspase 3 positive cells.
All cells excluding cell debris were first gated in a FSC/ SSC plot and subsequently subgrouped regarding their staining ability for activated caspase 3.

---

[x] this section is party adapted from Bundscherer *et al.* [48, 50]

Results

Figure 3.7A (Jurkat cells), Figure 3.7B (THP-1 cells) and Figure 3.7C (primary monocytes) illustrate the percentages of caspase 3 positive cells. Jurkat cells (Figure 3.7A) showed a non-thermal plasma treatment time dependent increase of late apoptotic cells. This ranged from 2.4 % at 5 s, which was comparable to the untreated control, increasing steadily to more than 80 % at 180 s of plasma treatment. Jurkat cells incubated with 100 µM H_2O_2 or 10 µM etoposide (Eto) displayed a high percentage of caspase 3 positive cells (85 % and 71 %).

THP-1 cells (Figure 3.7B) responded less sensitive to plasma treatment. Even a treatment time of 180 s did not increase the percentage of caspase 3 positive cells compared with the untreated control (0 s). Only a prolonged treatment time of 360 s caused a significant increase of late apoptotic cells of up to 25 %. However, only six percent of caspase 3 positive cells could be found in the control samples treated with 100 µM H_2O_2. In contrast to non-thermal plasma or H_2O_2 treated cells, etoposide induced apoptosis in 71 % of the cells.

Figure 3.7C displays the measured caspase 3 activation levels of isolated human monocytes. In contrast to the cell lines 17 % late apoptotic cells were already found in the untreated control. Up to a plasma treatment time of 15 s caspase 3 values of the investigated monocytes remained at the control-level. Plasma exposure times exceeding 15 s showed dose-dependent induction of caspase 3 activation up to a level of 80 % (360 s). Incubation with 100 µM H_2O_2 and 10 µM etoposide led to up-regulation of caspase 3 of 71 % and 75 %, respectively.
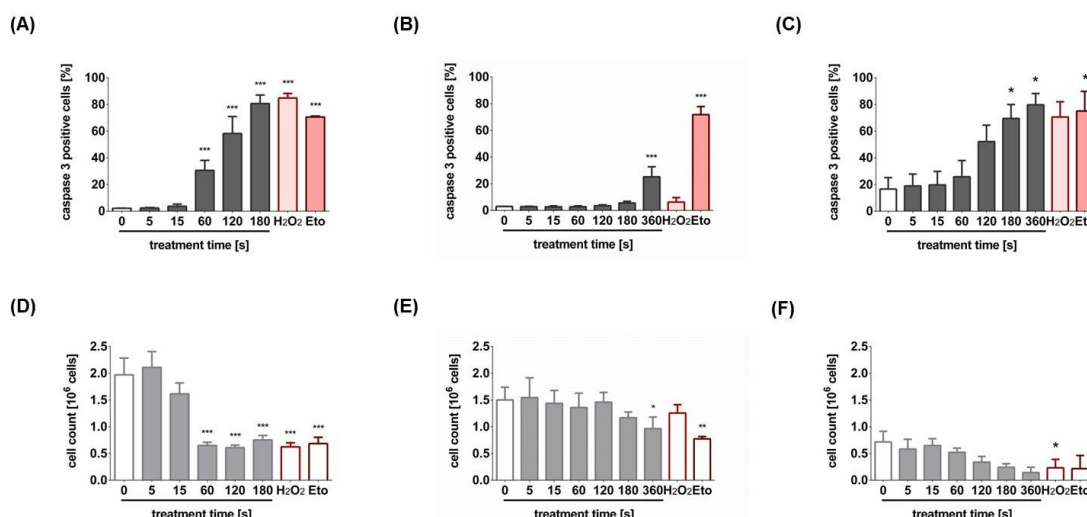
Figure 3.7: Flow cytometry analysis showing caspase 3 positive cells and absolute cell counts after indirect plasma treatment.
Percentage of caspase 3 positive Jurkat cells (A), THP-1 cells (B) and primary monocytes (C) were plotted according to plasma treatment time. Absolute cell counts of Jurkat (D), THP-1 (E) cells and primary monocytes (F) are displayed as a function of plasma treatment time. 100 µM H_2O_2 (red) and 10 µM etoposide (Eto; dark red) were used as a positive controls for apoptosis induction. Representative data are displayed with the mean and standard deviation of three independent experiments. Statistical significance of differences between treated and untreated cells was determined by one-way ANOVA and Dunnett´s post hoc-test and is displayed in the following way: $p < 0.05$ (*), $p < 0.01$ (**), $p < 0.001$ (***).

Since plasma-mediated growth retardation of the investigated cells was observed, cell counting was performed in association with the caspase 3 assay 18 h after plasma exposure. Corresponding absolute cell counts are shown in Figure 3.7D (Jurkat cells), Figure 3.7E (THP-1 cells) and Figure 3.7F (primary monocytes). The number of Jurkat cells (Figure 3.7D) decreased in a plasma treatment time dependent manner, which inversely correlates to the caspase 3 values. The short-term treatment times (5 s and 15 s) did not alter cell numbers significantly compared with the untreated control. Remarkably, a treatment time of 5 s revealed a slight increase of the cell count (2.11×10^6 cells) in comparison to the untreated control (1.97×10^6 cells). On the contrary, only 65 % to 75 % of the initially seeded cells (1×10^6 cells) could be detected in the 60 s, 120 s and 180 s plasma exposed, H_2O_2 or etoposide treated samples.

In contrast to Jurkat cells, a significant growth attenuation of THP-1 cells (Figure 3.7E) 18 h after plasma exposure was only observed in the 360 s plasma-treated sample. The sample treated for 5 s also showed a small increase of the cell number (1.55×10^6 cells) in comparison to the untreated control

Results

(1.50 × 10^6 cells). 100 µM H$_2$O$_2$ did not alter cell growth significantly (1.26 × 10^6 cells). In contrast, only 0.78 × 10^6 cells were counted after incubation with 10 µM etoposide.

Figure 3.7F displays the received cell numbers of the primary monocytes. In contrast to the cell lines, the cell number decreased rapidly during the incubation times for all conditions. Up to a treatment exposure time of 15 s (0.65 × 10^6 cells) only a slight decrease of the counted number was observed compared with the untreated control (0.72 × 10^6 cells). Samples treated for 120 s (0.24 × 10^6 cells) to 360 s (0.15 × 10^6 cells) showed a treatment time dependent decrease of the cell number. Also exposure to H$_2$O$_2$ or etoposide led to a decreased cell count of 0.23 × 10^6 cells and 0.22 × 10^6 cells, respectively.

3.3 Gene expression studies after plasma treatment

To gain insights into the plasma-induced genomic modulations, DNA microarray analysis of 24.000 genes in total was performed with both cell lines 3 h after treatment. For each cell line a short and an intermediate plasma treatment time was chosen, which were compared with an untreated control. Subsequently, selected target genes of both cell types were validated by quantitative PCR. Here, an additional long plasma treatment time was added and the gene expression trend was followed for a time span of 24 h.

3.3.1 Transcriptomics of Jurkat cells

DNA microarray

Jurkat cells, indirectly treated for 15 s and 30 s, were compared with untreated cells in a DNA microarray-based approach (NimbleGen). Data generated were analyzed by Patek Genomics Suite software. Comparing both treatment times with the control 338 genes (193 down- and 145 up-regulated) were detected to be more than two-fold differentially regulated. Furthermore, the comparison of

the short treatment time (15 s) alone to the untreated control, led to 681 modulated genes (402 down- and 279 up-regulated). While the intermediate plasma exposure (30 s) alone revealed 1,149 differentially expressed genes (760 down- and 389 up-regulated) compared with untreated control (the full gene lists are depicted in supplementary tables 1-3).

Figure 3.8 visualizes all differentially expressed genes in a heatmap format of 15 s and 30 s treated Jurkat cells in comparison to the untreated control (0 s) as determined by Patek Genomics Suite software. Here, genes were subgrouped dependent on the received fold changes. Remarkably, most genes were up- or down-regulated in a plasma treatment time dependent manner.
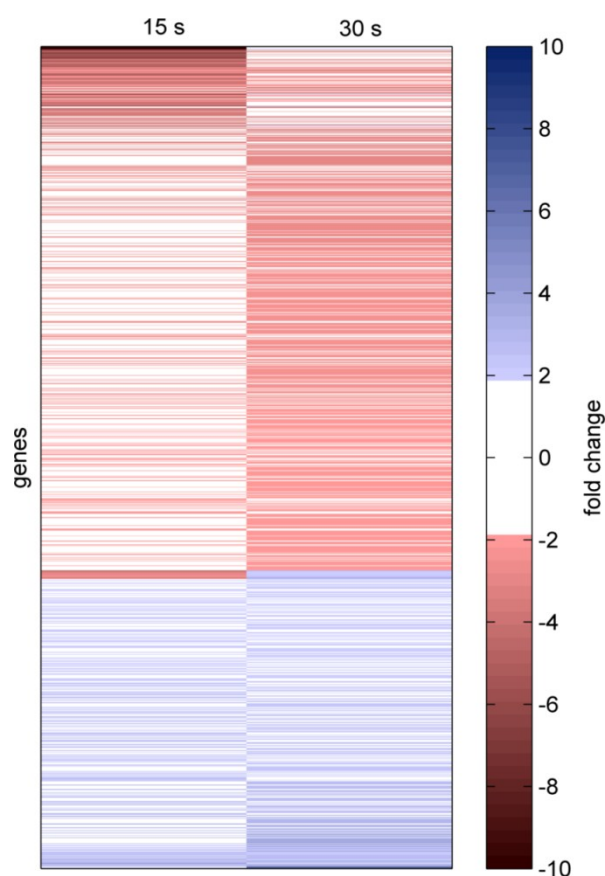
Figure 3.8: Heatmap analysis of plasma-modulated genes in Jurkat cells.
Plasma-regulated gene expression was identified by a genome-wide gene expression analysis in Jurkat cells. Data were processed using Patek Genomics Suite software and received fold changes were displayed in a heatmap chart. DNA microarray analysis was performed with pooled RNA samples of 8 independent experiments. Significantly down-regulated genes (fold change ≤ -2) are represented in red and up-regulated genes (fold change ≥ 2) in blue. Genes, which were not significantly regulated by plasma treatment are depicted in white (2 > fold change > -2).

Results

In the following, the case of both plasma treatment times together (15 s and 30 s) compared with the untreated control (0 s) is elaborated.

Subsequently, gene ontology (GO) analysis was performed using Panther classification system. Here, non-thermal plasma-modulated protein classes were determined as depicted in Figure 3.9, whereas 17 different protein classes including 198 total proteins could be detected. To name only the classes with the highest protein numbers, 45 receptor proteins, 29 signaling molecules and 19 transcription factors were found to be regulated by plasma treatment.

total = 198
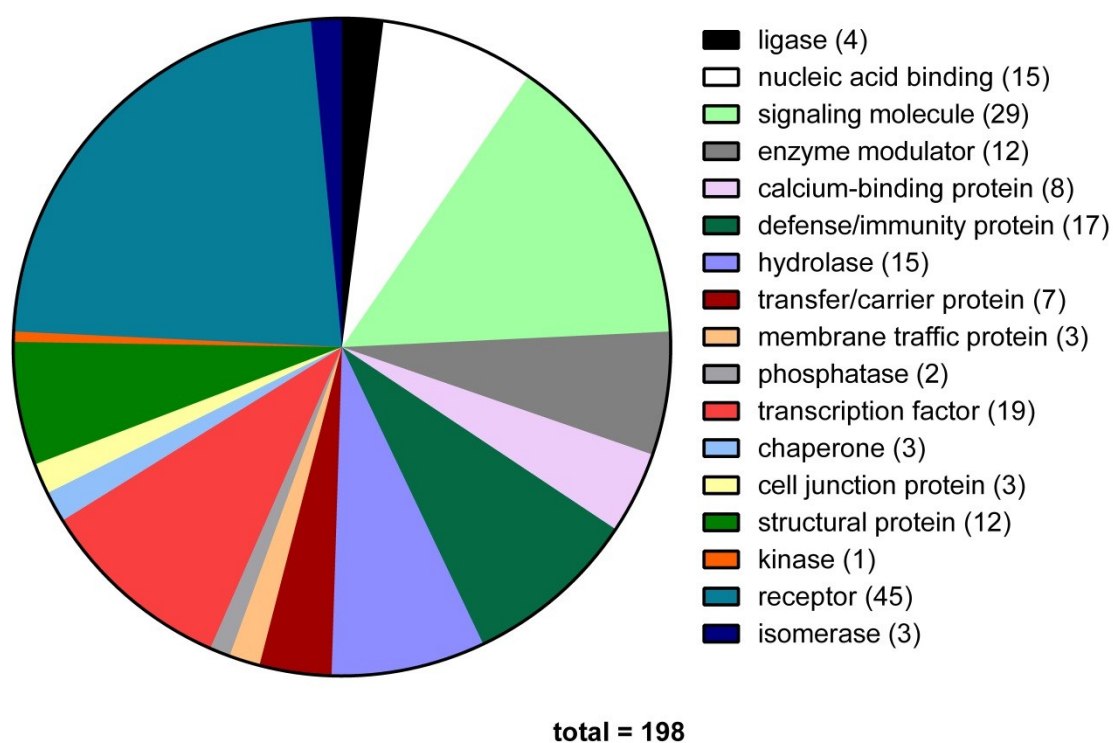
Figure 3.9: Gene ontology analysis of plasma-regulated protein classes in Jurkat cells.
For the DNA microarray approach, plasma-treated (15 s and 30 s) Jurkat cells were compared with untreated cells (0 s). Here, RNA samples were pooled of 8 independent experiments and subsequently applied on the microarray slides. DNA microarray data were subjected to gene ontology analysis by Panther software, whereas protein classes regulated by plasma treatment were depicted as a pie chart. The number of molecules found for the different classes is displayed in brackets behind the specific protein class.

In order to obtain more information about the plasma-modulated genes, pathway analysis of the identified genes was further performed by IPA software. A simplified overview of one main signaling pathway assessed by IPA is displayed in Figure 3.10. The transcription factors FOS and JUN are

components of activator protein 1 (AP-1), which is involved in various molecular mechanisms like proliferation, differentiation and apoptosis [117]. The phosphorylation of these transcription factors is amongst others regulated by the MAP kinases JNK, p38 MAPK, MEK and ERK [118, 119]. In the DNA microarray approach FOS was found to be 3.2-fold and JUN to be 3.0-fold up-regulated in the plasma-treated cell samples compared with the untreated control (Supplementary table 3). The plasma-based modulation of the expression of these transcription factors was further assessed by quantitative PCR.
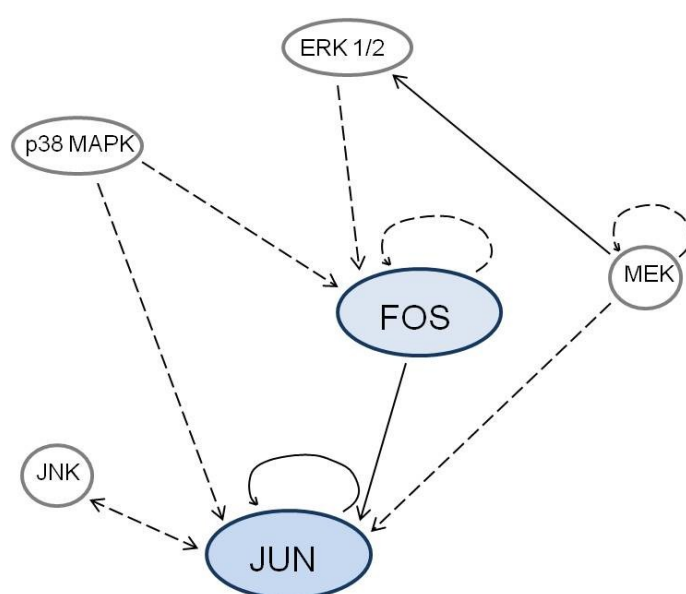
Figure 3.10: IPA pathway of plasma-treated Jurkat cells.
DNA microarray analysis was performed with plasma-treated (15 s and 30 s) and untreated (0 s) Jurkat cells Therefore, pooled RNA samples of eight independent experiments were used. Data were analyzed using IPA software. One received pathway is simplified depicted in the drawing. Up-regulated genes are illustrated in blue. A solid line represents a direct and a dashed line an indirect interaction between molecules. Image adapted from IPA signaling pathway.

quantitative PCR

Next to the short (15 s) and intermediate (30 s) treatment times a longer plasma exposure of 60 s was chosen for the investigated Jurkat cells. Moreover, an additional cell sample was treated with 100 µM H_2O_2. Cell samples for quantitative PCR validation were drawn 3 h, 6 h, 12 h and 24 h after plasma treatment to get an impression about the variation of the differentially expressed genes over time.

Results

Figure 3.11 displays the non-thermal plasma-induced regulation of the transcription factor FOS. According to the plasma treatment time an increase of the fold change could be observed at all investigated time points. However, incubation with 100 µM H_2O_2 led to the highest changes of FOS expression. The highest expression was found after an incubation time of 6 h. Here, the maximal plasma-induced fold change averaged 12.8 for the treatment of 60 s and the maximal H_2O_2-induced fold change constituted 34.6 ($p < 0.05$, *). After this incubation time, the expression of FOS was reduced for all samples. After 12 h and 24 h FOS expression dropped to the level of 3 h.
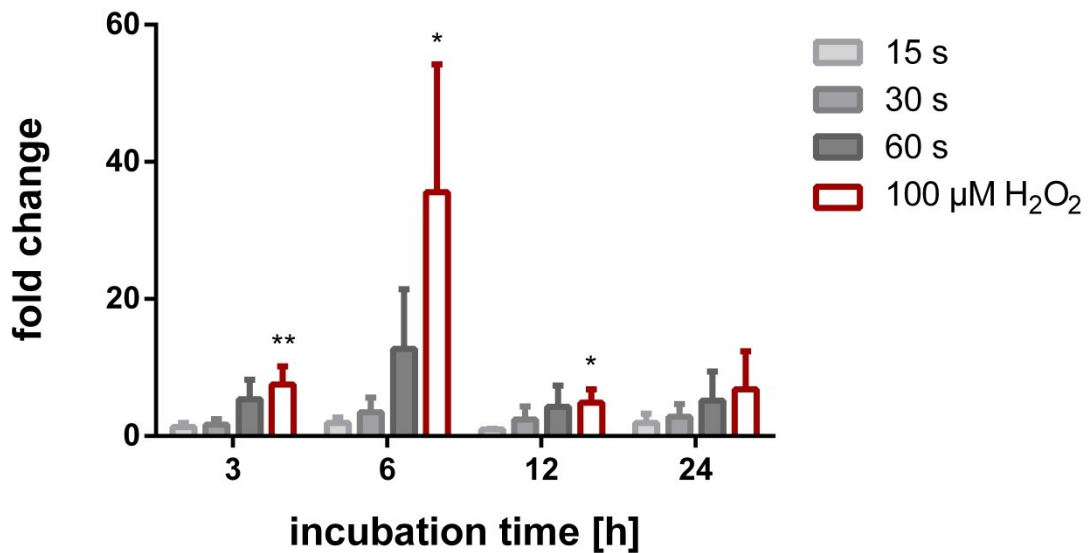
Figure 3.11: FOS gene regulation in plasma-treated Jurkat cells.
3 h, 6 h, 12 h and 24 h after plasma treatment, gene expression of FOS was determined in plasma (15 s, 30 s and 60 s) as well as H_2O_2 (100 µM; red) treated Jurkat cells. Modulated gene expression is displayed as fold changes referring to the untreated control (fold change of 1). Mean and standard deviation of three independent experiments are depicted. Statistical significance of differences between treated and untreated cells was determined by one-way ANOVA and Dunnett´s post hoc-test and is displayed in the following way: $p < 0.05$ (*), $p < 0.01$ (**), $p < 0.001$ (***).

In Figure 3.12 the modulation of JUN gene expression of Jurkat cells after non-thermal plasma treatment is shown. Similar to the modulator FOS, a plasma treatment time dependency could be detected for the JUN gene expression profile. Nevertheless, maximal expression levels were gained after an incubation time of 12 h. The maximal gene expression levels of the longest plasma treatment exposure of 60 s (fold change of 15.5) and the 100 µM H_2O_2

(fold change of 15.0) treatment resembled each other. After an incubation time of 24 h, the JUN-expression dropped to the level of 3 h.
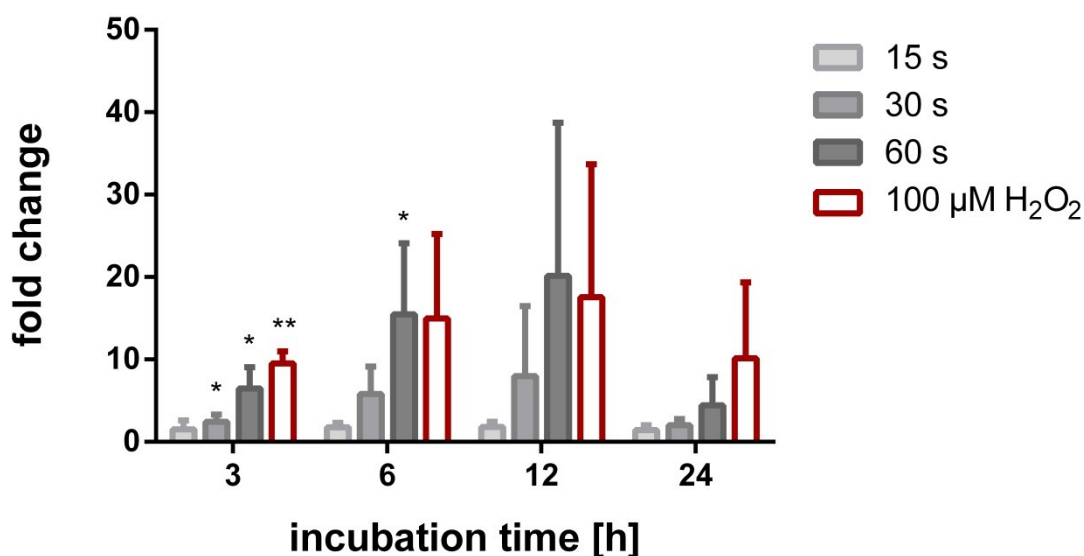
Figure 3.12: JUN gene regulation in plasma-treated Jurkat cells.
3 h, 6 h, 12 h and 24 h after plasma treatment, gene expression of JUN was determined in plasma (15 s, 30 s and 60 s) as well as H_2O_2 (100 µM; red) treated Jurkat cells. Modulated gene expression is displayed as fold changes referring to the untreated control (fold change of 1). Mean and standard deviation of three independent experiments are depicted. Statistical significance of differences between treated and untreated cells was determined by one-way ANOVA and Dunnett´s post hoc-test and is displayed in the following way: $p < 0.05$ (*), $p < 0.01$ (**), $p < 0.001$ (***).

3.3.2 Transcriptomics of THP-1 cells

DNA microarray

Similar to the Jurkat cells, two plasma treatment times were chosen for the DNA microarray approach (NimbleGen) of the THP-1 cells. Since THP-1 cells were identified to tolerate longer plasma exposure, the short plasma treatment time selected was 60 s and the intermediate 180 s. In contrast to the Jurkat cell line much less genes were identified for THP-1 to be regulated by plasma as determined by Patek Genomics Suite software. The comparison of both plasma treatment times together (60 s and 180 s) to the untreated control (0 s) discovered 27 genes in total (9 down- and 18 up-regulated) that were more than two-fold differentially expressed after plasma exposure. Moreover, comparing the short treatment time of 60 s to the control, identified 149 differentially transcribed genes (73 down- and 76 up-regulated). After an intermediate

treatment time of 180 s 43 differentially expressed genes (9 down- and 34 up-regulated) in comparison to the untreated control were detected (the full gene lists are depicted in supplementary tables 4-6). Figure 3.13 displays the heatmap of the differentially expressed genes of 60 s and 180 s plasma-exposed THP-1 cells compared with untreated (0 s) cells. Distribution of the different genes took place due to different fold change levels. In contrast to the Jurkat cells, in THP-1 cells more genes were regulated by plasma treatment in response to the short treatment time of 60 s than the intermediate treatment time of 180 s. Below, the comparison between both plasma treatment times (60 s and 180 s) is followed up.
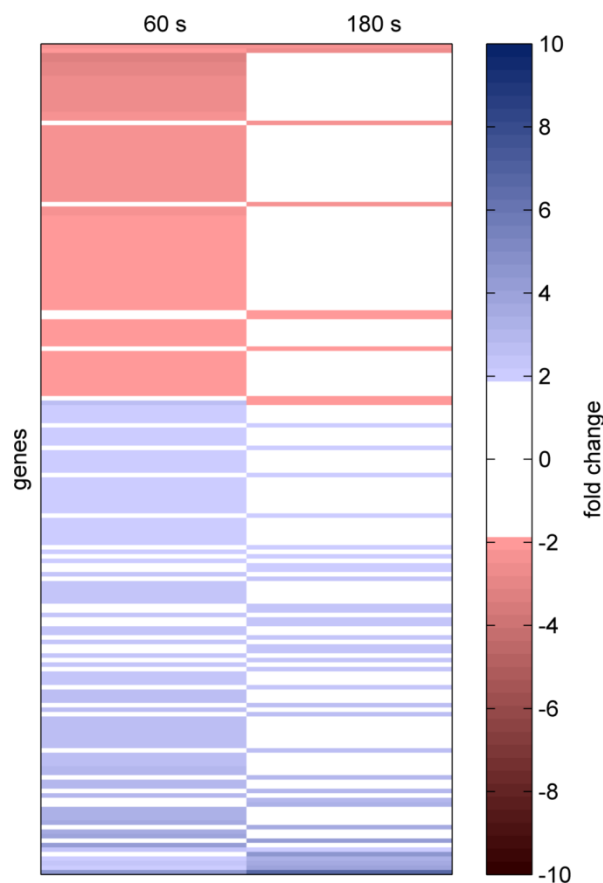
Figure 3.13: Heatmap analysis of plasma-modulated genes in THP-1 cells.
Plasma-regulated gene expression was identified by a genome-wide gene expression analysis in THP-1 cells. Data were processed using Patek Genomics Suite software and received fold changes were displayed in a heatmap chart. DNA microarray analysis was performed with pooled RNA samples of 8 independent experiments. Significantly down-regulated genes (fold change ≤ -2) are represented in red and up-regulated genes (fold change ≥ 2) in blue. Genes, which were not significantly regulated by plasma treatment are depicted in white (2 > fold change > -2).

To get an impression about the different protein classes affected by plasma treatment, DNA microarray data were further investigated by Panther classification system (Figure 3.14). 27 plasma-regulated proteins could be identified by GO analysis, whereas the classes of nucleic acid binding (5 proteins), transcription factors (5) and signaling molecules (3) were the most represented.

total = 27
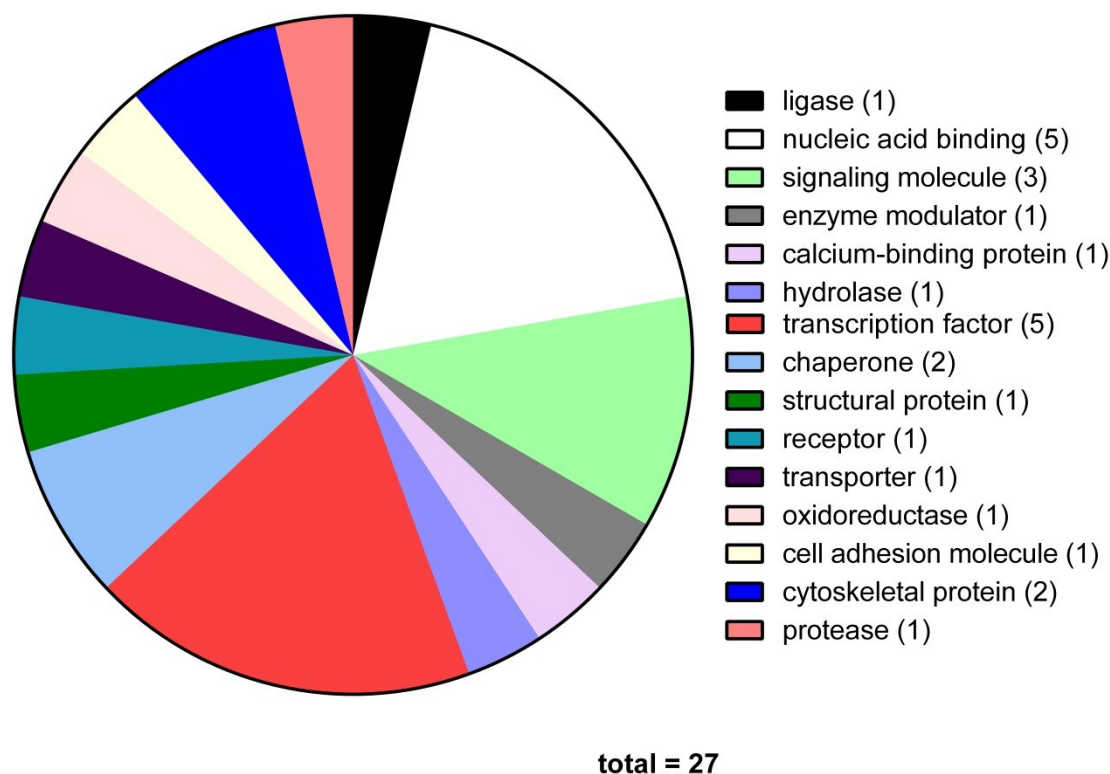
Figure 3.14: Gene ontology analysis of plasma-regulated protein classes in THP-1 cells.
For the DNA microarray approach, plasma-treated (60 s and 180 s) THP-1 cells were compared with untreated cells (0 s). Here, RNA samples were pooled of 8 independent experiments and subsequently applied on the microarray slides. DNA microarray data were subjected to gene ontology analysis by Panther software, whereas protein classes regulated by plasma treatment were depicted as a pie chart. The number of molecules found for the different classes is displayed in brackets behind the specific protein class.

Furthermore, pathway analysis by IPA software was performed. One interesting pathway is displayed in Figure 3.15. Like in the Jurkat cells one member of the AP-1 complex JUND was detected, which is important for cell fate decisions and indirectly regulated by the canonical MAP kinases [120, 121]. Amongst others, IL-8 is known to be synthesized by phosphorylation of JUN via JNK [122]. Additionally, an induction of JUN by activation of JNK can lead to

transactivation of HMOX-1 [123]. Comparing both plasma treatment times to the untreated control, a 2.2 fold activation of JUND, a 2.1 fold induction of IL-8 and a 5.6 fold activation of HMOX-1 gene expression was detected in the DNA microarray data (Supplementary table 6). These molecules and additionally GSR (glutathione reductase) that had a fold change of 2.3 comparing the 180 s treated cell sample to 0 s (Supplementary table 5), were further validated by quantitative PCR.
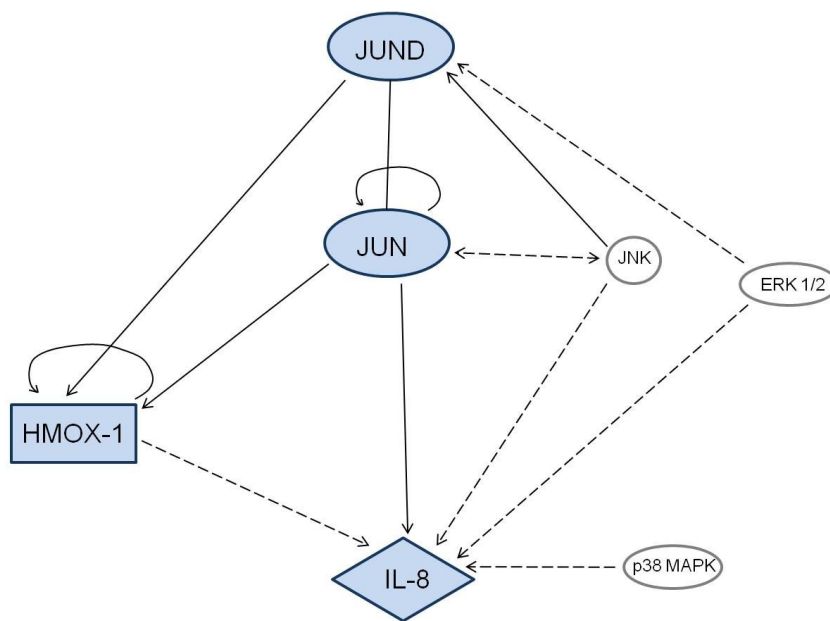
Figure 3.15: IPA pathway of plasma-treated THP-1 cells.
DNA microarray analysis was performed with plasma-treated (60 s and 180 s) and untreated (0 s) THP-1 cells Therefore, pooled RNA samples of eight independent experiments were used. Data were analyzed using IPA software. One received pathway is simplified depicted in the drawing. Up-regulated genes are illustrated in blue. A solid line represents a direct and a dashed line an indirect interaction between molecules. Image adapted from IPA signaling pathway.

quantitative PCR

An additional treatment time has been included in the qPCR-analyses of the selected molecules. Next to the short (60 s) and intermediate (180 s) treatment time a long plasma exposure of 360 s was chosen for the THP-1 monocytes. An additional sample was incubated with 100 µM H_2O_2. According to the Jurkat cell line, the expression levels of examined genes were analyzed 3 h, 6 h, 12 h and 24 h after treatment.

First, the gene expression of JUND, one domain of the JUN protein, was analyzed [124]. Distribution of the different JUND gene expression levels over time is displayed in Figure 3.16. Only a slight plasma-dependent induction of the expression of this molecule (< 2-fold regulated) was found in the qPCR experiment for the whole time span. The sample treated with 100 µM H_2O_2 even showed no regulation for all investigated time points.
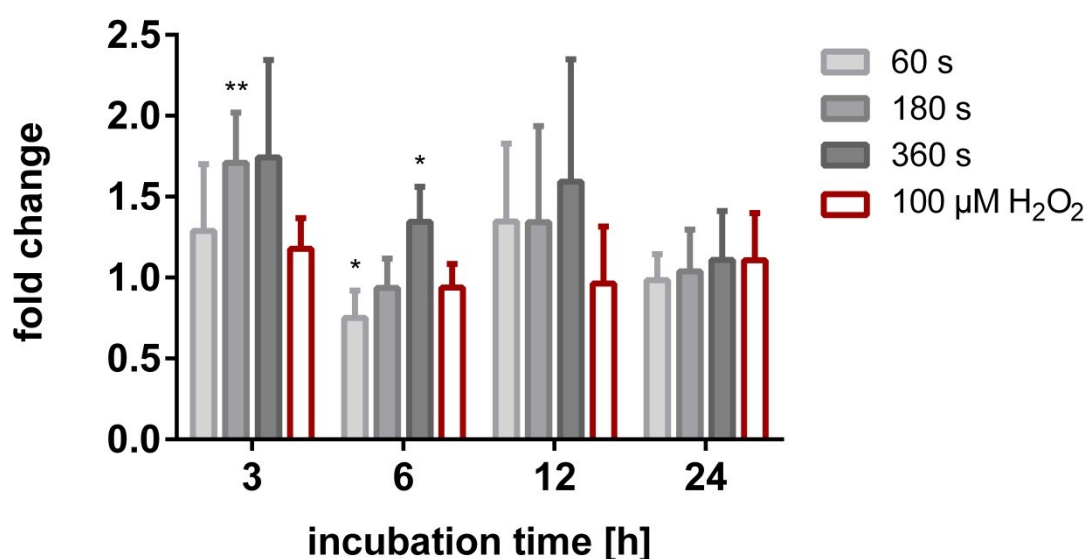
Figure 3.16: JUND gene regulation in plasma-treated THP-1 cells.
3 h, 6 h, 12 h and 24 h after plasma treatment, gene expression of JUND was determined in plasma (60 s, 180 s and 360 s) as well as H_2O_2 (100 µM; red) treated THP-1 cells. Modulated gene expression is displayed as fold changes referring to the untreated control (fold change of 1). Mean and standard deviation of three independent experiments are depicted. Statistical significance of differences between treated and untreated cells was determined by one-way ANOVA and Dunnett´s post hoc-test and is displayed in the following way: $p < 0.05$ (*), $p < 0.01$ (**), $p < 0.001$ (***).

Figure 3.17 shows the evaluated gene expression levels of IL-8 in THP-1 cells. Although cells treated for 60 s and 100 µM H_2O_2 showed no IL-8 gene regulation, 180 s and 360 s induced the IL-8 gene expression in a treatment time dependent manner. Maximal IL-8 gene regulation was observed after an incubation time of 6 h for the 360 s treated sample, which yielded a 15.3-fold change ($p < 0.01$, **). For incubation times longer than 6 h IL-8 gene expression dropped nearly to the base level.
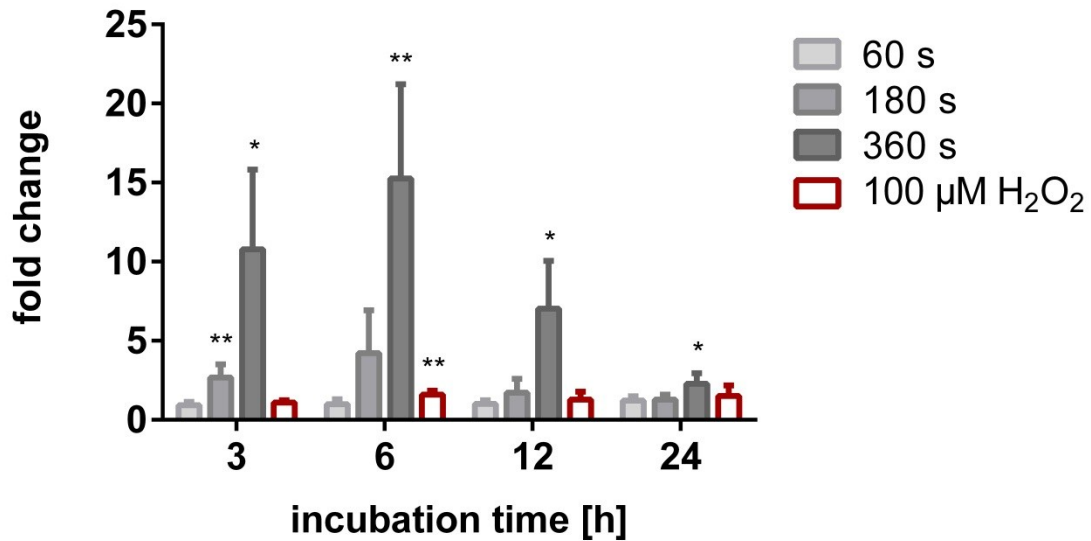
Figure 3.17: IL-8 gene regulation in plasma-treated THP-1 cells.
3 h, 6 h, 12 h and 24 h after plasma treatment, gene expression of IL-8 was determined in plasma (60 s, 180 s and 360 s) as well as H_2O_2 (100 µM; red) treated THP-1 cells. Modulated gene expression is displayed as fold changes referring to the untreated control (fold change of 1). Mean and standard deviation of three independent experiments are depicted. Statistical significance of differences between treated and untreated cells was determined by one-way ANOVA and Dunnett´s post hoc-test and is displayed in the following way: p < 0.05 (*), p < 0.01 (**), p < 0.001 (***).

HMOX-1 gene expression modulation by plasma treatment of THP-1 cells is depicted in Figure 3.18. Similar to IL-8 gene expression, the gene of HMOX-1 was induced by plasma treatment and had a maximal fold change of 29.5 (360 s; p < 0.05, *) at an incubation time of 6 h. H_2O_2 could also enhance HMOX-1 gene expression, similarly to the 60 s plasma-treated sample. Subsequently, the HMOX-1 signal dropped to the basal level until the incubation time of 24 h.

Furthermore, gene expression of glutathione reductase (GSR) was analyzed in plasma-treated THP-1 cells as depicted in Figure 3.19. While no plasma-mediated regulation of this gene was found after an incubation time of 3 h, a slight induction of GSR expression was shown in 180 s and 360 s treated samples after an incubation time of 6 h. Though, 12 h after plasma exposure, significant alterations of GSR gene expression were found mainly in THP-1 cells treated for 180 s and 360 s (p < 0.01, **). Here, expression of the GSR gene was induced up to a fold change of 2.0 and 2.3 in cells treated for 180 s and 360 s, respectively. After incubation time of 24 h no GSR plasma-modulated

gene regulation could be observed any more. In contrast to plasma, treatment with 100 µM H_2O_2 only induced GSR expression slightly up to a fold change of 1.4 after an 6 h incubation time.
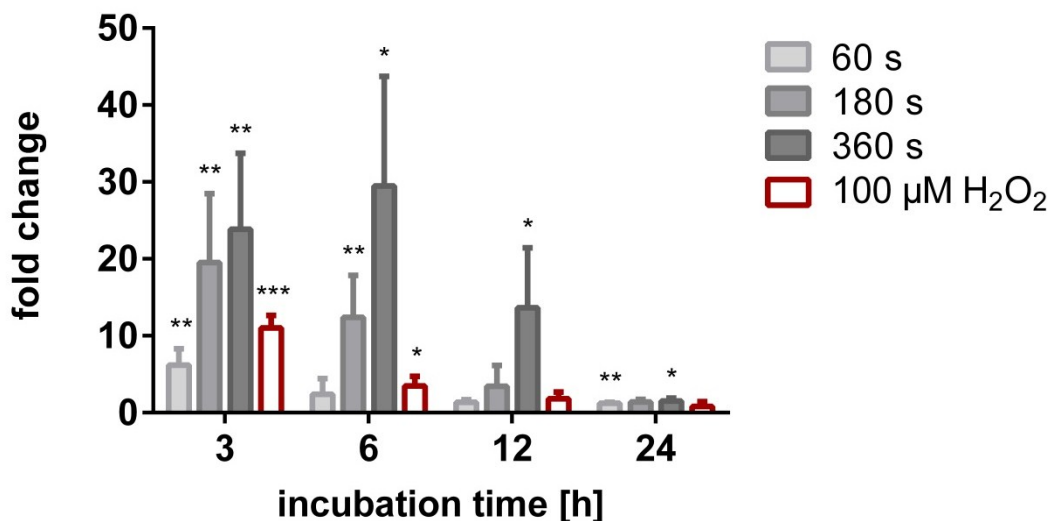
Figure 3.18: HMOX-1 gene regulation in plasma-treated THP-1 cells.
3 h, 6 h, 12 h and 24 h after plasma treatment, gene expression of HMOX-1 was determined in plasma (60 s, 180 s and 360 s) as well as H_2O_2 (100 µM; red) treated THP-1 cells. Modulated gene expression is displayed as fold changes referring to the untreated control (fold change of 1). Mean and standard deviation of three independent experiments are depicted. Statistical significance of differences between treated and untreated cells was determined by one-way ANOVA and Dunnett´s post hoc-test and is displayed in the following way: $p < 0.05$ (*), $p < 0.01$ (**), $p < 0.001$ (***).
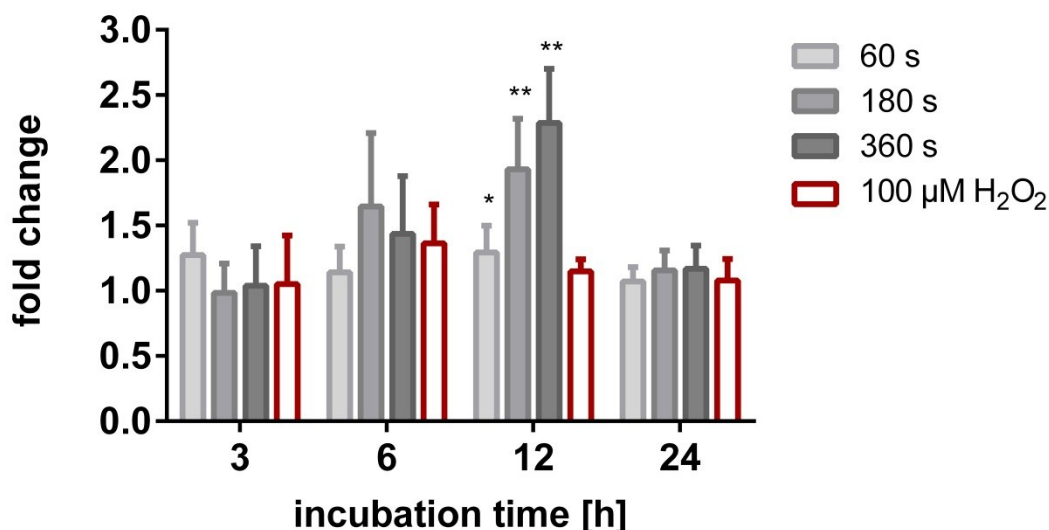

Figure 3.19: GSR gene regulation in plasma-treated THP-1 cells.
3 h, 6 h, 12 h and 24 h after plasma treatment, gene expression of GSR was determined in plasma (60 s, 180 s and 360 s) as well as H_2O_2 (100 µM; red) treated THP-1 cells. Modulated gene expression is displayed as fold changes referring to the untreated control (fold change of 1). Mean and standard deviation of three independent experiments are depicted. Statistical significance of differences between treated and untreated cells was determined by one-way ANOVA and Dunnett´s post hoc-test and is displayed in the following way: $p < 0.05$ (*), $p < 0.01$ (**), $p < 0.001$ (***).

Results

3.4 Plasma-mediated changes on protein level

After the analyses of a selection of differentially expressed genes, changes on protein level due to plasma treatment were examined in the Jurkat and THP-1 cell line as well as primary monocytes by western blot, ELISA and flow cytometry.

3.4.1 Plasma treatment-induced MAPK signaling[x]

Since it was striking that plasma induced genes that are associated with MAPK signaling, the relative phosphorylation or activation levels of these kinases were determined by western blotting technique and plotted as bar diagrams. Expression of β-Actin was additionally examined to ensure equal loading of the protein suspension onto the gels.

After plasma treatment, Jurkat cells, THP-1 cells and primary monocytes, were subjected to western blot analyses to investigate the activation of the pro-proliferative ERK-MEK signaling cascade, the pro-apoptotic signaling pathways of p38 MAPK and JNK as well as the protective chaperone HSP27. The activation of those molecules was determined by phospho-specific antibodies of the respective proteins. Own previous experiments indicated that ERK, MEK and HSP27 showed the strongest activation signals already after a short incubation time of 15 min, whereas p38 MAPK and JNK had activation maxima at 3 h after plasma treatment (data not shown). Thus, these incubation times were chosen for the analysis of the particular proteins. Since the apoptotic assays showed different plasma sensitivities of the investigated cell lines, different plasma treatment times were chosen for each cell line. Next to an untreated control (0 s), Jurkat cells were treated for 5 s, 15 s, 30 s and 60 s, and THP-1 cells were treated for 30 s, 60 s, 180 s and 360 s. For a better comparability between THP-1 monocyte cell line and primary monocytes, the

---

[x] this section is partly adapted from publications of Bundscherer *et al.* [48, 50]

58

same treatment times were used for isolated monocytes as for the cell line. Next to the non-thermal plasma treatment, cells were incubated with the apoptotic stimulant H_2O_2 (100 µM) as well as a proliferation inducing agent. Therefore, CD4$^+$ Jurkat T helper cells were stimulated with PHA (1 µg/mL) and THP-1 and primary monocytes with LPS (1 µg/mL) [125-127].

Jurkat cells

Figure 3.20 displays the western blot images of total and phosphorylated versions of the analytes as well as the thereof calculated activation of the investigated MAPK relative to the untreated control obtained in Jurkat cells. Plasma-exposed cells displayed an increased activation (phosphorylation) of the pro-proliferative signaling molecules MEK 1/2 (Figure 3.20A) and ERK 1/2 (Figure 3.20B) with a plasma treatment time dependency. A treatment intensity of 60 s doubled the signal of MEK 1/2 activation, induced a threefold activation of the ERK 1 signal and a 2.5-fold activation of ERK 2 compared with the untreated control (0 s). Also the stimulus PHA and the control H_2O_2 showed considerable activation signals.

Moreover, plasma exposure also activated the pro-apoptotic signaling proteins p38 MAPK (Figure 3.20C) and JNK 1/2 (Figure 3.20D) in a strong treatment time dependent manner. After a plasma treatment time of 60 s, the cells displayed an eleven-fold activation of p38 MAPK compared with the untreated control. JNK 1 and JNK 2 were activated in the 60 s exposed sample up to thirteen- and 21-fold, respectively. PHA did not alter MAPK activation compared with the untreated control. In contrast, activation of p38 MAPK and JNK 1/2 was strongly induced in the H_2O_2 control. Western blots of Jurkat cell lysates showed poor band intensities for both phospho-HSP27 and HSP27, which therefore could not be analyzed.

(A)

(B)

(C)

(D)
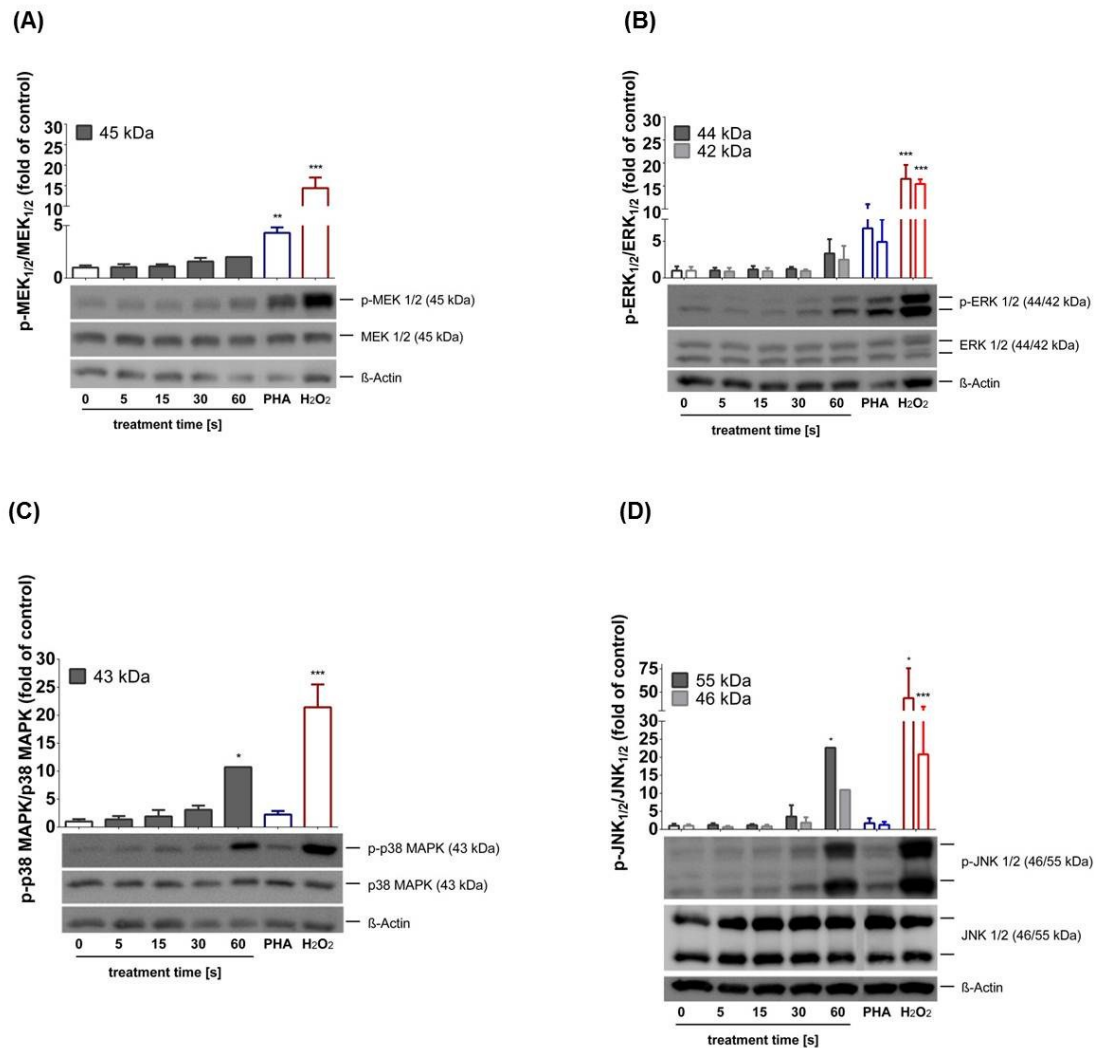
Figure 3.20: Quantitative western blot analyses of MAPK signaling pathways in Jurkat cells after non-thermal plasma treatment.
Signals of phosphorylated proteins were normalized to the signal of the corresponding total protein and the degree of activation was plotted normalized to the untreated control (0 s). β-Actin (45 kDa) was used as the loading control. (A) MEK 1/2 both at 45 kDa, (B) ERK 1/2 at 44 kDa and 42 kDa, (C) p38 MAPK at 43 kDa and (D) JNK 1/2 at 46 kDa and 55 kDa. 1 µg/mL PHA (blue) was used as a proliferation inducing agent, 100 µM H_2O_2 (red) to trigger cell death. The results are the means and standard deviation of three independent experiments. Statistical significance of differences between treated and untreated cells was determined by one-way ANOVA and Dunnett´s post hoc-test and is displayed in the following way: $p < 0.05$ (*), $p < 0.01$ (**), $p < 0.001$ (***).

THP-1 cells

In Figure 3.21 the received western blot images of THP-1 monocytes are depicted. THP-1 cells revealed only slight up-regulation of the pro-proliferative signaling molecules MEK 1/2 (Figure 3.21A) and ERK 1/2 (Figure 3.21B) at different plasma treatment time points. Both 180 s and 360 s plasma exposure induced a MEK 1/2 activation of 1.2-fold, indicating a twenty percent increase of

60

the untreated control. Furthermore, it could be demonstrated that ERK 1/2 was slightly but significantly activated after plasma exposure. In particular, ERK 1 was activated up to a maximum of 2.2-fold of the untreated control after 180 s of plasma exposure, while a treatment time of 360 s yielded an induction level of 1.9 compared with the untreated control. In contrast, ERK 2 was activated in a plasma treatment time dependent way up to a value of 1.7-fold of the control after 360 s of plasma treatment. The ERK-MEK pathway was shown to be induced also in the H_2O_2 control. However, LPS only slightly induced ERK 1 phosphorylation.

Both pro-apoptotic MAPK signaling pathways p38 MAPK (Figure 3.21C) and JNK 1/2 (Figure 3.21D) were activated by non-thermal plasma treatment in THP-1 cells. The mitogen-activated protein kinase p38 showed a correlation between activation and plasma treatment time. A non-thermal plasma treatment of 360 s revealed activation of 2.7-fold compared with the untreated control. JNK 1/2 displayed an elevated activation with increasing plasma treatment time – JNK 1 was induced up to twofold and JNK 2 up to 2.5-fold of the untreated control after 360 s plasma treatment duration. LPS and H_2O_2 treated cells additionally showed an up-regulation of JNK 1/2 and p38 MAPK.

Interestingly, the heat shock protein 27 (Figure 3.21E) was activated in plasma-treated THP-1 cells, with a strong plasma treatment time dependency. A treatment time of 360 s exhibited a 21-fold activation signal compared with the control. Also H_2O_2 treatment led to an induction of HSP27. Furthermore, a slight increase of HSP27 activation was found in the LPS control.
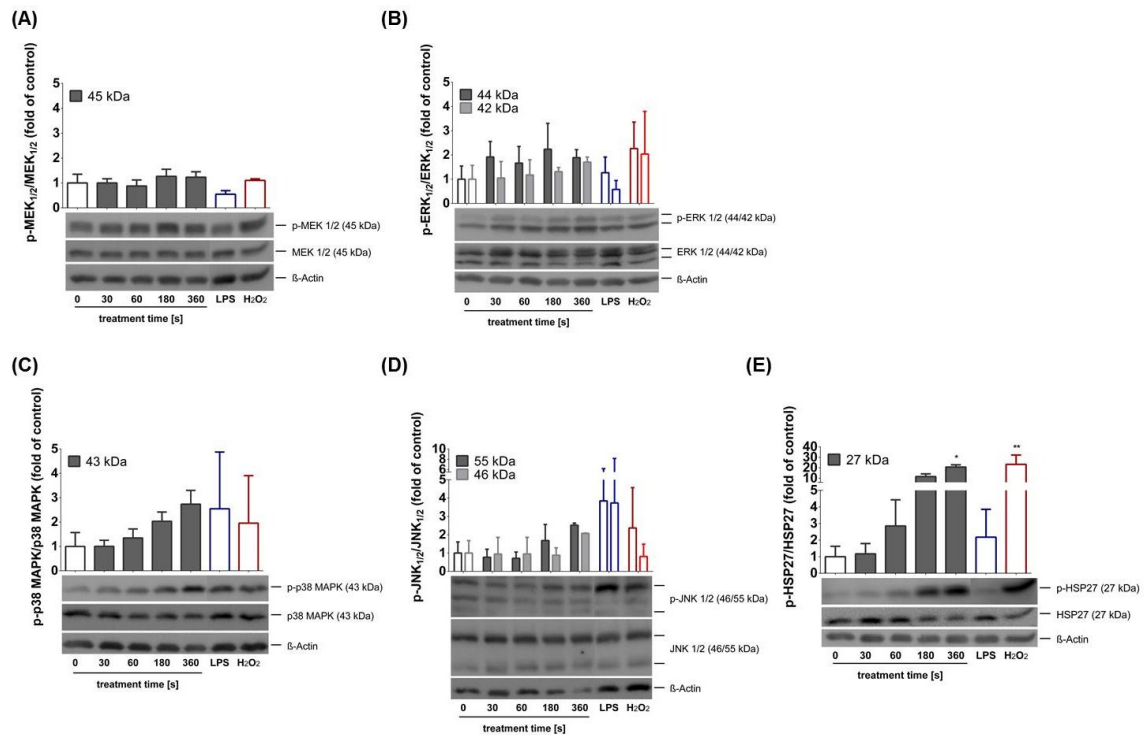
Figure 3.21: Quantitative western blot analyses of MAPK signaling pathways in THP-1 cells after non-thermal plasma treatment.
Signals of phosphorylated proteins were normalized to the signal of the corresponding total protein and the degree of activation was plotted normalized to the untreated control (0 s). β-Actin (45 kDa) was used as the loading control. (A) MEK 1/2 both at 45 kDa, (B) ERK 1/2 at 44 kDa and 42 kDa, (C) p38 MAPK at 43 kDa, (D) JNK 1/2 at 46 kDa and 55 kDa and (E) HSP27 at 27 kDa. 1 µg/mL LPS (blue) was used as a proliferation inducing agent, 100 µM H_2O_2 (red) to trigger cell death. The results are the means and standard deviation of three independent experiments. Statistical significance of differences between treated and untreated cells was determined by one-way ANOVA and Dunnett´s post hoc-test and is displayed in the following way: $p < 0.05$ (*), $p < 0.01$ (**), $p < 0.001$ (***).

Primary human monocytes

Figure 3.22 displays the received MAPK western blots of primary monocytes. Both short and long plasma treatments led to an activation of the pro-proliferative MEK-ERK pathway (Figure 3.22A and Figure 3.22B). As displayed in Figure 3.22A, MEK 1/2 (45 kDa) was activated by non-thermal plasma exposure in a treatment time dependent way. The shorter plasma treatment times of 30 s and 60 s already resulted in an induction of the relative phosphorylation level of MEK 1/2 (1.6- and 1.8-fold), while longer duration of plasma treatment led to significant activation ($p < 0.05$, *) up to 2.4-fold of untreated control after a treatment time of 360 s. A similar tendency could be demonstrated for the plasma-mediated activation of ERK 1/2 (Figure 3.22B). The relative phosphorylation level of ERK 1 (44 kDa) increased up to a

treatment time of 60 s (3.4-fold over 0 s) and persisted at this level also for the longer treatment times (180 s and 360 s). In contrast, the activation level of ERK 2 (42 kDa) increased up to a value of 8.6 after a treatment time of 180 s, while samples treated for 360 s showed an ERK 2 phosphorylation level of 6.3 compared to the untreated control. LPS up-regulated both MEK 1/2 (1.8-fold) and ERK 1/2 (3.6- and 8.3-fold). Additionally, H_2O_2 activated the relative phosphorylation level of MEK 1/2 (1.8-fold) and ERK 1/2 (both 2.6-fold).

In contrast to the pro-proliferative pathway, the pro-apoptotic cascades JNK and p38 MAPK were only induced after long plasma exposure times (Figure 3.22C and Figure 3.22D). The analysis of the apoptotic p38 MAPK pathway is illustrated in Figure 3.22C. There was no regulation of this molecule for the short plasma treatment times of 30 s and 60 s compared to the untreated control. However, longer plasma exposure resulted in an up-regulation of the relative phosphorylation level of p38 MAPK up to 1.6 and 1.5 after a treatment time of 180 s and 360 s, respectively. Similar to the activation of p38 MAPK, short plasma treatment times (30 s and 60 s) did not activate JNK 1/2, while longer plasma treatment times (180 s and 360 s) resulted in an up-regulation of JNK 1/2 (Figure 3.22D). JNK 1 (46 kDa) was induced up to 3.5-fold of control after 360 s ($p < 0.05$, *) of plasma exposure, while JNK 2 (55 kDa) showed an up-regulation up to 4.5 for a plasma treatment of 360 s. Like the short plasma treatment times, incubation with LPS (1 µg/mL) induced neither p38 MAPK nor JNK 1/2. Treatment with the apoptosis-inducing agent H_2O_2 (100 µM) led to an up-regulation of p38 MAPK to 1.7- and of JNK 1/2 to 3.1- and 4.7-fold ($p < 0.05$, *) of the control.

Western blots with lysates of isolated monocytes displayed poor band intensities for phospho- and total-HSP27, which therefore could not be analyzed.

Interestingly, it could be shown that the short plasma treatment times of 30 s and 60 s were able only to induce the pro-proliferative MEK-ERK pathway,

Results

while the pro-apoptotic cascades p38 MAPK and JNK were only switched on after the longer plasma durations of 180 s and 360 s.
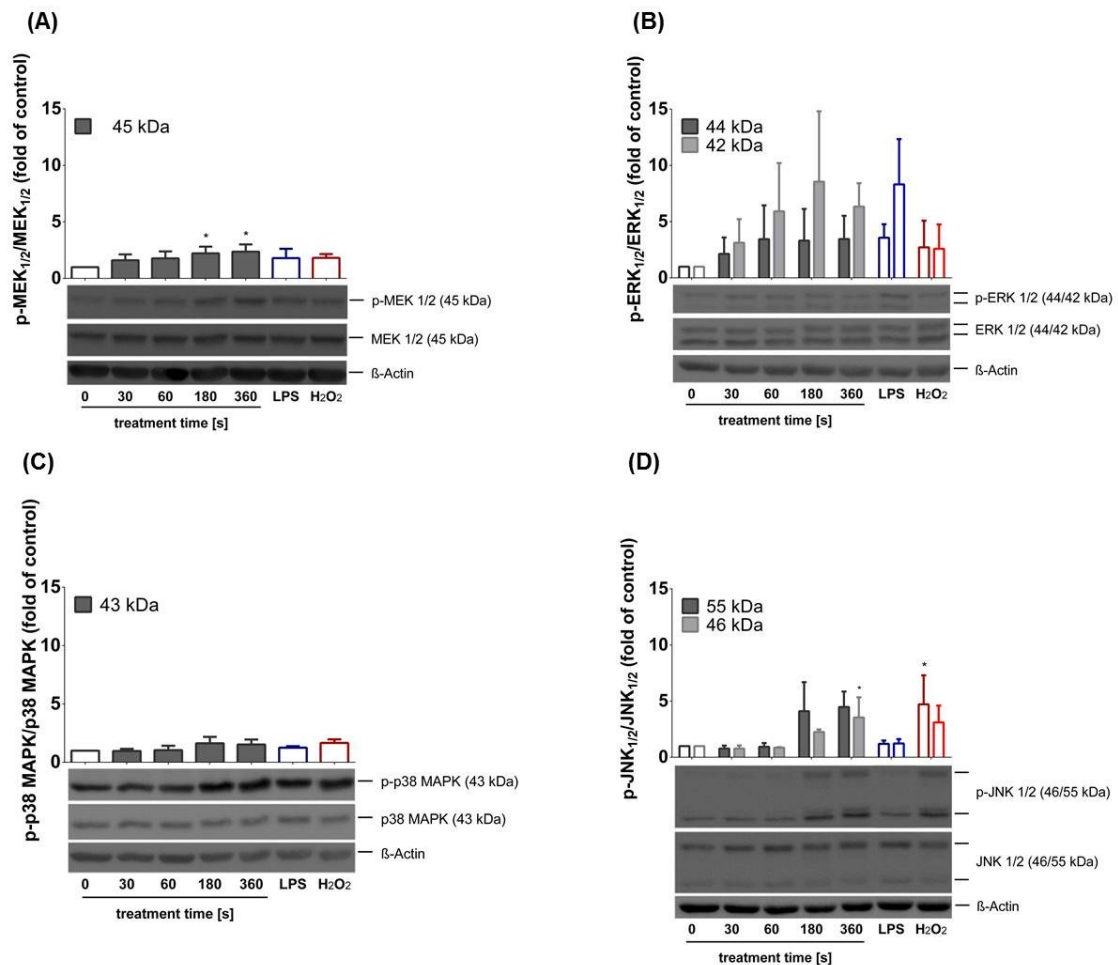

Figure 3.22: Quantitative western blot analyses of MAPK signaling pathways in primary monocytes after non-thermal plasma treatment.
Signals of phosphorylated proteins were normalized to the signal of the corresponding total protein and the degree of activation was plotted normalized to the untreated control (0 s). β-Actin (45 kDa) was used as the loading control. (A) MEK 1/2 both at 45 kDa, (B) ERK 1/2 at 44 kDa and 42 kDa, (C) p38 MAPK at 43 kDa, and (D) JNK 1/2 at 46 kDa. 1 µg/mL LPS (blue) was used as a proliferation inducing agent, 100 µM H_2O_2 (red) to trigger cell death. The results are the means and standard deviation of three independent experiments. Statistical significance of differences between treated and untreated cells was determined by one-way ANOVA and Dunnett´s post hoc-test and is displayed in the following way: $p < 0.05$ (*), $p < 0.01$ (**), $p < 0.001$ (***).

3.4.2   Modulated cytokine production of plasma-treated cells

To date there is little knowledge about the modulation of immune cells by plasma in respect to their cytokine expression profile. Therefore, a broad screening of a variety of cytokines was conducted by ELISA kits. Here, Jurkat, THP-1 and primary monocytes were analyzed regarding their cytokine secretion

profile. An additional setup was applied, where THP-1 cells and HaCaT keratinocytes were co-cultured. This co-culture approach was performed to simulate a wound environment. Plasma-mediated regulation of pro- as well as anti-inflammatory cytokines was detected for all investigated cell types 24 h after plasma treatment. Table 3.1 summarizes all examined cytokines and indicates their regulation.

Table 3.1: Cytokine screening by ELISA technique.

Name	Pro- (+) or anti- (-) inflammatory	Cell type	Plasma-induced changes
IL-1α	+	Jurkat cells	n.a.
		THP-1 cells	n.d.
		Primary monocytes	n.a.
		THP-1 and HaCaT cells	↑
IL-1β	+	Jurkat cells	n.d.
		THP-1 cells	n.d.
		Primary monocytes	n.c
		THP-1 and HaCaT cells	n.c.
IL-2	±	Jurkat cells	n.d.
		THP-1 cells	n.d.
		Primary monocytes	n.d.
		THP-1 and HaCaT cells	n.d.
IL-4	±	Jurkat cells	n.a.
		THP-1 cells	n.d.
		Primary monocytes	n.a.
		THP-1 and HaCaT cells	n.d.
IL-6	±	Jurkat cells	n.c.
		THP-1 cells	n.d.
		Primary monocytes	30 s ↑ and 60 s to 360 s ↓
		THP-1 and HaCaT cells	↑
IL-8	±	Jurkat cells	n.d.
		THP-1 cells	↑
		Primary monocytes	30 s and 60 s n.c., 180 s and 360 s ↓
		THP-1 and HaCaT cells	↑
IL-10	±	Jurkat cells	n.d.
		THP-1 cells	n.d.
		Primary monocytes	↓
		THP-1 and HaCaT cells	n.d.
IL-12	±	Jurkat cells	n.d.
		THP-1 cells	n.d.
		Primary monocytes	n.d.
		THP-1 and HaCaT cells	n.d.
IL-17A	+	Jurkat cells	n.d.
		THP-1 cells	n.c.
		Primary monocytes	n.a.
		THP-1 and HaCaT cells	n.d.
IL-22	±	Jurkat cells	n.c.
		THP-1 cells	n.c.
		Primary monocytes	n.d.
		THP-1 and HaCaT cells	n.a.
GM-CSF	±	Jurkat cells	n.c.
		THP-1 cells	n.d.
		Primary monocytes	↓
		THP-1 and HaCaT cells	↑
IFNγ	+	Jurkat cells	n.d.
		THP-1 cells	n.d.
		Primary monocytes	n.d.
		THP-1 and HaCaT cells	n.d.
TNFα	±	Jurkat cells	n.c.
		THP-1 cells	n.c.
		Primary monocytes	n.d.
		THP-1 and HaCaT cells	n.c.
TGFβ	±	Jurkat cells	n.c
		THP-1 cells	n.c
		Primary monocytes	n.d.
		THP-1 and HaCaT cells	n.a.

Abbreviations: ↑ = increased; ↓ = decreased; n.c. = not changed; n.d. = not detectable; n.a. = not analyzed.

Results

For Jurkat cells, no cytokine was found to be regulated by plasma treatment. Therefore, cytokine expression was only followed up for THP-1, primary monocytes as well as THP-1 cells, which were co-cultured with HaCaT keratinocytes.

THP-1 cells

IL-8 secretion of THP-1 cells in response to plasma treatment analyzed by ELISA technique is depicted in Figure 3.23. In all examined samples an induction of secreted IL-8 was detected with prolonged plasma treatment. A plasma treatment up to 180 s and incubation with 100 µM H_2O_2 did not significantly alter IL-8 secretion pattern compared with untreated cells. Remarkably, only THP-1 cells that were plasma-exposed for a long (360 s) time produced high amounts of IL-8 compared with the control. After an incubation time of 24 h, the measured IL-8 concentration of cell supernatants treated for 360 s averaged 474 pg/mL ($p < 0.001$, ***). While, only 107 pg/mL IL-8 was detectable in the supernatant of untreated cells at the same incubation time. In contrast to IL-8, IL-6 was not detectable in these cells.
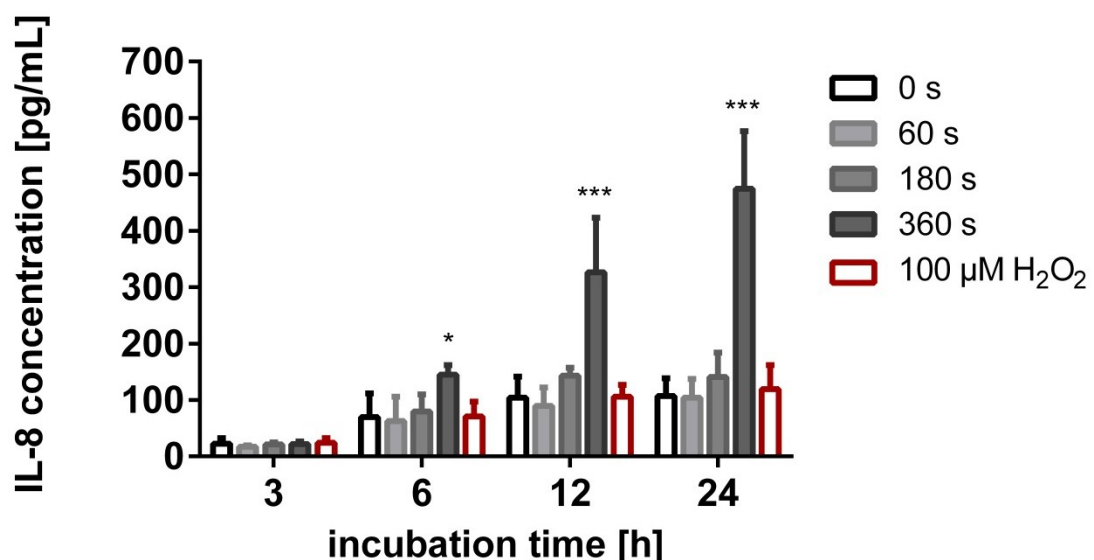
Figure 3.23: IL-8 secretion of THP-1 monocytes after plasma treatment.
IL-8 secretion into the supernatant was analyzed by ELISA technique 3 h, 6 h, 12 h and 24 h after plasma (60 s, 180 s and 360 s) as well as H_2O_2 (100 µM; red) treatment of THP-1 cells. Mean and standard deviation of three independent experiments are shown. Statistical significance of differences between treated and untreated cells was determined by one-way ANOVA and Dunnett´s post hoc-test and is displayed in the following way: $p < 0.05$ (*), $p < 0.01$ (**), $p < 0.001$ (***).

Primary Monocytes[x]

Next to the THP-1 monocytes, primary monocytes were further analyzed regarding their cytokine secretion. However, the amount of living primary monocytes dropped rapidly during incubation after plasma treatment, especially after a long plasma exposure (part 3.2). Thus, detection of secreted cytokines by ELISA was challenging, since it could not be assumed that one million cells produced the obtained amount of cytokines as it was the case for THP-1 cells [128]. Therefore, the cytokine production level was determined by intracellular staining and flow cytometry analysis. Due to test requirements, the intracellular expression levels had to be examined after an incubation time of 6 h. Here, intracellular expression levels of the pro-inflammatory cytokines IL-8 and IL-6 were regulated by plasma treatment. Results are displayed in Figure 3.24 as percent of cells expressing these cytokines. Interestingly, while 79 % of untreated monocytes (0 s) were positively stained for IL-8, only 32 % expressed IL-6.
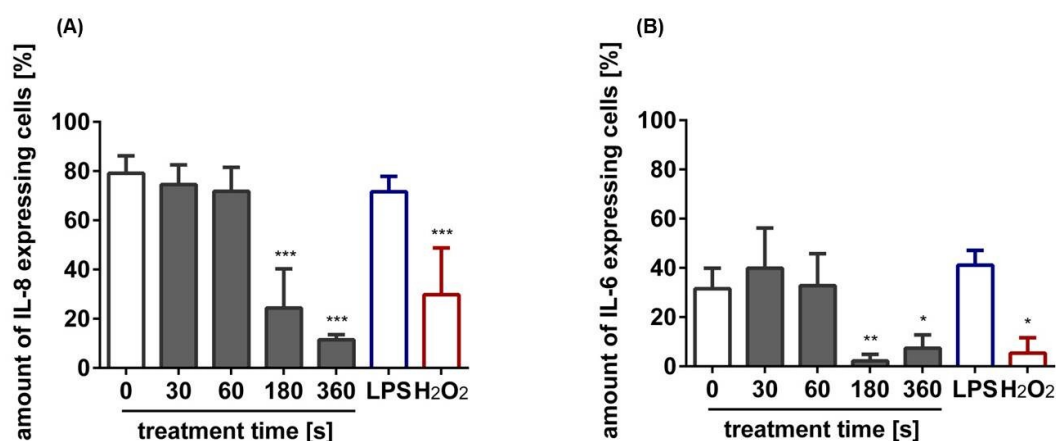
Figure 3.24: Intracellular cytokine expression in primary monocytes measured by flow cytometry.
6 h after indirect plasma treatment with the kinpen 09, monocytes were permeabilized and stained with APC-conjugated IL-8 (A) and PE-conjugated IL-6 antibodies (B). Then, the intracellular cytokine expression levels were determined by flow cytometry measurements. 100 µM H_2O_2 (red) was used to induce apoptosis and 1 µg/mL LPS (blue) to stimulate the monocytes. Representative data are displayed with the mean and standard deviation of three independent experiments. Statistical significance of differences between treated and untreated cells was determined by one-way ANOVA and Dunnett´s post hoc-test and is displayed in the following way: $p < 0.05$ (*), $p < 0.01$ (**), $p < 0.001$ (***).

---

[x] this section is partly adapted from Bundscherer *et al.* [48]

Results

After the short plasma treatment times of 30 s and 60 s no significant modulation of IL-8 expression (Figure 3.24A) compared to the untreated control (0 s) was observed in the investigated cells. The longer plasma exposure times of 180 s and 360 s resulted in a significant decrease ($p < 0.001$, ***) of cells expressing IL-8 to 11 % after a treatment time of 360 s.

Incubation with 1 µg/mL LPS showed a similar number of cells expressing IL-8 as the untreated control and the short treatment times (72 % IL-8 positive). In contrast, treatment with 100 µM H_2O_2 reduced the intracellular IL-8 expression to 30 % ($p < 0.001$, ***).

Next to IL-8, the amount of cells expressing IL-6 was determined (Figure 3.24B). An induction of cells expressing this cytokine could be observed after a plasma treatment time of only 30 s (40 % IL-6 positive). A treatment of 60 s (33 % IL-6 positive) resembled the untreated control (32 % IL-6 positive), while longer plasma treatment times resulted in a significant reduction of the amount of IL-6 expressing cells to 2 % ($p < 0.01$, **) after a 180 s plasma exposure.

LPS stimulation yielded an up-regulation of cells expressing IL-6 (42 % IL-6 positive) as expected. Similar to the long treatment times, incubation with 100 µM H_2O_2 led to a significant decreased IL-6 expression (5 % IL-6 positive, $p < 0.05$, *) compared with the untreated control.

3.4.3 Cytokine expression of co-cultured THP-1 and HaCaT keratinocytes

To simulate a wound, where skin and immune cells interact via soluble mediators like cytokines a co-culture approach was performed with HaCaT keratinocytes and THP-1 monocytes (in cooperation with A. Barton), which were reported to not effect viability of each other [129]. Here, cells were either treated for 180 s or left untreated. Additionally, LPS (1 µg/mL) was added to 180 s plasma-exposed cells. This component of gram negative bacteria should simulate the microorganisms, which often colonize a wound. Furthermore, THP-1 and HaCaT cells were studied under these conditions on their own. Figure 3.25 displays the evaluated cytokine secretion trends of IL-8 (Figure 3.25A), IL-6 (Figure 3.25B), GM-CSF (Figure 3.25C) and TNFα (Figure 3.25D).

The highest IL-8 concentrations (Figure 3.25A) were found in the samples cultivated with LPS and treated for 180 s ($p < 0.001$, ***). Here, IL-8 secretion of mono-cultured THP-1 cells and co-cultured cells displayed an IL-8 concentration of 3,993 pg/mL and 4,560 pg/mL, respectively. Mono-cultured HaCaT cells only secreted 650 pg/mL IL-8. For the HaCaT (250 pg/mL) as well as the co-cultured (193 pg/mL) cells also a slight induction of IL-8 secretion was observed after a 180 s plasma treatment only compared with untreated control (HaCaT 193 pg/mL and co-cultured cells 145 pg/mL). In THP-1 cells no alteration between the 180 s treated sample and the untreated control was detected (both 47 pg/mL).

A similar result was found for IL-6 secretion (Figure 3.25B). The highest IL-6 concentration was found in LPS and plasma-treated co-cultured cells (1,500 pg/mL). While IL-6 secretion of HaCaT cells averaged at 842 pg/mL and of THP-1 cells at 530 pg/mL under the same treatment conditions (all $p < 0.001$, ***). Additionally, an induction of IL-6 concentration was observed after plasma treatment only in both mono-cultivated HaCaT (514 pg/mL; $p < 0.001$, ***) and co-cultivated THP-1 and HaCaT cells (307 pg/mL; $p < 0.05$, *) compared with the untreated controls (both around 90 pg/mL). In contrast, in THP-1 cells, IL-6 secretion of 180 s plasma-treated and untreated cells were below the detection level.

GM-CSF secretion (Figure 3.25C) was not detectable in mono-cultivated THP-1 cells at any condition. Even though measurable GM-CSF concentration was not very high, an increase of this cytokine was found in HaCaT keratinocytes from untreated (4 pg/mL) over 180 s plasma-treated (7.5 pg/mL) to 180 s and LPS-treated (15 pg/mL; $p < 0.001$, ***) condition. The same tendency was observed in co-cultured THP-1 and HaCaT cells. Here, untreated cells secreted 4 pg/mL GM-CSF, cells incubated with 180 s plasma-exposed medium 5 pg/mL GM-CSF and 180 s and LPS treated cells 22 pg/mL GM-CSF ($p < 0.001$, ***).

In Figure 3.25D TNFα secretion of all investigated cells is depicted. Remarkably, only a treatment of 180 s and 1 µg/mL LPS induced an elevated

Results

TNFα secretion level of mono-cultured THP-1 cells (33 pg/mL; $p < 0.001$, ***).
All other conditions did not change the TNFα concentration (all about 5 pg/mL).
Even under co-culture of HaCaT and THP-1 cells there was no TNFα
detectable, indicating that HaCaT cells might be responsible for this TNFα
reduction.
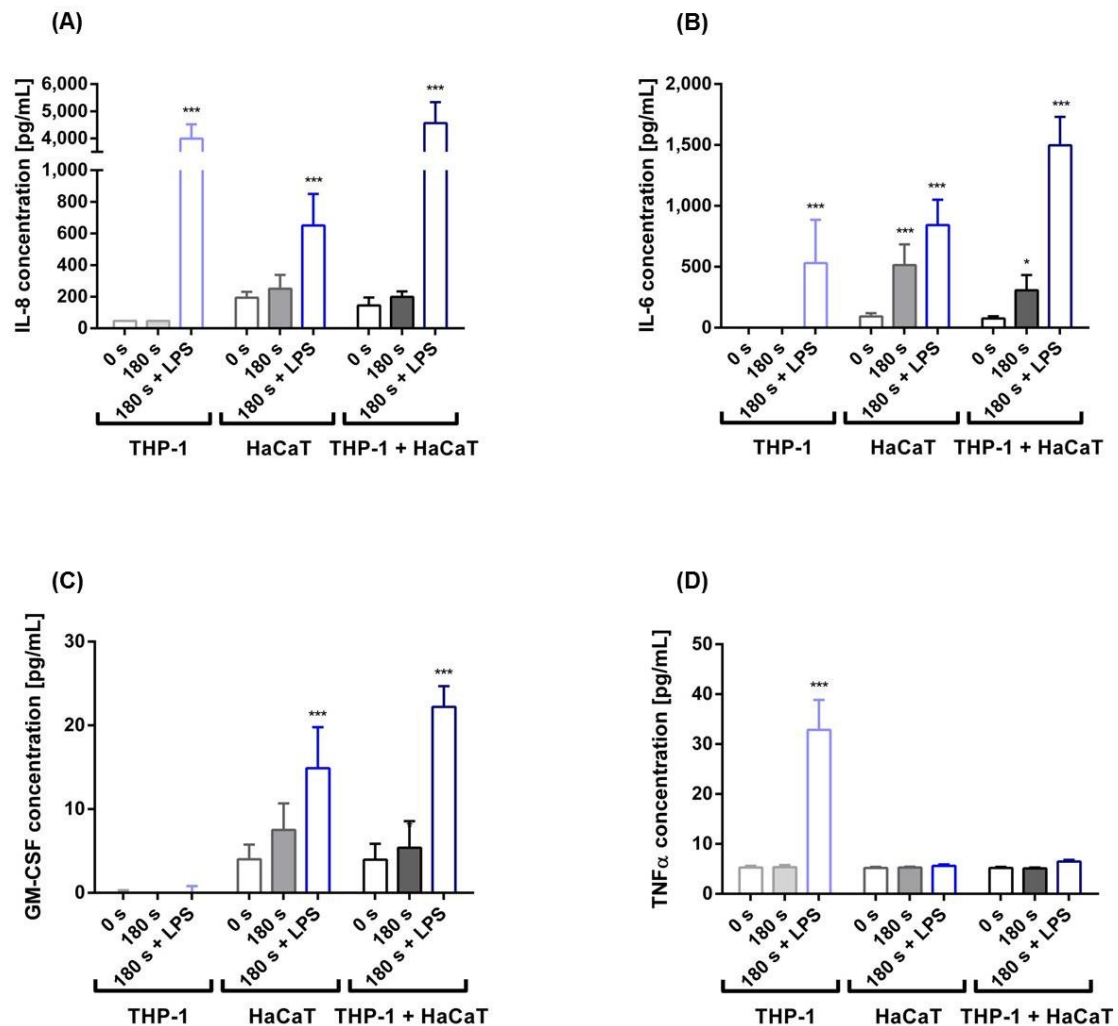
Figure 3.25: Plasma-induced cytokine expression of mono- and co-cultivated THP-1 and HaCaT cells.
After an incubation time of 24 h, plasma exposed (180 s ± 1 µg/mL LPS, blue) THP-1, HaCaT keratinocytes and co-cultured THP-1 and HaCaT cells were analyzed regarding their cytokine secretion by ELISA. Part (A) shows the measured IL-8, part (B) IL-6, part (C) GM-CSF and part (D) TNFα values. Four independent experiments have been performed, of which mean and standard deviation are displayed. Statistical significance of differences between treated and untreated cells was determined by one-way ANOVA and Dunnett´s post hoc-test and is displayed in the following way: $p < 0.05$ (*), $p < 0.01$ (**), $p < 0.001$ (***).

4 Discussion

The aim of this study was to examine if immune cells can be modulated by non-thermal plasma. This was investigated in detail at different levels, namely gene expression and protein production. In addition protein activation (phosphorylation of signaling molecules) was detected in response to plasma application. The results show for the first time that intracellular signals in immune cells strongly correlate with the duration of plasma exposure and the subsequent incubation time. Detailed knowledge about these mechanisms allow a target-oriented application of plasma for example in stimulation of wound healing.

4.1 Impact of non-thermal plasma treatment on cell survival

It has been shown in several studies that non-thermal atmospheric pressure plasma is able to induce apoptosis in different cell types, i.e. leukocytes, cancer cells and skin cells [104, 130, 131]. Therefore, the first focus of this thesis was the investigation of cell survival and apoptosis induction for the different immune cell types, $CD4^+$ T helper cells and monocytes after plasma treatment with a kinpen 09 device (part 3.1 and 3.2). It could be shown that different cell types of the immune system differed in their sensitivity towards plasma.

Both annexin V/ 7AAD (Figure 3.4 and Figure 3.5) and caspase 3 assay (Figure 3.7) revealed an increased number of apoptotic cells in a plasma treatment time dependent manner in nearly all tested samples of the investigated cell types. Here, primary leukocytes showed a considerably higher amount of cells undergoing programmed cell death than their cell line counterparts. The reason why the examined cell lines tolerated higher plasma doses than the primary cells might be the fact that both cell lines descend from leukemia patients [12, 24, 100]. Their immortalization and adaption to cell culture conditions may have led to increased capability dealing with oxidative stress and preventing apoptosis. Moreover, blood monocytes and the respective THP-1 cell line were

Discussion

less sensitive to the induction of apoptosis than blood CD4$^+$ T helper cells and the Jurkat cell line in response to plasma. For THP-1 cells, only the longest treatment time of 360 s revealed an increased number of apoptotic cells. These results indicate strong resistance of monocytes towards plasma chemistry and radicals and that there must be differences in the defense and repair mechanisms between the investigated cells [100].

Next to the caspase 3 assay, cell counting was performed for the investigated cell types (Jurkat, THP-1 and primary monocytes). While the amount of apoptotic cells increased with the plasma treatment time, the cell numbers decreased. Next to the induction of programmed cell death the reduced cell count might be explained by cell cycle arrest in order to repair DNA damage, caused by plasma exposure [50, 130, 132]. In contrast to the cell lines, the inserted cell numbers were considerably reduced after the incubation time for primary monocytes for all examined conditions. In this context it has to be considered that primary monocytes have a relative short life span and are known to undergo spontaneous apoptosis on a daily basis [14]. Both cell lines similarly showed a slight increase in cell number after short plasma exposure (5 s). However, the time point of investigation 18 h after treatment (caspase 3 assay) was possibly too early to detect significantly increased differences in cell numbers. Thus, long term effects were determined by growth curves with the cell lines for a time period of 6 days. According to the apoptosis assays, growth curves showed that Jurkat cells were more susceptible to plasma treatment, since all investigated treatment times reduced the cell growth. In contrast, the cell growth curve trend was even higher for THP-1 cells treated for 30 s and 60 s than untreated control samples. The elevated cell counts indicate the stimulation of pro-proliferative processes in the cells after short plasma treatment. In this respect it is of great interest that Kalghatgi *et al.* observed similar effects for endothelial cells. Nevertheless, these cell numbers were not significantly increased and might be due to relatively high cell growth rates *per se* [50, 93].

72

Next to plasma treatment, cells were incubated with $100\,\mu M\,H_2O_2$ and $10\,\mu M$ etoposide, two substances that are known to evoke apoptosis [125, 133]. In all experiments dealing with survival and apoptosis of leukocytes, incubation with $100\,\mu M\,H_2O_2$ resembled a treatment time of 180 s. Direct H_2O_2 measurements in plasma-treated liquids revealed this concentration of $100\,\mu M$ after 180 s plasma exposure and are therefore in good agreement (personal communication with H. Tresp). However, in THP-1 monocytes treatment with $100\,\mu M\,H_2O_2$ did not induce apoptosis, while etoposide ($10\,\mu M$) was able to provoke apoptosis by induction of caspase 3 in these cells. On the one hand this might be due to an insufficient concentration of H_2O_2, since Okahashi *et al.* evidenced that application of H_2O_2 is a potent apoptosis inducer for THP-1 cells after applying $200\,\mu M$ [134]. On the other hand, this can be explained by different mode of action of the apoptosis-inducing agents H_2O_2 and etoposide. While H_2O_2 is known to cause chemical oxidation of cellular components leading to indirect DNA damage, etoposide is a direct DNA damaging substance (topoisomerase II inhibitor) that is known to cause double strand breaks [125, 135]. Different studies already evidenced that H_2O_2 is one of the major stable products in kinpen 09 (argon) plasma-treated cell culture medium [136, 137]. Thus, H_2O_2 seems to be one of the main long-living plasma components to affect cell viability in susceptible cells [100].

Altogether, CD4$^+$ T helper cells were more susceptible to plasma and H_2O_2 exposure compared to monocytes. One possibility for these differences between the cell types is the different origins of these cells. While CD4$^+$ T helper cells originate from lymphoid stem cells, monocytes descend from myeloid stem cells [5, 6]. Furthermore, the strong resistance of monocytes towards plasma chemistry and radicals may be also attributed to the fact that these phagocytes endogenously produce ROS such as H_2O_2 themselves during the respiratory burst to inactivate engulfed microorganisms [21, 50]. Thus, they express high copy numbers of anti-oxidant enzymes to protect themselves from the cytotoxic effects directed against microorganisms, for instance glutathione peroxidases, thioredoxin reductases and catalases [50, 138, 139].

Discussion

Next to the formation of H_2O_2, increased cell death and decreased cell viability may be amongst others affected by changes of the surrounding pH value. It has been already shown that the pH value of kinpen 09 treated medium was increased in a treatment time dependent manner [100], which can be explained by a degassing effect (release of carbon dioxide) due to the argon flow of the plasma jet the main component of the RPMI medium buffer system being the carbonate buffer sodium bicarbonate [100, 140]. The elevated pH level of the culture medium may contribute to apoptosis induction since it is known that alkaline stress can cause apoptosis in human cells [100, 141]. Additionally, it is already known that reactive species like superoxide anions and hydroxyl radicals are formed by plasma treatment of liquids [100, 136] and their stability also depends on pH value. This was accounted for by pre-incubation of the culture medium in a CO_2-incubator 18 h prior to each experiment. Moreover, it has to be further investigated what kind of reactive species are produced in plasma-treated liquids and which impacts these molecules have on cellular level.

In summary, it could be shown that the percentage of apoptotic leucocytes increased and the cell survival rate decreased with prolongation of the plasma treatment time. However, the magnitude of apoptosis induction was strongly dependent on the investigated cell type. Monocytes were less sensitive than $CD4^+$ T helper cells, whereas the cell lines displayed higher survival rates compared with their human blood counterparts [100].

4.2 Plasma-induced alteration of gene expression

Although multiple studies described the DNA damaging effect of non-thermal plasma treatment on mammalian cells [142, 143], only a few detailed approaches have been performed so far concerning the gene regulation by plasma exposure [96, 97, 144]. However, the mentioned studies only examined the impacts of plasma on skin cells (keratinocytes and fibroblasts), whereas immune cells have been widely neglected. In order to fill this gap, DNA microarray and subsequently qPCR analysis for distinct target genes were done

with both Jurkat CD4$^+$ T helper cells (part 3.3.1) as well as THP-1 monocytes (part 3.3.2).

Upon plasma treatment, Jurkat cells regulated much more genes compared to THP-1 cells as detected by DNA microarray analysis (Figure 3.8 and Figure 3.13). This is consistent with the finding that the Jurkat cell line was much more susceptible to plasma exposure referring to apoptosis induction (part 3.2). However, only a small number of regulated genes were found in both immune cell types in contrast to plasma-treated HaCaT keratinocytes (60 s), where Schmidt *et al.* found more than 1,000 differentially expressed genes [144]. One possible explanation could be that the incubation time of 3 h chosen in this study was relative short in comparison to the microarray approach of HaCaT cells that included incubation times from 3 h to 24 h. Nevertheless, immune cells have a totally different constitution handling oxidative stress, notably monocytes that produce RONS themselves [21, 145, 146]. Amongst others transcription factors and signaling molecules belonged to the protein classes with the most transcriptional alterations due to plasma treatment for Jurkat as well as for THP-1 cells found by Panther classification system (Figure 3.9 and Figure 3.14). Therefore, signaling pathways with the distinct molecules, found by IPA software, were further investigated by qPCR. In particular, gene expression of FOS and JUN was determined in Jurkat cells, while gene transcription of JUND, IL-8, HMOX-1 and GSR was examined in THP-1 cells.

Both expression of the transcription factors FOS and JUN, components of the AP-1 (activator protein 1), was induced in a plasma exposure time dependent way in Jurkat cells (Figure 3.11 and Figure 3.12). These transcription factors are known to be associated with different kinases of the MAPK signaling pathway. JUN is mainly phosphorylated by JNK, which enhances its transactivation potential [147]. Since an induction of the JNK pathway could be proven in this study (part 3.4.1), this activation of JUN expression will be one possible activation mechanism of non-thermal plasma treated cells. It is also a fact that FOS can be amongst others activated by ERK and p38 MAPK [148, 149] – another set of MAP kinases, which were found activated by non-thermal

Discussion

plasma (part 3.4.1). JUND gene expression was only slightly activated in THP-1 cells by non-thermal plasma treatment (Figure 3.16). JUND, a component of JUN, can be activated by phosphorylation of ERK and JNK, which has been reported to lead to survival signaling [120, 121]. This could be an explanation why plasma-treated THP-1 cells display higher survival rates than Jurkat cells when exposed for a short period (part 3.1). Furthermore, JUND has been reported to be essential for macrophage activation and cytokine secretion, which is important for a proper wound healing process [150]. Those findings support the data of an increased secretion of IL-8 due to a plasma treatment of THP-1 cells (Figure 3.23). In summary, FOS, JUN and JUND were regulated by plasma treatment in the investigated cells. These components of the AP-1 complex play key roles in cell fate decisions like DNA repair, apoptosis, cell survival, proliferation, activation and differentiation [117, 149].

Furthermore, transcription of the inflammatory cytokine IL-8 was induced in THP-1 cells by plasma treatment, especially after long plasma exposure of 360 s (Figure 3.17). As depicted in Figure 4.1 it was reported by Hoffmann *et al.* that ERK 1/2, as well as JNK 1/2 are able to stimulate the gene expression of IL-8, while p38 MAPK was shown to do post-transcriptional regulation of IL-8. However, ERK 1/2 was shown to be a weak inducer of IL-8 transcription. Amongst others, AP-1 is a transcriptional activator of IL-8, which is required for maximal gene expression [64]. IL-8 is crucial for the wound healing process, because it functions as a neutrophil chemoattractant and also enhances the respiratory burst and ROS generation of neutrophils [151]. Thus it can be hypothesized that this induction could be of importance for the initiation of wound healing, especially the hemostasis and inflammation phase.
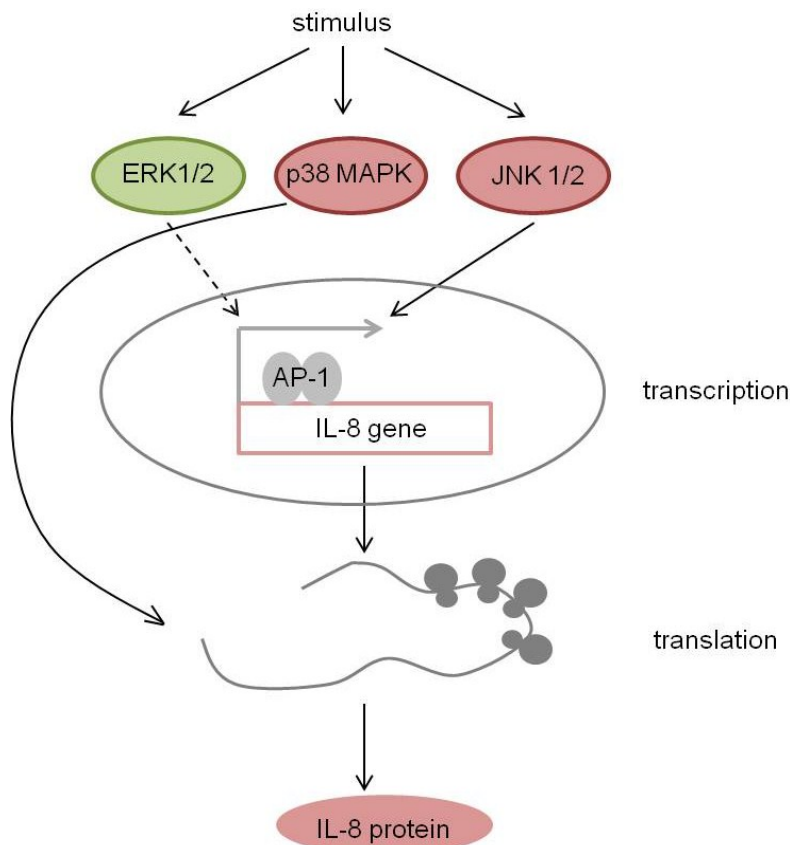
Figure 4.1: Schematic overview of the signal transduction steps of IL-8 gene regulation.
The canonical MAP kinases ERK 1/2, p38 MAPK and JNK 1/2 are activated through different mediators e.g. cytokines or growth factors. JNK 1/2 as well as ERK 1/2 are able to induce IL-8 gene transcription. Here, AP-1 is one possible transcription factor. Furthermore, p38 MAPK is known to stabilize IL-8 mRNA during the translation to the IL-8 protein. A solid line represents a strong and a dashed line a weak induction between molecules. Image adapted from [64].

Additionally, THP-1 cells showed a plasma-mediated increase of HMOX-1 (Figure 3.18), the gene encoding the heme oxygenase-1. Amongst others HMOX-1 gene expression can be transactivated by the transcription factor AP-1 in response to oxidative stress [152], since it catalyzes the oxidation of free heme to generate carbon monoxide (CO), biliverdin and iron (Fe^{2+}). Thus, this enzyme ensures anti-inflammatory, anti-oxidative and anti-apoptotic properties, which could be a possible explanation for the ability of plasma-treated THP-1 cells to avoid apoptosis [153]. Since HMOX-1 is under transcriptional regulation of not only AP-1 but also NRF2 (nuclear respiratory factor 2) [154], a number of other mechanisms might play a role in plasma-induced up-regulation of HMOX-1. Interestingly, HaCaT keratinocytes strongly increase their expression of HMOX-1 upon plasma treatment, which could be associated to translocation of NRF2 to the nucleus [155].

Discussion

Like heme oxygenase-1, glutathione reductase (GSR), which is another important enzyme of the cellular anti-oxidant defense system, was up-regulated after plasma treatment (Figure 3.19). This was also the case for plasma-treated HaCaT cells [144], pointing towards a cell-independent response mechanism towards plasma. Reduced glutathione (GSH) is an essential scavenger of free ROS (OH$^\bullet$ and H_2O_2) and peroxides, whereas it functions as an electron donor to form its oxidized form (GSSG) [156]. The oxidized form GSSG can be reduced to GSH by the enzyme GSR. In this way cells ensure that more GSSG is recycled to GSH, in order to scavenge more free radicals and therefore protect the macromolecules of the cell. An up-regulation of GSR displays a pronounced way of cells to protect themselves to endogenous ROS [157]. Since cells were only treated once and for a short period, the cellular protection lasted longer than the plasma-mediated ROS effects. This could explain the stimulation that has been seen in the plasma-treated THP-1 cells (Figure 3.2). Interestingly, glutathione-thiyl radicals (GS$^\bullet$) have been recently identified in plasma-treated THP-1 cells (personal communication with H. Tresp), pointing out that this reaction could be of importance in molecular mechanisms triggered by plasma treatment.

In summary, various plasma-modulated genes were identified for both cell lines, whereas an interference with the MAPK signaling pathways and IL-8 production was identified. Furthermore, it was shown that the activation levels of all examined genes peaked at either 6 h or 12 h after plasma treatment and were more or less reduced to the baseline level after an incubation time of 24 h. Moreover, in contrast to the apoptosis experiments (part 3.2), treatment with 100 µM H_2O_2 yielded different gene expression levels than cells treated for 180 s. However, unpublished data from the authors working group revealed that H_2O_2 is a stable component of plasma-treated medium (personal communication with J. Winter). Hence, other RONS may play an inferior role in plasma-cell-interaction although this needs further research.

78

4.3 Modulation on protein level after non-thermal plasma treatment

Furthermore, alterations in the activation levels of MAPKs and production of different cytokines were found in the investigated immune cells due to plasma treatment as discussed in the following two sections.

4.3.1 Plasma-mediated MAPK signaling

Since plasma exposure induced the expression of various genes associated with the MEK-ERK, p38 MAPK and JNK pathways, the activation of these canonical MAPKs and the related heat shock protein 27 (HSP27) was determined by western blotting technique for plasma-treated Jurkat cells, THP-1 and primary monocytes (part 3.4.1).

For all investigated cell types it could be shown that the ERK-MEK pathway as well as the p38 MAPK and JNK cascades were activated in a treatment time dependent manner in response to plasma treatment (Figure 3.20, Figure 3.21 and Figure 3.22). However, HSP27 activation could only be detected in THP-1 monocytes.

Comparing both cell lines, THP-1 cells generally responded less sensitive to plasma treatment than Jurkat cells. This could be demonstrated by lower activation signals of the pro-proliferative MEK-ERK signaling pathway as well as pro-apoptotic p38 MAPK and JNK cascades after applying the same plasma treatment times. Next to the strong resistance of monocytes towards plasma chemistry and radicals already discussed in part 4.1, the capability of plasma-treated THP-1 cells to evade pro-apoptotic signaling pathways might be due to the expression of HSP27 (Figure 3.21). HSP27 is known to oligomerize to prevent a cytochrome c dependent activation of caspase 3 [50, 158]. This indicates that HSP27 activation might play a key role in these cells in evading apoptosis after plasma treatment. In contrast, expression of HSP27 and p-HSP27 was too low in all Jurkat samples to be measured accurately. This

Discussion

finding is consistent with data from De *et al.*, who showed that Jurkat cells lack sufficient HSP27 expression [50, 159]. It is to take into consideration that T cells have completely other cellular functions and signaling structures than monocytes. For instance, p38 MAPK and JNK not only induce apoptosis but also contribute to TCR signaling in these cells [50, 160]. Additionally, p38 MAPK signaling is known to be required for T cell mediated immunity. Induction of p38 MAPK leads to IFNγ production of CD4$^+$ T helper cells that can activate macrophages and consequently might also trigger an immune response [50, 161].

Interestingly, for primary monocytes it could be shown that the short plasma treatment times (30 s and 60 s) were able only to induce the pro-proliferative MEK-ERK pathway, while the pro-apoptotic cascades p38 MAPK and JNK were only switched on after the longer plasma durations (180 s and 360 s). Activation of both MEK 1/2 and ERK 1/2 of plasma-treated primary monocytes revealed the same trends as the plasma-treated THP-1 monocyte cell line. However, the yielded levels were considerably higher for the investigated primary cells. The activation of the MEK-ERK pathway is known to be important for the transformation from monocytes to M1 macrophages, which is essential for a proper wound healing process. Furthermore, it has been reported that the MEK-ERK signaling pathway was weakened in diabetic rats, which was associated with impaired wound regeneration [48, 162, 163]. Thus, plasma treatment could be one option to reactivate this pathway in monocytes and subsequently contribute to a proper wound healing process.

Both the p38 MAPK and JNK cascade have been reported to be involved in oxidative stress mediated-apoptosis induction [48, 164]. Especially long-term plasma treatment times led to an accumulation of reactive species in the cell culture medium [48, 114]. This could be a possible explanation why p38 MAPK and JNK 1/2 were only activated after the long plasma exposure times (180 s and 360 s). This is consistent with caspase 3 data of primary monocytes (Figure 3.7), which showed that about 70 % of 180 s and 80 % of 360 s plasma-treated monocytes were positive for this apoptotic marker [48]. In contrast to THP-1

cells, no distinct bands could be detected for HSP27 and phospho-HSP27 on the corresponding western blot membranes. One explanation could be that primary monocytes do not overexpress HSP27 in response to plasma treatment, which would also clarify why they are reacting more sensitive to this treatment. Another interpretation is the possibility of oligomerization between HSP27 and other heat shock proteins, which would result in an alteration of the molecular mass [165].

To trigger the pro-proliferative MEK-ERK signaling cascade, PHA (1 μg/mL) was used as a control for Jurkat CD4$^+$ T helper cells and LPS (1 μg/mL) for THP-1 as well as primary monocytes. As described by Li *et al.* the ERK-MEK pathway was activated in Jurkat cells by PHA treatment – an established stimulus for T lymphocytes [50, 127]. In the literature, an activation of ERK in response to LPS stimulation (10 μg/mL) in THP-1 cells was described with a maximum at 15 min after treatment [50, 166]. However, in this study only ERK 1 showed slight up-regulation in THP-1 cells activated with 1 μg/mL LPS after the same incubation time. In this set-up this low LPS concentration used was not sufficient to induce a significant activation of the ERK-MEK cascade. However, LPS induced JNK and p38 MAPK activation in THP-1 cells, which agrees with data published by Guha *et al.*, who described an activation of these MAPKs in human monocytes in response to LPS treatment [50, 167]. Nevertheless, the used LPS concentration was sufficient to up-regulate both MEK 1/2 and ERK 1/2 in the primary monocytes, which agrees with the findings described by Liu *et al.* for monocytes [48, 63]. In contrast, incubation with LPS induced neither p38 MAPK nor JNK 1/2 in primary monocytes. This result is consistent with data from Heidenreich *et al.* who showed that LPS is able to activate monocytes by expression of CD14, which leads to increased survival and evasion of apoptosis [126].

Cells incubated with 100 μM H_2O_2 served as positive controls for the activation of the pro-apoptotic pathways for all investigated cell types. All investigated MAPK cascades were not only induced by plasma- but also by H_2O_2-treatment. H_2O_2 was identified as one major ROS in the plasma jet kinpen 09 and in

treated liquids. Moreover, it possesses a relative longevity compared with other produced species [50, 106, 137]. ROS production could be also a possible explanation why the ERK-MEK cascade is induced in response to plasma as well as to H_2O_2. Next to stimulating substances, this pro-survival pathway is known to be activated by oxidative stress in different cell types [50, 168, 169]. However, it is a known fact that H_2O_2 at low doses is able to stimulate cells growth [50, 170]. As shown by Matsukawa and colleagues, H_2O_2 also activated the pro-apoptotic MAPK cascades [50, 171], similar to the plasma activation of the investigated immune cells. In THP-1 cells, H_2O_2 additionally induced the chaperon HSP27, which is known to be activated through MAPKAP kinase-2, a kinase, which itself can be induced by p38 MAPK [50, 57, 58]. This also supports or findings of the elevated phosphorylation states of the p38 MAPK in the investigated immune cells.

In conclusion, all investigated cell types showed more or less strong plasma-mediated activation of the different MAP kinases, indicating that these kinases are important intracellular plasma responses.

4.3.2 Plasma-modulated cytokine secretion

MAPK signaling is associated with the expression and secretion of various inflammatory cytokines, including IL-6 and IL-8 [64, 66]. Hence, cytokine production was examined in plasma-treated Jurkat cells, THP-1 cells, primary monocytes, as well as THP-1 cells co-cultured with HaCaT keratinocytes. Even though a wide range of cytokines was tested, most of them showed no alteration due to plasma treatment or were below the detection level (Table 3.1).

Cytokine secretion in mono-cultured cells

In good agreement with the plasma-regulated induction of IL-8 gene expression (Figure 3.17), IL-8 secretion could be shown to be induced with plasma treatment in THP-1 cells (Figure 3.23). Even though there was no significant alteration of IL-8 secretion for THP-1 cells plasma-treated for 180 s or

100 µM H_2O_2, THP-1 cells that were plasma-exposed for 360 s yielded a significantly increased IL-8 concentration in the cell culture medium, especially after the incubation times of 12 h and 24 h. This induction of pro-inflammatory IL-8 could contribute to an increased accumulation of neutrophils during inflammation phase of wound healing, which was already observed by Arndt *et al.* in a mouse model that was treated with non-thermal plasma [97, 151]. A possible explanation for the IL-8 induction after a treatment time of 360 s is that the highest activation levels of the kinases ERK 1/2, p38 MAPK and JNK 1/2 were reached after this plasma treatment time in these cells (Figure 3.21). As reported by Hoffmann *et al.* and displayed in Figure 4.1, these MAPKs are known to promote IL-8 gene expression and translation [64]. Interestingly, intracellular IL-8 content of primary monocytes stayed constant for the short treatment times (30 s and 60 s) and decreased with longer plasma treatment times (180 s and 360 s) 6 h after plasma treatment (Figure 3.24). Here the comparison between primary monocytes and THP-1 monocytes is only possible with restriction. The apoptotic cascades p38 MAPK and JNK were only activated in primary monocytes in response to the long plasma treatment times, which were shown to induce high apoptosis rates compared to the short treatment times (Figure 3.7) and also to the THP-1 cell line. This induction of apoptosis and the fact that ERK 1/2 is not a very potent stimulant of IL-8 gene expression could be the reason why IL-8 production was not activated in response to plasma treatment [48, 64]. Additionally, the incubation time of 6 h that was chosen due to the intracellular staining requirements, might have been too short, since the highest IL-8 concentrations for THP-1 cells were measured 12 h and 24 h after plasma treatment (Figure 3.23).

In contrast to IL-8, an up-regulation of intracellular IL-6 could be demonstrated for primary monocytes treated for 30 s. While a treatment time of 60 s resembled the untreated control, longer plasma exposure led to a decrease of the intracellular IL-6 level. The inflammatory mediator IL-6 has been shown to be up-regulated upon ERK 1/2 activation in human monocytes [48, 66]. IL-6 production in response to ERK 1/2 signaling could be one explanation for the induced number of IL-6 expressing cells after a plasma treatment time of 30 s. It

Discussion

has also been reported that NRF2 is able to induce IL-6 expression, which potentially plays a role in oxidative stress defense [48, 172]. That could also clarify the elevated IL-6 level after 30 s of plasma treatment. Oxidative stress can be amongst others triggered by direct impact of ROS [173]. These species are generated through the interaction of a plasma jet effluent and the ambient air [48, 85]. The concentrations of the ROS transferred to the culture medium might have been below a cytotoxicity threshold for the short plasma treatment times in contrast to long plasma exposure [48]. Here, the cytotoxic level of generated ROS might have been too high, which is known to induce high apoptosis rates (part 3.2). Moreover, it is now widely accepted that small amounts of ROS stimulate cells and may activate cytokine production [174].

Incubation with 1 µg/mL LPS led to a similar IL-8 expression level of primary monocytes as the untreated control and the short treatment times. Schaub *et al.* evidenced a stimulation of IL-8 secretion of monocytes through LPS [175]. However, this study was performed with a ten times higher LPS concentration (10 µg/mL), which could explain the different outcome of this experiment [48]. In contrast, LPS stimulation yielded an up-regulation of the intracellular IL-6 level, which is consistent with data from Schildberger *et al.*, who demonstrated an enhanced IL-6 secretion after LPS stimulation [176].

IL-8 secretion of THP-1 cells that were treated with 100 µM H_2O_2 were not altered compared to control. This finding is in good agreement with nearly constant levels of IL-8 gene expression upon treatment with the same amount of H_2O_2. Incubation with 100 µM H_2O_2 did significantly reduced the intracellular IL-8 and IL-6 levels in primary monocytes similar to the long treatment times. Since this treatment resulted in a decreased number of cells expressing IL-8 like the long treatment times, it can be assumed that H_2O_2 produced in plasma-treated liquids [137] plays an essential role in the decrease of cell viability (part 3.2) and the subsequent reduction of these cytokines.

In summary, THP-1 cells as well as primary monocytes displayed plasma-regulated production of IL-8. An elevation of this cytokine was observed for

THP-1 cells. However, a decrease for IL-8 was detected intracellular in primary monocytes with increasing plasma treatment time. Primary monocytes additionally showed an induction of IL-6 production after a short plasma treatment time (30 s), while longer treatment resulted in decreased IL-6 expression.

Cytokine secretion in a co-culture approach

In order to investigate, whether and how epithelial HaCaT cells and immune cells interact with each other via cytokine secretion, a co-culture approach was conducted. Cytokine production of co-cultivated THP-1 and HaCaT cells was compared to mono-cultivated THP-1 and HaCaT cells. Cells were either left untreated, were plasma-treated (180 s) or were plasma-(180 s) and LPS-(1 µg/mL) treated. Four cytokines were found to be affected under these conditions – IL-8, IL-6, GM-CSF and TNFα (Figure 3.25).

Generally, secretion of IL-8 and IL-6 behaved in a similar way. Induction of these cytokines was observed in mono-cultivated HaCaT and in combination with THP-1 cells upon plasma treatment, while mono-cultivated HaCaT cells always revealed slightly higher levels. Whereas no IL-6 and low not regulated IL-8 concentrations were found in untreated and 180 s treated THP-1 cells. Thus, the increased cytokine amount in the co-culture seems to be released mainly by plasma-treated HaCaT keratinocytes. The induction of IL-6 gene expression in HaCaT keratinocytes in response to plasma treatment was already demonstrated by Barton *et al.* and is supposed to be induced by RONS generated in the plasma-treated cell culture medium [96, 172, 177]. However, IL-8 was already found to be regulated in THP-1 cells after applying a long plasma treatment time of 360 s (Figure 3.23), which was supposed to be triggered by ERK, p38 MAPK and JNK signaling [64]. These cascades could be also the reason for the IL-8 induction in HaCaT and co-cultured cells, since they are also known to be switched on in HaCaT cells in response to plasma treatment [178]. Incubation with plasma- and LPS-exposed medium led to the highest cytokine secretion of all investigated condition, whereas the co-

Discussion

cultivated cells revealed the highest IL-8 and IL-6 concentrations. Remarkably are the very high concentrations of the cytokines in the co-culture approach that slightly exceeded the sum of individual cells. This outcome can be explained with the fact that both cell lines are reported to secrete IL-8 as well as IL-6 upon stimulation with LPS [179, 180]. GM-CSF secretion revealed a similar trend as described for IL-8 and IL-6 even though all GM-CSF levels were relatively low. In THP-1 mono-cultivated cells this cytokine was below the detection limit in all investigated conditions. HaCaT as well as co-cultured cells displayed an increase in GM-CSF production after plasma treatment. Plasma-induced GM-CSF gene expression in HaCaT cells was recently evidenced by Barton *et al.* [96]. Since keratinocytes are known to produce this cytokine during early wound healing phases to attract phagocytic immune cells and to promote epidermal keratinocyte proliferation [181], it is not surprising that the additional presence of LPS enhanced the secreted concentration of GM-CSF. Interestingly, an induction of TNFα secretion was only observed in THP-1 cells that were treated with plasma and LPS. It was already reported that LPS is able to induce TNFα expression in these cells [180]. However, also the co-cultured cells that were plasma- as well as LPS-treated showed no regulation of this cytokine. Thus, it is assumed that TNFα produced by THP-1 cells bound with high affinity to the TNFα receptors on the cell surface of keratinocytes, which led to TNFα-mediated IL-8 and IL-6 production in these cells [182, 183]. This might be a possible explanation why co-cultivated plasma- and LPS-treated cells revealed the highest levels of these cytokines, although the concentrations of these cytokines were slightly under the mono-cultivated HaCaTs for untreated and plasma-treated conditions.

These results are very promising, since plasma-treated HaCaT keratinocytes and THP-1 cells in the presence of the bacterial component LPS are able to induce the expression of the inflammatory cytokines IL-8, IL-6 and GM-CSF, which are needed for a proper wound healing process.

In conclusion, this thesis demonstrated that human immune cells display different sensitivities towards cell survival and proliferation in response to

plasma treatment. Furthermore, it was shown that non-thermal plasma can stimulate human cell activities by activating different signaling cascades, the expression of various genes and production of different cytokines. These findings suggest that non-thermal plasma-treated immune cells might be able to actively contribute to wound healing.

5 Outlook

For the first time, we gained insights into intra- and inter- cellular signaling events after non-thermal plasma exposure in human immune cells. Here, the CD4$^+$ T helper cell line Jurkat and the monocyte cell line THP-1 as well as the corresponding primary cells have been examined. Although a lot of new findings evolved from this work, many new questions emerged.

Within this work, protein phosphorylation of some distinct proteins has been investigated, though direct modification due to oxidation or nitrosylation has not been looked at of protein level. Here, mass spectrometry could shed some light in this issue.

Although working with cell lines is more convenient and an effective tool for establishing experiments, it is necessary for future research to keenly focus on the effects of non-thermal plasma treatment on primary immune cells. These cells are closer to the *in vivo* situation and may reveal differences between healthy donors and patients with chronic wounds. In this issue it could be of great value to correlate genomic with proteomic analyses. Additionally, not only T cells and monocytes should be studied but also neutrophils, macrophages and dendritic cells are of importance in the wound healing process. Since various cells are involved in wound healing, mouse models that develop either an acute or a chronic wound could be a good option to study this complex interaction of skin and immune cells in respect to their reaction to plasma treatment.

Furthermore, studies regarding plasma-cell interactions as well as liquid and plasma diagnostics should be intensified. For a better understanding of the plasma-mediated effects it is important to know what molecules are generated by plasma and how they can affect both, immune and skin cells.

6 Summary

Non-thermal atmospheric pressure plasma has drawn more and more attention to the field of wound healing research during the last two decades. It is characterized by a unique composition, which includes free radicals, ions, electrons, excited and neutral species, electric fields, UV, infra-red, and thermal radiation. Furthermore, non-thermal plasma exhibits temperatures that are below those inducing thermal cell damage. Next to its well-established anti-bacterial properties, plasma can have lethal as well as stimulating effects on mammalian cells. Therefore, the medical application of non-thermal plasma on chronic wounds seems to be a promising tool to enable healing processes. However, less is known about the induction of intracellular signaling pathways in human cells after plasma exposure. While some studies already investigated the cellular plasma-mediated impacts on skin cells, immune cells have been widely neglected. Nevertheless, immune cells play a leading part in the process of wound recovery and removal of pathogens as well as debris.

Therefore, this thesis examined the cellular effects of a non-thermal atmospheric pressure plasma treatment on human immune cells using the argon plasma jet kinpen 09. Here, the CD4$^+$ T helper cell line Jurkat, the monocyte cell line THP-1 as well as the corresponding primary cells were investigated.

First, cell survival and apoptosis induction was assessed in response to non-thermal plasma treatment by growth curves and flow cytometric assays. On the one hand it could be shown that primary cells are more susceptible to plasma treatment than the respective cell lines. On the other hand, monocytes responded less sensitive to plasma exposure than lymphocytes, indicating strong resistance of monocytes towards radicals and other reactive oxygen species (ROS).

Furthermore, this thesis outlined the impact of non-thermal plasma treatment on the gene expression level of immune cells. Therefore, DNA microarray analysis

Summary

was performed with the cell lines Jurkat and THP-1. It became obvious that plasma exposure modulated the expression of several genes in both cell types. Interestingly, there was only little concordance between both cell lines. Differential expression of distinct target genes was further validated by quantitative PCR in the immune cell lines. Here, elevated gene expression levels of JUN (Jun proto-oncogene) and FOS (FBJ murine osteosarcoma viral oncogene homolog) in Jurkat cells and increased transcription of JUND in THP-1 cells in response to plasma treatment were made visible. JUN, FOS and JUND are components of the transcription factor AP-1 (activator protein 1), which is involved amongst others in gene expression of interleukin 8 (IL-8) and heme oxygenase 1 (HMOX-1). Consequently, transcriptional induction of the inflammatory cytokine IL-8 as well as the enzymes HMOX-1 and GSR (glutathione reductase) was detected in plasma-treated THP-1 cells. The up-regulation of these anti-oxidant enzymes could be one possibility why THP-1 monocytes tolerate much higher plasma treatment durations than Jurkat cells, where this regulation could not be found.

In addition, alterations in the protein activation levels were analyzed in plasma-treated Jurkat, THP-1 cells and primary monocytes. Since some of the identified target genes are known to be associated with the MAPK (mitogen-activated protein kinase) pathways, the regulation of these cascades was further investigated by western blot analysis. In all investigated cell types the pro-proliferative signaling molecules ERK 1/2 (extracellular signal-regulated kinase 1/2) and MEK 1/2 (MAPK/ERK kinase 1/2) as well as the pro-apoptotic signaling proteins p38 MAPK (p38 mitogen-activated protein kinase) and JNK 1/2 (c-Jun N-terminal kinase 1/2) were activated in a plasma treatment time dependent manner. Remarkably, primary monocytes revealed an induction of the pro-proliferative MEK-ERK pathway already after short plasma treatment times (30 s and 60 s), while the pro-apoptotic cascades p38 MAPK and JNK were only activated after longer plasma exposure durations (180 s and 360 s). This demonstrates that the choice of the right treatment time allows switching on specific pathways or leaving them deactivated. In contrast to Jurkat and primary monocytes, the anti-apoptotic HSP27 (heat shock protein 27) was only induced

in THP-1 cells in response to plasma exposure, indicating a possible mechanism how THP-1 cells may deal plasma-mediated ROS stress.

Moreover, modulation of cytokine production and secretion was examined in the different immune cell types and co-cultured THP-1 and HaCaT keratinocytes by ELISA or flow cytometry. Jurkat cells showed no plasma-mediated regulation of cytokine expression. In contrast, THP-1 cells revealed an increased IL-8 secretion after long plasma time duration (360 s). Additionally, the intracellular expression levels of IL-6 and IL-8 were modulated in primary monocytes by plasma exposure. While short plasma treatment caused no alteration of the number of cells expressing IL-8 an up-regulation of the intracellular IL-6 level occurred after 30 s of plasma treatment. Long plasma treatment times resulted in a significant decrease of the intracellular IL-8 and IL-6 production levels. Furthermore, co-cultured THP-1 and HaCaT cells as well as mono-cultured THP-1 and HaCaT cells were examined regarding their cytokine secretion profile. Here, cells treated with plasma (180 s) as well as LPS (lipopolysaccharides) and plasma (180 s and LPS) were compared with untreated cells. IL-6, IL-8 and GM-CSF secretion was induced by both plasma and plasma combined with LPS treatment in mono-cultivated HaCaT cells and co-cultured cells. Though, the highest cytokine secretion levels were reached in the plasma and LPS exposed co-culture. In contrast, mono-cultivated THP-1 cells only showed an increased secretion of IL-6, IL-8 and TNFα after incubation with plasma together with LPS exposed medium.

In conclusion, this study revealed for the first time the non-thermal plasma-modulated expression of numerous genes and cytokines and the activation state of various signaling cascades in human immune cells. Thus, it contributes to gain a better understanding of the immune-modulatory impacts of plasma that might promote the wound healing process.

7 Zusammenfassung

Unter Atmosphärendruck erzeugtes Niedertemperaturplasma hat in den letzten zwei Jahrzehnten immer mehr an Aufmerksamkeit in der Wundheilungsforschung auf sich gezogen. Niedertemperaturplasma zeichnet sich durch eine einzigartige Zusammensetzung aus, da es freie Radikale, Ionen, Elektronen sowie angeregte und neutrale Spezies, elektrische Felder, UV-, Infrarot- und Wärmestrahlung einschließt. Plasma kann neben seinen bekannten antibakteriellen Eigenschaften sowohl letale als auch stimulierende Effekte auf Säugetierzellen ausüben. Aus diesem Grund scheint die medizinische Anwendung von Niedertemperaturplasma auf chronischen Wunden eine erfolgversprechende Anwendung zu sein, die den Wundheilungsprozess unterstützt. In der Wissenschaft ist bis heute wenig über die Auswirkung von Plasma auf intrazelluläre Signalwege humaner Zellen bekannt. Während einzelne Studien Effekte von Plasma auf Hautzellen erforscht haben, wurde die Auswirkung von Plasma auf Immunzellen weitestgehend vernachlässigt. Jedoch spielen Immunzellen eine wichtige Rolle im Wundheilungsprozess sowie bei der Beseitigung von Pathogenen und Zelltrümmern.

Die vorliegende Arbeit untersucht mit Hilfe eines durch Argon betriebenen Plasmajets (kinpen 09) die zellulären Effekte von Niedertemperaturplasma auf humane Immunzellen. Im Fokus der vorliegenden Untersuchung stehen sowohl die CD4$^+$ T Helferzelllinie Jurkat als auch die Monozytenzelllinie THP-1 sowie die entsprechenden Primärzellen.

Zu Beginn wurden die Zellviabilität und die Apoptoseinduktion nach Behandlung mit Niedertemperaturplasma mittels Wachstumskurven sowie Durchflusszytometrie untersucht. Dabei wurde zum einen nachgewiesen, dass Primärzellen empfänglicher für die Plasmabehandlung sind als ihre entsprechenden Zelllinien. Zum anderen wurde gezeigt, dass die Lymphozyten deutlich empfindlicher auf die Plasmabehandlung reagierten als die Monozyten. Das kann als Hinweis darauf verstanden werden, dass Monozyten eine starke

Abwehrfunktion gegenüber Radikalen und anderen reaktiven Sauerstoffspezies (ROS/ reactive oxygen species) besitzen.

Ein weiterer Schwerpunkt dieser Arbeit lag auf der Erforschung von Auswirkungen einer Niedertemperaturplasmabehandlung auf die Genexpression von Immunzellen. Dafür wurden genomweite Genexpressionsanalysen mittels einer DNA Microarray Untersuchung der Zelllinien Jurkat und THP-1 durchgeführt. Dabei konnte gezeigt werden, dass Plasmaexposition in beiden untersuchten Zellarten die Expression verschiedener Gene beeinträchtigt. Interessanterweise wurden nur wenige Übereinstimmungen zwischen den beiden Zelllinien gefunden. Die differenzielle Expression bestimmter Zielgene in den Immunzelllinien wurde mittels quantitativer PCR weiter validiert. Hierbei konnte eine erhöhte Genexpression von JUN (Jun proto-oncogene) und FOS (FBJ murine osteosarcoma viral oncogene homolog) in Jurkat Zellen und eine verstärkte Transkription von JUND in THP-1 Zellen gezeigt werden. JUN, FOS und JUND gehören zum Transkriptionsfaktor AP-1 (activator protein 1), der unter anderem an der Genexpression von Interleukin-8 (IL-8) und der Hämoxygenase-1(HMOX-1/ heme oxygenase 1) beteiligt ist. Die Gentranskription des inflammatorischen Zytokins IL-8 und der Enzyme HMOX-1 sowie Glutathion Reduktase (GSR/ glutathione reductase) wurde in plasmabehandelten THP-1 Zellen induziert. Die Hochregulation dieser antioxidativ wirkenden Enzyme könnte eine Möglichkeit sein, weshalb THP-1 Monozyten eine höhere Plasmabehandlungsdauer tolerieren als Jurkat Zellen, in denen diese Regulation nicht gefunden wurde.

Des Weiteren wurden Veränderungen des Proteinaktivierungslevels in Jurkat Zellen, THP-1 Zellen und primären Monozyten nach einer Plasmabehandlung untersucht. Da mehrere der identifizierten Zielgene mit den MAPK (mitogen-activated protein kinase) Signalwegen zusammenhängen, wurde die Regulation dieser Kaskaden mit Western Blot Analysen untersucht. Dabei konnte in allen untersuchten Zellarten eine plasmabehandlungszeitabhängige Aktivierung sowohl der proproliferativen Moleküle ERK 1/2 (extracellular signal-regulated kinase 1/2) und MEK 1/2 (MAPK/ERK kinase 1/2) als auch der

Zusammenfassung

proapoptotischen Signalproteine p38 MAPK (p38 mitogen-activated protein kinase) und JNK 1/2 (c-Jun N-terminal kinase 1/2) nachgewiesen werden. Besonders auffallend war, dass der proproliferative MEK-ERK Signalweg in primären Monozyten schon nach kurzen Behandlungszeiten (30 s und 60 s) angeschaltet wurde, wohingegen die proapoptotischen Kaskaden p38 MAPK und JNK erst nach längeren Plasmabehandlungszeiten (180 s und 360 s) induziert wurden. Dies zeigt, dass allein durch die richtige Wahl der Behandlungszeit eine Option besteht, die entsprechenden Signale mithilfe von gezielten Plasmabehandlungen anzuregen oder deaktiviert zu belassen. Im Gegensatz zu Jurkat Zellen und primären Monozyten wurde durch Plasmabehandlung in THP-1 Zellen zusätzlich das antiapoptotische Hitzeschockprotein 27 (HSP27/ heat shock protein 27) aktiviert, was ein mögliches Charakteristikum dieser Zellen sein könnte, dem plasmavermittelten oxidativen Stress zu begegnen.

Zudem wurde die veränderte Zytokinproduktion und Sekretion in unterschiedlichen Immunzelltypen und kokultivierten THP-1 und HaCaT Keratinozyten durch ELISA- oder Durchflusszytometrieuntersuchungen analysiert. Jurkat Zellen wiesen dabei keine plasmavermittelte Regulation der Zytokinexpression auf. Dagegen konnte in THP-1 Zellen eine erhöhte IL-8 Sekretion nach einer langen Plasmabehandlungszeit (360 s) nachgewiesen werden. Darüber hinaus wurden die intrazellulären IL-6 und IL-8 Expressionslevel in primären Monozyten durch Plasmabehandlung reguliert. Während eine kurze Plasmaexposition keinen veränderten Anteil von IL-8 exprimierenden Zellen mit sich zog, konnte eine Hochregulation des intrazellulären IL-6 Levels nach einer Behandlungszeit von 30 s nachgewiesen werden. Lange Plasmabehandlungszeiten führten allerdings zu einer signifikanten Reduktion von IL-6 und IL-8 exprimierenden Zellen. Des Weiteren wurden kokultivierte THP-1 und HaCaT Keratinozyten hinsichtlich ihrer Zytokinsekretionsprofile untersucht. Dabei wurden Zellen sowohl mit Plasma (180 s) als auch mit Lipopolysacchariden (LPS/ lipopolysaccharides) und Plasma (LPS und 180 s) behandelt und mit unbehandelten Zellen verglichen. Hierbei konnte gezeigt werden, dass die IL-6, IL-8 und GM-CSF Sekretion nach

einer reinen Plasmabehandlung und nach einer kombinierten Plasma- und LPS-Behandlung sowohl in monokultivierten HaCaT Zellen als auch in kokultivierten Zellen induziert wurde. Die höchsten Zytokinsekretionslevel wurden jedoch in den kokultivierten Zellen ermittelt, welche sowohl mit Plasma als auch LPS behandelt wurden. Dagegen konnte in monokultivierten Plasma- und LPS-behandelten THP-1 Zellen lediglich eine erhöhte Sekretion von IL-6, IL-8 und TNFα identifiziert werden.

Erstmalig konnte in der vorliegenden Arbeit gezeigt werden, dass Niedertemperaturplasma die Expression zahlreicher Gene und Zytokine und den Aktivierungszustand von verschiedenen Signalkaskaden in humanen Immunzellen verändern kann. Daher trägt die Arbeit zu einem besseren Verständnis der Auswirkungen von Plasma auf Zellen des Immunsystems und deren Regulation bei, welche für den Wundheilungsprozess förderlich sein könnten.

8 Literature

[1]   **Medzhitov R and Janeway C Jr.** (2000): *Innate immunity*. N Engl J Med. 343 (5): 338-44.

[2]   **Janeway C, Murphy K, Travers P and Walport M**. (2007): *Immunobiology*. 7 ed. Garland Science; New York. 928.

[3]   **Bonilla FA and Oettgen HC**. (2010): *Adaptive immunity*. J Allergy Clin Immunol. 125 (2 Suppl 2): S33-40.

[4]   **Todar K**. *Todar´s online texbook of bacteriology.* [20.11.2013]. Available from: www.textbookofbacteriology.net.

[5]   **Akashi K, Traver D, Miyamoto T and Weissman IL**. (2000): *A clonogenic common myeloid progenitor that gives rise to all myeloid lineages*. Nature. 404 (6774): 193-7.

[6]   **Kondo M, Weissman IL and Akashi K**. (1997): *Identification of clonogenic common lymphoid progenitors in mouse bone marrow*. Cell. 91 (5): 661-72.

[7]   **Broere F, Apasov SG, Sitkovsky MV and van Eden W**. (2011): *A2 T cell subsets and T cell-mediated immunity*. 3 ed. Birkhäuser Basel; Basel. 15-27.

[8]   **Banchereau J and Steinman RM**. (1998): *Dendritic cells and the control of immunity*. Nature. 392 (6673): 245-52.

[9]   **da Silva Martins M and Piccirillo CA**. (2012): *Functional stability of Foxp3+ regulatory T cells*. Trends Mol Med. 18 (8): 454-62.

[10]   **Luckheeram RV, Zhou R, Verma AD and Xia B**. (2012): *CD4(+)T cells: differentiation and functions*. Clin Dev Immunol. 2012: 1-12.

[11] **Cai Y, Shen X, Ding C, Qi C, Li K, Li X, Jala VR, Zhang HG, Wang T, Zheng J and Yan J**. (2011): *Pivotal role of dermal IL-17-producing gammadelta T cells in skin inflammation*. Immunity. 35 (4): 596-610.

[12] **Schneider U, Schwenk HU and Bornkamm G**. (1977): *Characterization of EBV-genome negative "null" and "T" cell lines derived from children with acute lymphoblastic leukemia and leukemic transformed non-Hodgkin lymphoma*. Int J Cancer. 19 (5): 621-6.

[13] **Whitelaw DM**. (1972): *Observations on human monocyte kinetics after pulse labeling*. Cell Tissue Kinet. 5 (4): 311-7.

[14] **Parihar A, Eubank TD and Doseff AI**. (2010): *Monocytes and macrophages regulate immunity through dynamic networks of survival and cell death*. J Innate Immun. 2 (3): 204-15.

[15] **Hume DA**. (2006): *The mononuclear phagocyte system*. Curr Opin Immunol. 18 (1): 49-53.

[16] **Zanoni I, Ostuni R, Marek LR, Barresi S, Barbalat R, Barton GM, Granucci F and Kagan JC**. (2011): *CD14 controls the LPS-induced endocytosis of Toll-like receptor 4*. Cell. 147 (4): 868-80.

[17] **Akira S and Takeda K**. (2004): *Toll-like receptor signalling*. Nat Rev Immunol. 4 (7): 499-511.

[18] **Dale DC, Boxer L and Liles WC**. (2008): *The phagocytes: Neutrophils and monocytes*. Blood. 112 (4): 935-45.

[19] **Leon B, Lopez-Bravo M and Ardavin C**. (2005): *Monocyte-derived dendritic cells*. Semin Immunol. 17 (4): 313-8.

[20] **MacMicking J, Xie QW and Nathan C**. (1997): *Nitric oxide and macrophage function*. Annu Rev Immunol. 15: 323-50.

[21] **Forman HJ and Torres M**. (2002): *Reactive oxygen species and cell signaling: Respiratory burst in macrophage signaling*. Am J Respir Crit Care Med. 166 (12 Pt 2): S4-8.

[22]   **Baran CP, Zeigler MM, Tridandapani S and Marsh CB**. (2004): *The role of ROS and RNS in regulating life and death of blood monocytes*. Curr Pharm Des. 10 (8): 855-66.

[23]   **Mahdavian Delavary B, van der Veer WM, van Egmond M, Niessen FB and Beelen RH**. (2011): *Macrophages in skin injury and repair*. Immunobiology. 216 (7): 753-62.

[24]   **Tsuchiya S, Yamabe M, Yamaguchi Y, Kobayashi Y, Konno T and Tada K**. (1980): *Establishment and characterization of a human acute monocytic leukemia cell line (THP-1)*. Int J Cancer. 26 (2): 171-6.

[25]   **Greaves NS, Ashcroft KJ, Baguneid M and Bayat A**. (2013): *Current understanding of molecular and cellular mechanisms in fibroplasia and angiogenesis during acute wound healing*. J Dermatol Sci. 72 (3): 206-17.

[26]   **Park JE and Barbul A**. (2004): *Understanding the role of immune regulation in wound healing*. Am J Surg. 187 (5A): 11S-6S.

[27]   **Eming SA, Krieg T and Davidson JM**. (2007): *Inflammation in wound repair: Molecular and cellular mechanisms*. J Invest Dermatol. 127 (3): 514-25.

[28]   **Diegelmann RF and Evans MC**. (2004): *Wound healing: an overview of acute, fibrotic and delayed healing*. Front Biosci. 9: 283-9.

[29]   **Martin P**. (1997): *Wound healing--aiming for perfect skin regeneration*. Science. 276 (5309): 75-81.

[30]   **Werner S and Grose R**. (2003): *Regulation of wound healing by growth factors and cytokines*. Physiol Rev. 83 (3): 835-70.

[31]   **Enoch S and Leaper DJ**. (2005): *Basic science of wound healing*. Surgery (Oxford). 23 (2): 37-42.

[32]   **Lucas T, Waisman A, Ranjan R, Roes J, Krieg T, Muller W, Roers A and Eming SA**. (2010): *Differential roles of macrophages in diverse phases of skin repair*. J Immunol. 184 (7): 3964-77.

[33]   **Reinke JM and Sorg H**. (2012): *Wound repair and regeneration*. Eur Surg Res. 49 (1): 35-43.

[34]   **Witte MB and Barbul A**. (2002): *Role of nitric oxide in wound repair*. Am J Surg. 183 (4): 406-12.

[35]   **Loots MA, Lamme EN, Zeegelaar J, Mekkes JR, Bos JD and Middelkoop E**. (1998): *Differences in cellular infiltrate and extracellular matrix of chronic diabetic and venous ulcers versus acute wounds*. J Invest Dermatol. 111 (5): 850-7.

[36]   **Parsek MR and Singh PK**. (2003): *Bacterial biofilms: An emerging link to disease pathogenesis*. Annu Rev Microbiol. 57: 677-701.

[37]   **Costerton W, Veeh R, Shirtliff M, Pasmore M, Post C and Ehrlich G**. (2003): *The application of biofilm science to the study and control of chronic bacterial infections*. J Clin Invest. 112 (10): 1466-77.

[38]   **Clark RA, Ghosh K and Tonnesen MG**. (2007): *Tissue engineering for cutaneous wounds*. J Invest Dermatol. 127 (5): 1018-29.

[39]   **Wei W, Liu Q, Tan Y, Liu L, Li X and Cai L**. (2009): *Oxidative stress, diabetes, and diabetic complications*. Hemoglobin. 33 (5): 370-7.

[40]   **Eming SA, Koch M, Krieger A, Brachvogel B, Kreft S, Bruckner-Tuderman L, Krieg T, Shannon JD and Fox JW**. (2010): *Differential proteomic analysis distinguishes tissue repair biomarker signatures in wound exudates obtained from normal healing and chronic wounds*. J Proteome Res. 9 (9): 4758-66.

[41]   **Pastar I, Khan AA, Stojadinovic O, Lebrun EA, Medina MC, Brem H, Kirsner RS, Jimenez JJ, Leslie C and Tomic-Canic M**. (2012):

Induction of specific microRNAs inhibits cutaneous wound healing. J Biol Chem. 287 (35): 29324-35.

[42]   **Wild T and Auböck J**. (2007): *Manual der Wundheilung; Chirurgisch-dermatologischer Leitfaden der modernen Wundbehandlung*. 1 ed. Springer; Wien. 354.

[43]   **Catalano E, Cochis A, Varoni E, Rimondini L and Azzimonti B**. (2013): *Tissue-engineered skin substitutes: An overview*. J Artif Organs. 1-7.

[44]   **Alberts B, Johnson A, Lewis J, Raff M, Roberts K and Walter P**. (2007): *Molecular biology of the cell*. 5 ed. Garland Science; New York. 1392.

[45]   **Copper GM and Hausman RE**. (2013): *The cell: A molecular approach*. 6 ed. Sinauer Associates; Sunderland. 832.

[46]   **Geest CR and Coffer PJ**. (2009): *MAPK signaling pathways in the regulation of hematopoiesis*. J Leukoc Biol. 86 (2): 237-50.

[47]   **Seger R and Krebs EG**. (1995): *The MAPK signaling cascade*. FASEB J. 9 (9): 726-35.

[48]   **Bundscherer L, Nagel S, Hasse S, Tresp H, Wende K, Walther R, Reuter S, Weltmann KD, Masur K and Lindequist U**. (submitted 2014): *Non-thermal plasma treatment induces MAPK signaling in human monocytes*. Cent Eur J Chem.

[49]   **Wada T and Penninger JM**. (2004): *Mitogen-activated protein kinases in apoptosis regulation*. Oncogene. 23 (16): 2838-49.

[50]   **Bundscherer L, Wende K, Ottmüller K, Barton A, Schmidt A, Bekeschus S, Hasse S, Weltmann KD, Masur K and Lindequist U**. (2013): *Impact of non-thermal plasma treatment on MAPK signaling pathways of human immune cell lines*. Immunobiology. 218 (10): 1248–55.

[51] **Shaul YD and Seger R**. (2007): *The MEK/ERK cascade: From signaling specificity to diverse functions*. Biochim Biophys Acta. 1773 (8): 1213-26.

[52] **Davis RJ**. (2000): *Signal transduction by the JNK group of MAP kinases*. Cell. 103 (2): 239-52.

[53] **Schaeffer HJ and Weber MJ**. (1999): *Mitogen-activated protein kinases: Specific messages from ubiquitous messengers*. Mol Cell Biol. 19 (4): 2435-44.

[54] **Jakob U, Gaestel M, Engel K and Buchner J**. (1993): *Small heat shock proteins are molecular chaperones*. J Biol Chem. 268 (3): 1517-20.

[55] **Ricci JE, Maulon L, Battaglione-Hofman V, Bertolotto C, Luciano F, Mari B, Hofman P and Auberger P**. (2001): *A Jurkat T cell variant resistant to death receptor-induced apoptosis. Correlation with heat shock protein (Hsp) 27 and 70 levels*. Eur Cytokine Netw. 12 (1): 126-34.

[56] **Schafer C, Clapp P, Welsh MJ, Benndorf R and Williams JA**. (1999): *HSP27 expression regulates CCK-induced changes of the actin cytoskeleton in CHO-CCK-A cells*. Am J Physiol. 277 (6 Pt 1): C1032-43.

[57] **Chen SF, Nieh S, Jao SW, Liu CL, Wu CH, Chang YC, Yang CY and Lin YS**. (2012): *Quercetin suppresses drug-resistant spheres via the p38 MAPK-Hsp27 apoptotic pathway in oral cancer cells*. PLoS ONE. 7 (11): e49275.

[58] **Stokoe D, Engel K, Campbell DG, Cohen P and Gaestel M**. (1992): *Identification of MAPKAP kinase 2 as a major enzyme responsible for the phosphorylation of the small mammalian heat shock proteins*. FEBS Lett. 313 (3): 307-13.

[59] **Shibata S, Tada Y, Asano Y, Hau CS, Kato T, Saeki H, Yamauchi T, Kubota N, Kadowaki T and Sato S**. (2012): *Adiponectin regulates cutaneous wound healing by promoting keratinocyte proliferation and migration via the ERK signaling pathway*. J Immunol. 189 (6): 3231-41.

[60]   **Javelaud D, Laboureau J, Gabison E, Verrecchia F and Mauviel A**. (2003): *Disruption of basal JNK activity differentially affects key fibroblast functions important for wound healing*. J Biol Chem. 278 (27): 24624-8.

[61]   **Chen C, Chen YH and Lin WW**. (1999): *Involvement of p38 mitogen-activated protein kinase in lipopolysaccharide-induced iNOS and COX-2 expression in J774 macrophages*. Immunology. 97 (1): 124-9.

[62]   **Watanabe K, Shuto T, Sato M, Onuki K, Mizunoe S, Suzuki S, Sato T, Koga T, Suico MA, Kai H and Ikeda T**. (2011): *Lucidenic acids-rich extract from antlered form of Ganoderma lucidum enhances TNFalpha induction in THP-1 monocytic cells possibly via its modulation of MAP kinases p38 and JNK*. Biochem Biophys Res Commun. 408 (1): 18-24.

[63]   **Liu MK, Herrera-Velit P, Brownsey RW and Reiner NE**. (1994): *CD14-dependent activation of protein kinase C and mitogen-activated protein kinases (p42 and p44) in human monocytes treated with bacterial lipopolysaccharide*. J Immunol. 153 (6): 2642-52.

[64]   **Hoffmann E, Dittrich-Breiholz O, Holtmann H and Kracht M**. (2002): *Multiple control of interleukin-8 gene expression*. J Leukoc Biol. 72 (5): 847-55.

[65]   **Winzen R, Kracht M, Ritter B, Wilhelm A, Chen CY, Shyu AB, Muller M, Gaestel M, Resch K and Holtmann H**. (1999): *The p38 MAP kinase pathway signals for cytokine-induced mRNA stabilization via MAP kinase-activated protein kinase 2 and an AU-rich region-targeted mechanism*. EMBO J. 18 (18): 4969-80.

[66]   **Sim YS, Kim SY, Kim EJ, Shin SJ and Koh WJ**. (2012): *Impaired expression of MAPK is associated with the downregulation of TNF-alpha, IL-6, and IL-10 in Mycobacterium abscessus lung disease*. Tuberc Respir Dis (Seoul). 72 (3): 275-83.

[67]   **Rennekampff HO, Hansbrough JF, Kiessig V, Dore C, Sticherling M and Schroder JM**. (2000): *Bioactive interleukin-8 is expressed in wounds and enhances wound healing*. J Surg Res. 93 (1): 41-54.

[68]   **Stroth U**. (2011): *Plasmaphysik: Phänomene, Grundlagen, Anwendungen*. 1 ed. Vieweg+Teubner Verlag/ Springer Fachmedien Wiesbaden GmbH; Wiesbaden. 488.

[69]   **Goldston RJ and Rutherford PH**. (1995): *Introduction to plasma physics*. 1 ed. Institute of Physics Publishing; London. 510.

[70]   **Heinlin J, Isbary G, Stolz W, Morfill G, Landthaler M, Shimizu T, Steffes B, Nosenko T, Zimmermann J and Karrer S**. (2011): *Plasma applications in medicine with a special focus on dermatology*. J Eur Acad Dermatol Venereol. 25 (1): 1-11.

[71]   **Weltmann KD, Polak M, Masur K, von Woedtke T, Winter J and Reuter S**. (2012): *Plasma processes and plasma sources in medicine*. Contrib Plasma Phys. 52 (7): 644-54.

[72]   **Lieberman MA and Lichtenberg AJ**. (2005): *Principles of plasma discharges and materials processing*. 2 ed. John Wiley & Sons; Hoboken. 800.

[73]   **Weltmann KD, Kindel E, von Woedtke T, Hähnel M, Stieber M and Brandenburg R**. (2010): *Atmospheric-pressure plasma sources: Prospective tools for plasma medicine*. Pure Appl Chem. 82 (6): 1223–37.

[74]   **Meichsner J, Schmidt M, Schneider R and Wagner HE**. (2012): *Nonthermal plasma chemistry and physics*. 1 ed. Crc Press; Boca Raton. 564.

[75]   **Stoffels E, Flikweert AJ, Stoffels WW and Kroesen GMW**. (2002): *Plasma needle: A non-destructive atmospheric plasma source for fine surface treatment of (bio)materials*. Plasma Sources Sci Technol. 11 (4): 383-8.

[76] **Winter J, Dunnbier M, Schmidt-Bleker A, Meshchanov A, Reuter S and Weltmann KD**. (2012): *Aspects of UV-absorption spectroscopy on ozone in effluents of plasma jets operated in air*. J Phys D: Appl Phys 45 (38): 1-7.

[77] **Pipa AV, Reuter S, Foest R and Weltmann KD**. (2012): *Controlling the NO production of an atmospheric pressure plasma jet*. J Phys D: Appl Phys. 45 (8): 1-7.

[78] **Graves DB**. (2012): *The emerging role of reactive oxygen and nitrogen species in redox biology and some implications for plasma applications to medicine and biology*. J Phys D: Appl Phys. 45 (26): 1-42.

[79] **Soneja A, Drews M and Malinski T**. (2005): *Role of nitric oxide, nitroxidative and oxidative stress in wound healing*. Pharmacol Rep. 57 Suppl: 108-19.

[80] **Sen CK**. (2003): *The general case for redox control of wound repair*. Wound Repair Regen. 11 (6): 431-8.

[81] **Nathan C and Ding A**. (2010): *SnapShot: Reactive oxygen intermediates (ROI)*. Cell. 140 (6): 951- e2.

[82] **McDonnell G and Russell AD**. (1999): *Antiseptics and disinfectants: Activity, action, and resistance*. Clin Microbiol Rev. 12 (1): 147-79.

[83] **Hardwick JB, Tucker AT, Wilks M, Johnston A and Benjamin N**. (2001): *A novel method for the delivery of nitric oxide therapy to the skin of human subjects using a semi-permeable membrane*. Clin Sci (Lond). 100 (4): 395-400.

[84] **Haubner F, Ohmann E, Pohl F, Strutz J and Gassner HG**. (2012): *Wound healing after radiation therapy: Review of the literature*. Radiat Oncol. 7: 162.

[85] **Reuter S, Tresp H, Wende K, Hammer MU, Winter J, Masur K, Schmidt-Bleker A and Weltmann KD**. (2012): *From RONS to ROS:*

Tailoring plasma jet treatment of skin cells. IEEE Trans Plasma Sci. 40 (11): 2986 - 93

[86] **Koban I, Holtfreter B, Hubner NO, Matthes R, Sietmann R, Kindel E, Weltmann KD, Welk A, Kramer A and Kocher T**. (2011): *Antimicrobial efficacy of non-thermal plasma in comparison to chlorhexidine against dental biofilms on titanium discs in vitro - proof of principle experiment*. J Clin Periodontol. 38 (10): 956-65.

[87] **Oehmigen K, Winter J, Hahnel M, Wilke C, Brandenburg R, Weltmann KD and von Woedtke T**. (2011): *Estimation of possible mechanisms of escherichia coli inactivation by plasma treated sodium chloride solution*. Plasma Process Polym. 8 (10): 904-13.

[88] **Polak M, Winter J, Schnabel U, Ehlbeck J and Weltmann KD**. (2012): *Innovative plasma generation in flexible biopsy channels for inner-tube decontamination and medical applications*. Plasma Process Polym. 9 (1): 67-76.

[89] **Fricke K, Koban I, Tresp H, Jablonowski L, Schroder K, Kramer A, Weltmann KD, von Woedtke T and Kocher T**. (2012): *Atmospheric pressure plasma: A high-performance tool for the efficient removal of biofilms*. PLoS ONE. 7 (8): e42539.

[90] **Fridman G, Peddinghaus M, Balasubramanian M, Ayan H, Fridman A, Gutsol A and Brooks A**. (2006): *Blood coagulation and living tissue sterilization by floating-electrode dielectric barrier discharge in air*. Plasma Chem Plasma Process. 26 (4): 425-42.

[91] **Isbary G, Morfill G, Schmidt HU, Georgi M, Ramrath K, Heinlin J, Karrer S, Landthaler M, Shimizu T, Steffes B, Bunk W, Monetti R, Zimmermann JL, Pompl R and Stolz W**. (2010): *A first prospective randomized controlled trial to decrease bacterial load using cold atmospheric argon plasma on chronic wounds in patients*. Br J Dermatol. 163 (1): 78-82.

[92]   **Kaushik NK, Kim YH, Han YG and Choi EH**. (2013): *Effect of jet plasma on T98G human brain cancer cells*. Curr Appl Phys. 13 (1): 176-80.

[93]   **Kalghatgi S, Friedman G, Fridman A and Clyne AM**. (2010): *Endothelial cell proliferation is enhanced by low dose non-thermal plasma through fibroblast growth factor-2 release*. Ann Biomed Eng. 38 (3): 748-57.

[94]   **Wende K, Landsberg K, Lindequist U, Weltmann KD and von Woedtke T**. (2010): *Distinctive activity of a nonthermal atmospheric-pressure plasma jet on eukaryotic and prokaryotic cells in a cocultivation approach of keratinocytes and microorganisms*. IEEE Trans Plasma Sci. 38 (9): 2479-85.

[95]   **Kalghatgi SU, Fridman G, Fridman A, Friedman G and Clyne AM**. (2008): *Non-thermal dielectric barrier discharge plasma treatment of endothelial cells*. Conf Proc IEEE Eng Med Biol Soc. 2008: 3578-81.

[96]   **Barton A, Wende K, Bundscherer L, Hasse S, Schmidt A, Bekeschus S, Weltmann KD, Lindequist U and Masur K**. (submitted 2013): *Non-thermal plasma increases expression of wound healing related genes in a keratinocyte cell line*. Plasma Med.

[97]   **Arndt S, Unger P, Wacker E, Shimizu T, Heinlin J, Li YF, Thomas HM, Morfill GE, Zimmermann JL, Bosserhoff AK and Karrer S**. (2013): *Cold atmospheric plasma (CAP) changes gene expression of key molecules of the wound healing machinery and improves wound healing in vitro and in vivo*. PLoS ONE. 8 (11): e79325.

[98]   **Zenker M**. (2008): *Argon plasma coagulation*. GMS Krankenhhyg Interdiszip. 3 (1): 1-5.

[99]   **Kramer A, Lademann J, Bender C, Sckell A, Hartmann B, Münch S, Hinz P, Ekkernkamp A, Matthes R, Koban I, Partecke I, Heidecke CD, Masur K, Reuter S, Weltmann KD, Koch S and Assadian O**. (2013):

Suitability of tissue tolerable plasmas (TTP) for the management of chronic wounds. Clin Plasma Med. 1 (1): 11-8.

[100] **Bundscherer L, Bekeschus S, Tresp H, Hasse S, Reuter S, Weltmann KD, Lindequist U and Masur K**. (in press 2014): *Viability of human blood leucocytes compared with their respective cell lines after plasma treatment*. Plasma Med.

[101] **Toulon A, Breton L, Taylor KR, Tenenhaus M, Bhavsar D, Lanigan C, Rudolph R, Jameson J and Havran WL**. (2009): *A role for human skin-resident T cells in wound healing*. J Exp Med. 206 (4): 743-50.

[102] **Haertel B, Volkmann F, von Woedtke T and Lindequist U**. (2012): *Differential sensitivity of lymphocyte subpopulations to non-thermal atmospheric-pressure plasma*. Immunobiology. 217 (6): 628-33.

[103] **Shi XM, Zhang GJ, Yuan YK, Ma Y, Xu GM and Yang Y**. (2008): *Effects of low-temperature atmospheric air plasmas on the activity and function of human lymphocytes*. Plasma Process Polym. 5 (5): 482-8.

[104] **Bekeschus S, Masur K, Kolata J, Wende K, Schmidt A, Bundscherer L, Barton A, Kramer A, Bröker B and Weltmann KD**. (2013): *Human mononuclear cell survival and proliferation is modulated by cold atmospheric plasma jet*. Plasma Process Polym. 10 (8): 706-13.

[105] **Weltmann KD, Kindel E, Brandenburg R, Meyer C, Bussiahn R, Wilke C and von Woedtke T**. (2009): *Atmospheric pressure plasma jet for medical therapy: Plasma parameters and risk estimation*. Contrib Plasma Phys. 49 (9): 631-40.

[106] **Winter J, Wende K, Masur K, Iseni S, Dünnbier M, Hammer MU, Tresp H, Weltmann KD and Reuter S**. (2013): *Feed gas humidity: A hidden parameter affects cold atmospheric pressure plasma jet and plasma-treated human skin cells*. J Phys D: Appl Phys 46 (29): 1-11.

[107] **Bolstad BM, Irizarry RA, Astrand M and Speed TP**. (2003): *A comparison of normalization methods for high density oligonucleotide array data based on variance and bias*. Bioinformatics. 19 (2): 185-93.

[108] **Irizarry RA, Hobbs B, Collin F, Beazer-Barclay YD, Antonellis KJ, Scherf U and Speed TP**. (2003): *Exploration, normalization, and summaries of high density oligonucleotide array probe level data*. Biostatistics. 4 (2): 249-64.

[109] **Elmore S**. (2007): *Apoptosis: A review of programmed cell death*. Toxicol Pathol. 35 (4): 495-516.

[110] **Verhoven B, Schlegel RA and Williamson P**. (1995): *Mechanisms of phosphatidylserine exposure, a phagocyte recognition signal, on apoptotic T lymphocytes*. J Exp Med. 182 (5): 1597-601.

[111] **Koopman G, Reutelingsperger CP, Kuijten GA, Keehnen RM, Pals ST and van Oers MH**. (1994): *Annexin V for flow cytometric detection of phosphatidylserine expression on B cells undergoing apoptosis*. Blood. 84 (5): 1415-20.

[112] **Philpott NJ, Turner AJ, Scopes J, Westby M, Marsh JC, Gordon-Smith EC, Dalgleish AG and Gibson FM**. (1996): *The use of 7-amino actinomycin D in identifying apoptosis: Simplicity of use and broad spectrum of application compared with other techniques*. Blood. 87 (6): 2244-51.

[113] **Shi Y**. (2003): *Structural biology of programmed cell death*. Humana Press; New York. 47-65.

[114] **Ma RN, Feng HQ, Liang YD, Zhang Q, Tian Y, Su B, Zhang J and Fang J**. (2013): *An atmospheric-pressure cold plasma leads to apoptosis in Saccharomyces cerevisiae by accumulating intracellular reactive oxygen species and calcium*. J Phys D: Appl Phys. 46 (28).

[115] **Tuhvatulin AI, Sysolyatina EV, Scheblyakov DV, Logunov DY, Vasiliev MM, Yurova MA, Danilova MA, Petrov OF, Naroditsky BS,**

Morfill GE, Grigoriev AI, Fortov VE, Gintsburg AL and Ermolaeva SA. (2012): *Non-thermal plasma causes p53-dependent apoptosis in human colon carcinoma cells*. Acta Naturae. 4 (3): 82-7.

[116] **Chang HY and Yang X**. (2000): *Proteases for cell suicide: Functions and regulation of caspases*. Microbiol Mol Biol Rev. 64 (4): 821-46.

[117] **Vesely PW, Staber PB, Hoefler G and Kenner L**. (2009): *Translational regulation mechanisms of AP-1 proteins*. Mutat Res. 682 (1): 7-12.

[118] **Roux PP and Blenis J**. (2004): *ERK and p38 MAPK-activated protein kinases: A family of protein kinases with diverse biological functions*. Microbiol Mol Biol Rev. 68 (2): 320-44.

[119] **Kayahara M, Wang X and Tournier C**. (2005): *Selective regulation of c-jun gene expression by mitogen-activated protein kinases via the 12-o-tetradecanoylphorbol-13-acetate- responsive element and myocyte enhancer factor 2 binding sites*. Mol Cell Biol. 25 (9): 3784-92.

[120] **Lamb JA, Ventura JJ, Hess P, Flavell RA and Davis RJ**. (2003): *JunD mediates survival signaling by the JNK signal transduction pathway*. Mol Cell. 11 (6): 1479-89.

[121] **Vinciguerra M, Vivacqua A, Fasanella G, Gallo A, Cuozzo C, Morano A, Maggiolini M and Musti AM**. (2004): *Differential phosphorylation of c-Jun and JunD in response to the epidermal growth factor is determined by the structure of MAPK targeting sequences*. J Biol Chem. 279 (10): 9634-41.

[122] **Venza I, Cucinotta M, Caristi S, Mancuso G and Teti D**. (2007): *Transcriptional regulation of IL-8 by Staphylococcus aureus in human conjunctival cells involves activation of AP-1*. Invest Ophthalmol Vis Sci. 48 (1): 270-6.

[123] **Oguro T, Hayashi M, Nakajo S, Numazawa S and Yoshida T**. (1998): *The expression of heme oxygenase-1 gene responded to oxidative stress produced by phorone, a glutathione depletor, in the rat liver; the*

relevance to activation of c-jun n-terminal kinase. J Pharmacol Exp Ther. 287 (2): 773-8.

[124] **Angel P and Karin M**. (1991): *The role of Jun, Fos and the AP-1 complex in cell-proliferation and transformation*. Biochim Biophys Acta. 1072 (2-3): 129-57.

[125] **Daroui P, Desai SD, Li TK, Liu AA and Liu LF**. (2004): *Hydrogen peroxide induces topoisomerase I-mediated DNA damage and cell death*. J Biol Chem. 279 (15): 14587-94.

[126] **Heidenreich S, Schmidt M, August C, Cullen P, Rademaekers A and Pauels HG**. (1997): *Regulation of human monocyte apoptosis by the CD14 molecule*. J Immunol. 159 (7): 3178-88.

[127] **Li YQ, Hii CS, Der CJ and Ferrante A**. (1999): *Direct evidence that ERK regulates the production/secretion of interleukin-2 in PHA/PMA-stimulated T lymphocytes*. Immunology. 96 (4): 524-8.

[128] **Nagel S**. (2013): *Auswirkung von nicht-thermischem physikalischem Plasma auf die MAPK-Signalwege von primären humanen Monozyten* [Bachelor Thesis]. Greifswald, Germany: Ernst-Moritz-Arndt University of Greifswald.

[129] **Hennen J, Aeby P, Goebel C, Schettgen T, Oberli A, Kalmes M and Blömeke B**. (2011): *Cross talk between keratinocytes and dendritic cells: Impact on the prediction of sensitization*. Toxicol Sci. 123 (2): 501-10.

[130] **Ahn HJ, Kim KI, Kim G, Moon E, Yang SS and Lee JS**. (2011): *Atmospheric-pressure plasma jet induces apoptosis involving mitochondria via generation of free radicals*. PLoS ONE. 6 (11): e28154.

[131] **Blackert S, Haertel B, Wende K, von Woedtke T and Lindequist U**. (2013): *Influence of non-thermal atmospheric pressure plasma on cellular structures and processes in human keratinocytes (HaCaT)*. J Dermatol Sci. 70 (3): 173-81.

[132] **Wende K, Blackert S, Haertel B, Harms M, Holtz S, Masur K, von Woedtke T and Lindequist U**. (2014): *Transient oxidative stress in HaCaT keratinocytes after atmospheric pressure plasma jet treatment is influenced by cell environment*. Cell Biol Int. 38 (4): 412-25.

[133] **Montecucco A and Biamonti G**. (2007): *Cellular response to etoposide treatment*. Cancer Lett. 252 (1): 9-18.

[134] **Okahashi N, Nakata M, Sumitomo T, Terao Y and Kawabata S**. (2013): *Hydrogen peroxide produced by oral Streptococci induces macrophage cell death*. PLoS ONE. 8 (5): e62563.

[135] **Tammaro M, Barr P, Ricci B and Yan H**. (2013): *Replication-dependent and transcription-dependent mechanisms of DNA double-strand break induction by the topoisomerase 2-targeting drug Etoposide*. PLoS ONE. 8 (11): e79202.

[136] **Tresp H, Hammer MU, Winter J, Weltmann KD and Reuter S**. (2013): *Quantitative detection of plasma-generated radicals in liquids by electron paramagnetic resonance spectroscopy*. J Phys D: Appl Phys 46 (43): 435401.

[137] **Tresp H, Hammer MU, Weltmann KD and Reuter S**. (in press 2014): *Plasma generated reactive species in biologically relevant solutions*. Plasma Med.

[138] **Ebert-Dumig R, Seufert J, Schneider D, Kohrle J, Schutze N and Jakob F**. (1999): *Expression of selenoproteins in monocytes and macrophages--implications for the immune system*. Med Klin (Munich). 94 Suppl 3: 29-34.

[139] **Klebanoff SJ, Locksley RM, Jong EC and Rosen H**. (1983): *Oxidative response of phagocytes to parasite invasion*. Ciba Found Symp. 99: 92-112.

[140] **Buxton GV and Elliot AJ**. (1986): *Rate constant for reaction of hydroxyl radicals with bicarbonate ions*. Int J Radiat Appl Instrum C Radiat Phys Chem. 27 (3): 241-3.

[141] **Cutaia M, Black AD, Cohen I, Cassai ND and Sidhu GS**. (2005): *Alkaline stress-induced apoptosis in human pulmonary artery endothelial cells*. Apoptosis. 10 (6): 1457-67.

[142] **Kalghatgi S, Kelly CM, Cerchar E, Torabi B, Alekseev O, Fridman A, Friedman G and Azizkhan-Clifford J**. (2011): *Effects of non-thermal plasma on mammalian cells*. PLoS ONE. 6 (1): e16270.

[143] **Kim GJ, Kim W, Kim KT and Lee JK**. (2010): *DNA damage and mitochondria dysfunction in cell apoptosis induced by nonthermal air plasma*. Appl Phys Lett. 96 (2): 1-3.

[144] **Schmidt A, Wende K, Bekeschus S, Bundscherer L, Barton A, Ottmüller K, Weltmann KD and Masur K**. (2013): *Non-thermal plasma treatment is associated with changes in transcriptome of human epithelial skin cells*. Free Radic Res. 47 (8): 577-92.

[145] **Lichtenfels R, Mougiakakos D, Johansson CC, Dressler SP, Recktenwald CV, Kiessling R and Seliger B**. (2012): *Comparative expression profiling of distinct T cell subsets undergoing oxidative stress*. PLoS ONE. 7 (7): e41345.

[146] **Kuppan G, Balasubramanyam J, Monickaraj F, Srinivasan G, Mohan V and Balasubramanyam M**. (2010): *Transcriptional regulation of cytokines and oxidative stress by gallic acid in human THP-1 monocytes*. Cytokine. 49 (2): 229-34.

[147] **Hess J, Angel P and Schorpp-Kistner M**. (2004): *AP-1 subunits: Quarrel and harmony among siblings*. J Cell Sci. 117 (Pt 25): 5965-73.

[148] **Monje P, Hernandez-Losa J, Lyons RJ, Castellone MD and Gutkind JS**. (2005): *Regulation of the transcriptional activity of c-Fos by ERK. A novel role for the prolyl isomerase PIN1*. J Biol Chem. 280 (42): 35081-4.

[149] **Tanos T, Marinissen MJ, Leskow FC, Hochbaum D, Martinetto H, Gutkind JS and Coso OA**. (2005): *Phosphorylation of c-Fos by members of the p38 MAPK family. Role in the AP-1 response to UV light*. J Biol Chem. 280 (19): 18842-52.

[150] **Behmoaras J, Bhangal G, Smith J, McDonald K, Mutch B, Lai PC, Domin J, Game L, Salama A, Foxwell BM, Pusey CD, Cook HT and Aitman TJ**. (2008): *Jund is a determinant of macrophage activation and is associated with glomerulonephritis susceptibility*. Nat Genet. 40 (5): 553-9.

[151] **Mukaida N, Harada A and Matsushima K**. (1998): *Interleukin-8 (IL-8) and monocyte chemotactic and activating factor (MCAF/MCP-1), chemokines essentially involved in inflammatory and immune reactions*. Cytokine Growth Factor Rev. 9 (1): 9-23.

[152] **Lin CY, Hsiao WC, Huang CJ, Kao CF and Hsu GS**. (2013): *Heme oxygenase-1 induction by the ROS-JNK pathway plays a role in aluminum-induced anemia*. J Inorg Biochem. 128 (2013): 221-8.

[153] **Wu ML, Ho YC, Lin CY and Yet SF**. (2011): *Heme oxygenase-1 in inflammation and cardiovascular disease*. Am J Cardiovasc Dis. 1 (2): 150-8.

[154] **Itoh K, Mochizuki M, Ishii Y, Ishii T, Shibata T, Kawamoto Y, Kelly V, Sekizawa K, Uchida K and Yamamoto M**. (2004): *Transcription factor Nrf2 regulates inflammation by mediating the effect of 15-deoxy-Delta(12,14)-prostaglandin j(2)*. Mol Cell Biol. 24 (1): 36-45.

[155] **Dietrich S**. (2013): *Nrf2-vermittelte oxidative Stressantwort nach nicht-thermischer Plasmabehandlung in humanen Keratinozyten* [Bachelor Thesis]. Greifswald, Germany: Ernst-Moritz-Arndt University of Greifswald.

[156] **Mytilineou C, Kramer BC and Yabut JA**. (2002): *Glutathione depletion and oxidative stress*. Parkinsonism Relat Disord. 8 (6): 385-7.

[157] **Berkholz DS, Faber HR, Savvides SN and Karplus PA**. (2008): *Catalytic cycle of human glutathione reductase near 1 A resolution*. J Mol Biol. 382 (2): 371-84.

[158] **Sakamoto H, Mashima T, Yamamoto K and Tsuruo T**. (2002): *Modulation of heat-shock protein 27 (Hsp27) anti-apoptotic activity by methylglyoxal modification*. J Biol Chem. 277 (48): 45770-5.

[159] **De AK and Strickland J**. (2007): *Sensitivity of flow cytometric assay for measurement of human intracellular heat shock protein 27*. J Immunoassay Immunochem. 28 (3): 189-98.

[160] **Alegre ML, Frauwirth KA and Thompson CB**. (2001): *T-cell regulation by CD28 and CTLA-4*. Nat Rev Immunol. 1 (3): 220-8.

[161] **Rincon M, Flavell RA and Davis RA**. (2000): *The JNK and P38 MAP kinase signaling pathways in T cell-mediated immune responses*. Free Radic Biol Med. 28 (9): 1328-37.

[162] **Wang X and Studzinski GP**. (2001): *Activation of extracellular signal-regulated kinases (ERKs) defines the first phase of 1,25-dihydroxyvitamin D3-induced differentiation of HL60 cells*. J Cell Biochem. 80 (4): 471-82.

[163] **Xu K and Yu FS**. (2011): *Impaired epithelial wound healing and EGFR signaling pathways in the corneas of diabetic rats*. Invest Ophthalmol Vis Sci. 52 (6): 3301-8.

[164] **Torres M and Forman HJ**. (2003): *Redox signaling and the MAP kinase pathways*. Biofactors. 17 (1-4): 287-96.

[165] **Rogalla T, Ehrnsperger M, Preville X, Kotlyarov A, Lutsch G, Ducasse C, Paul C, Wieske M, Arrigo AP, Buchner J and Gaestel M**. (1999): *Regulation of Hsp27 oligomerization, chaperone function, and protective activity against oxidative stress/tumor necrosis factor alpha by phosphorylation*. J Biol Chem. 274 (27): 18947-56.

[166] **Durando MM, Meier KE and Cook JA**. (1998): *Endotoxin activation of mitogen-activated protein kinase in THP-1 cells; diminished activation following endotoxin desensitization*. J Leukoc Biol. 64 (2): 259-64.

[167] **Guha M and Mackman N**. (2001): *LPS induction of gene expression in human monocytes*. Cell Signal. 13 (2): 85-94.

[168] **Mehdi MZ, Azar ZM and Srivastava AK**. (2007): *Role of receptor and nonreceptor protein tyrosine kinases in H2O2-induced PKB and ERK1/2 signaling*. Cell Biochem Biophys. 47 (1): 1-10.

[169] **Schieven GL and Ledbetter JA**. (1994): *Activation of tyrosine kinase signal pathways by radiation and oxidative stress*. Trends Endocrinol Metab. 5 (9): 383-8.

[170] **Burdon RH, Alliangana D and Gill V**. (1995): *Hydrogen peroxide and the proliferation of BHK-21 cells*. Free Radic Res. 23 (5): 471-86.

[171] **Matsukawa J, Matsuzawa A, Takeda K and Ichijo H**. (2004): *The ASK1-MAP kinase cascades in mammalian stress response*. J Biochem. 136 (3): 261-5.

[172] **Wruck CJ, Streetz K, Pavic G, Gotz ME, Tohidnezhad M, Brandenburg LO, Varoga D, Eickelberg O, Herdegen T, Trautwein C, Cha K, Kan YW and Pufe T**. (2011): *Nrf2 induces interleukin-6 (IL-6) expression via an antioxidant response element within the IL-6 promoter*. J Biol Chem. 286 (6): 4493-9.

[173] **Koskenkorva-Frank TS, Weiss G, Koppenol WH and Burckhardt S**. (2013): *The complex interplay of iron metabolism, reactive oxygen species, and reactive nitrogen species: Insights into the potential of various iron therapies to induce oxidative and nitrosative stress*. Free Radic Biol Med. 65C: 1174-94.

[174] **Chapple IL**. (1997): *Reactive oxygen species and antioxidants in inflammatory diseases*. J Clin Periodontol. 24 (5): 287-96.

Literature

[175] **Schaub M, Harwaldt P, Wilhelm J, Heidt MC, Grebe M, Tillmanns H and Stadlbauer TH**. (2009): *FR167653 ameliorates expression of proinflammatory mediators in human umbilical venous endothelial cells and human monocytes*. Transplant Proc. 41 (6): 2616-20.

[176] **Schildberger A, Rossmanith E, Eichhorn T, Strassl K and Weber V**. (2013): *Monocytes, peripheral blood mononuclear cells, and THP-1 cells exhibit different cytokine expression patterns following stimulation with lipopolysaccharide*. Mediators Inflamm. 2013: 1-10.

[177] **Yao L, Hu DN, Chen M and Li SS**. (2012): *Subtoxic levels hydrogen peroxide-induced expression of interleukin-6 by epidermal melanocytes*. Arch Dermatol Res. 304 (10): 831-8.

[178] **Ottmüller K**. (2012): *Non-thermal plasma-induced MAPK and p53 signaling in keratinocytes and immune cells* [Diploma Thesis]. Greifswald, Germany: Ernst-Moritz-Arndt University of Greifswald.

[179] **Lv F, You W, Yu Y, Hu JB, Zhang B and Wang J**. (2013): *Effects of the 24 N-terminal amino acids of p55PIK on endotoxinstimulated release of inflammatory cytokines by hacat cells*. J Huazhong Univ Sci Technolog Med Sci. 33 (4): 587-93.

[180] **Budai MM, Varga A, Milesz S, Tozser J and Benko S**. (2013): *Aloe vera downregulates LPS-induced inflammatory cytokine production and expression of NLRP3 inflammasome in human macrophages*. Mol Immunol. 56 (4): 471-9.

[181] **Braunstein S, Kaplan G, Gottlieb AB, Schwartz M, Walsh G, Abalos RM, Fajardo TT, Guido LS and Krueger JG**. (1994): *GM-CSF activates regenerative epidermal growth and stimulates keratinocyte proliferation in human skin in vivo*. J Invest Dermatol. 103 (4): 601-4.

[182] **Sun J, Han J, Zhao Y, Zhu Q and Hu J**. (2012): *Curcumin induces apoptosis in tumor necrosis factor-alpha-treated HaCaT cells*. Int Immunopharmacol. 13 (2): 170-4.

[183] **Trefzer U, Brockhaus M, Lötscher H, Parlow F, Budnik A, Grewe M, Christoph H, Kapp A, Schöpf E, Luger TA and Krutmann J**. (1993): *The 55-kD tumor necrosis factor receptor on human keratinocytes is regulated by tumor necrosis factor-alpha and by ultraviolet B radiation*. J Clin Invest. 92 (1): 462-70.

Appendix

Supplementary Data

Supplementary gene list tables of DNA microarray are provided on a CD that is attached to the PhD thesis and available upon request.

Supplementary table 1: List of plasma-modulated genes in Jurkat cells treated for 15 s.

Supplementary table 2: List of plasma-modulated genes in Jurkat cells treated for 30 s.

Supplementary table 3: List of plasma-modulated genes in Jurkat cells treated for 15 s and 30 s.

Supplementary table 4: List of plasma-modulated genes in THP-1 cells treated for 60 s.

Supplementary table 5: List of plasma-modulated genes in THP-1 cells treated for 180 s.

Supplementary table 6: List of plasma-modulated genes in THP-1 cells treated for 60 s and 180 s.

Publications and Presentations

Publications:

Bundscherer L, Wende K, Ottmüller K, Barton A, Schmidt A, Bekeschus S, Hasse S, Weltmann KD, Masur K, Lindequist U. (2013): *Impact of non-thermal plasma treatment on MAPK signaling pathways of human immune cell lines.* Immunobiology 218 (10): 1248 – 55.

Schmidt A, Wende K, Bekeschus S, Bundscherer L, Barton A, Ottmüller K, Weltmann KD, Masur K. (2013): *Non-thermal plasma treatment is associated with changes in transcriptome of human epithelial skin cells.* Free Radic Res. 47 (8): 577 – 92.

Bekeschus S, Masur K, Kolata J, Wende K, Schmidt A, Bundscherer L, Barton A, Kramer A, Bröker B, Weltmann KD. (2013): *Human mononuclear cell survival and proliferation is modulated by cold atmospheric plasma jet.* Plasma Process Polym 10 (8): 706 – 13.

Barton A, Wende K, Bundscherer L, Hasse S, Schmidt A, Bekeschus S, Weltmann KD, Lindequist U, Masur K. (submitted 2013): *Non-thermal plasma increases expression of wound healing related genes in a keratinocyte cell line.* Plasma Med.

Bundscherer L, Bekeschus S, Tresp H, Hasse S, Reuter S, Weltmann KD, Lindequist U, Masur K. (in press 2014): *Viability of human blood leucocytes compared with their respective cell lines after plasma treatment.* Plasma Med.

Wende K, Barton A, Bekeschus S, Bundscherer L, Schmidt A, Weltmann KD, Masur K. (in press 2014): *Proteomic tools to characterize non-thermal plasma effects in eukaryotic cells.* Plasma Med.

Bundscherer L, Nagel S, Hasse S, Tresp H, Wende K, Walther R, Reuter S, Weltmann KD, Masur K, Lindequist U. (submitted 2014): *Non-thermal plasma treatment induces MAPK signaling in human monocytes.* Cent Eur J Chem.

Conference Proceedings:

Reuter S, Winter J, Wende K, Hasse S, Schroeder D, Bundscherer L, Barton A, Masur K, Knake N, Schulz-von der Gathen V, Weltmann KD. (2011): *Reactive oxygen species (ROS) in an argon plasma jet investigated with respect to ROS mediated apoptosis in human cells.* 30th International Conference on Phenomena in Ionized Gases (ICPIG).

Bundscherer L, Barton A, Masur K, Weltmann KD. (2012): *Impact of physical plasma on T lymphocytes.* 39th Annual Meeting of the Arbeitsgemeinschaft Dermatologische Forschung (ADF). Exp Dermatol.

Barton A, Holtz S, Bundscherer L, Masur K, Weltmann KD. (2012): *Influence of atmospheric pressure plasma on keratinocytes.* 39th Annual Meeting of the Arbeitsgemeinschaft Dermatologische Forschung (ADF). Exp Dermatol.

Bundscherer L, Schmidt A, Barton A, Hasse S, Wende K, Bekeschus S, Lindequist U, Weltmann KD, Masur K. (2013): *NTP-mediated changes of gene expression patterns in human cell lines.* 40th IEEE International Conference on Plasma Science (ICOPS).

Barton A, Wende K, Bundscherer L, Weltmann KD, Lindequist U, Masur K. (2013): *Non-Thermal Atmospheric Pressure Plasma Treatment of Human Cells: The Effect of Ambient Conditions. 21th International Symposium on Plasma Chemistry (*ISPC 21).

Oral Presentations:

Bundscherer L[*], **Hasse S, Barton A, Wende K, Weltmann KD, Lindequist U, Masur K.** (2011): *Plasma-mediated activation of immune cells.* 1. Workshop ZIK *plasmatis*, Rostock, Germany.

Bundscherer L[*], **Barton A, Lindequist U, Weltmann KD, Masur K.** (2011): *Studies of plasma-based activation of immune cells.* 3. Autumn School of Immunology – Current Concepts in Immunology, Bad Schandau, Germany.

Bundscherer L[*], **Ottmüller K, Schmidt A, Wende K, Barton A, Bekeschus S, Lindequist U, Weltmann KD, Masur K.** (2012): *Effect of non-thermal atmospheric pressure plasma treatment on signaling pathways of human immune cell lines.* 1st Young Professionals Workshop on Plasma Medicine, Boltenhagen, Germany.

Bundscherer L[*], **Schmidt A, Barton A, Hasse S, Wende K, Bekeschus S, Lindequist U, Weltmann KD, Masur K.** (2013): *NTP-mediated changes of gene expression patterns in human cell lines.* 40th IEEE International Conference on Plasma Science (ICOPS), San Francisco, USA.

Bundscherer L[*], **Wende K, Ottmüller K, Schmidt A, Barton A, Hasse S, Bekeschus S, Lindequist U, Weltmann KD, Masur K.** (2013): *Impact of atmospheric pressure plasma on MAPK signaling pathways in human immune cells lines.* 5th Central European Symposium on Plasma Chemistry (CESPC 5), Balatonalmádi, Hungary.

---

[*] presenting author

Publications and Presentations

Bundscherer L[*]**, Nagel S, Wende K, Ottmüller K, Hasse S, Weltmann KD, Lindequist U, Masur K.** (2013): *Induction of MAPK-mediated IL-8 secretion of human monocytes in response to non-thermal plasma treatment.* 2nd Young Professionals Workshop on Plasma Medicine, Kölpinsee, Germany.

Poster Presentations:

Bundscherer L[*]**, Barton A, Hasse S, Wende K, Bekeschus S, Lindequist U, Kramer A, Weltmann KD, Masur K.** (2011): *Impact of on-thermal atmospheric pressure plasma on immune cells.* 10. Workshop Plasmamedizin (ak-adp), Erfurt, Germany.

Bundscherer L[*]**, Barton A, Lindequist U, Kramer A, Weltmann KD, Masur K.** (2012): *Impact of physical plasma on T lymphocytes.* 39th Annual Meeting of the Arbeitsgemeinschaft Dermatologische Forschung (ADF), Marburg, Germany.

Bundscherer L[*]**, Barton A, Wende K, Masur K, Lindequist U, Kramer A, Weltmann KD.** (2012): *Impact of non-thermal atmospheric pressure plasma on T lymphocytes and monocytes.* 4th international conference on plasma medicine (ICPM4), Orléans, France.

Schulz U[*]**, Bundscherer L, von Woedtke T, Masur K, Morgenstern O.** (2012): *A cell culture based assay for studies on inhibitors of the inducible nitric oxide synthase (iNOS) and effects of cold atmospheric pressure plasma treatment of keratinocytes and leucocytes.* Jahrestagung 2012 der Deutschen Pharmazeutischen Gesellschaft, Greifswald, Germany.

---

[*] presenting author

Bundscherer L[**], Bekeschus S[**], Barton A, Wende K[*], Schmidt A, Hasse S, Bröker B, Lindequist U, Weltmann KD, Masur K[*]. (2013): *Viability after plasma treatment of ex vivo leucocytes compared with their respective cell lines.* NextMed 2013, San Diego, USA.

Bundscherer L[*], Wende K, Ottmüller K, Barton A, Hasse S, Schmidt A, Bekeschus S, Weltmann KD, Lindequist U, Masur K. (2013): *Impact of non-thermal atmospheric pressure plasma on immune cell lines.* 10th International Conference on New Trends in Immunosuppression and Immunotherapy (Immuno 2013), Barcelona, Spain.

Barton A, Hasse S[*]**, Bundscherer L, Wende K, Weltmann KD, Lindequist U, Masur K.** (2014): *Growth factors and cytokines are regulated by non-thermal atmospheric pressure plasma.* 41th Annual Meeting of the Arbeitsgemeinschaft Dermatologische Forschung (ADF), Cologne, Germany.

[**] contributed equally

[*] presenting author

Acknowledgements

First, I would like to express my deepest gratitude to Professor Dr. Ulrike Lindequist for her supportive encouragement that guided me throughout the PhD thesis. It was very reassuring to know that it was always possible to ask for her advice. I also would like to thank Dr. Kai Masur very much for giving me the opportunity to work on this fascinating topic and for his ambitious support during this study.

I would like to thank my supervisor Dr. Sybille Hasse very much for her great ideas, advice and support when revising my PhD thesis and publications. Moreover, her motivating way was very helpful throughout my time as PhD student. I am also very grateful to Dr. Kristian Wende who had a lot of constructive and insightful suggestions for my thesis as well as publications and Dr. Anke Schmidt whose guidance on DNA microarray was very helpful.

A very special thanks goes to Annemarie Barton who I could always rely on. I really enjoyed our collaboration with fruitful discussions and also the fun we had! Many thanks to Stefanie Nagel for her enormous and reliable help as my student assistant and Liane Kantz for her valuable technical assistance in the lab. Besides, I also would like to thank Ansgar Schmidt-Bleker for helping me with the illustration of the DNA microarray cluster analysis and Helena Tresp for the great collaboration and discussions!

In addition, I want to thank all the members of the ZIK *plasmatis* group for the great atmosphere and all the fun we had, especially Christin, Sylvain, Mario, Jörn, Malte and Stephan.

Finally, I would like to thank my family for supporting my studies and also my friends who had an open mind for all the questions and difficulties I had during my PhD time. My special thanks belongs to Matthias who had always been there for me at any time of the day or night!